



**The story of resorcinol crystals and a new perspective for
stabilizing high-pressure polymorphs at ambient conditions**

**Historia kryształów rezorcynolu i nowe sposoby stabilizowania
wysokociśnieniowych polimorfów w warunkach normalnych**

Fatemeh Safari

A thesis presented to the Faculty of Chemistry, Adam Mickiewicz University, Poznań, in the partial fulfilment of requirements for the degree of Doctor of Philosophy in Chemistry

Supervised by Prof. Dr. Hab. Andrzej Katrusiak

Co-supervised by Dr. Ewa Patyk-Kaźmierczak

January 2022

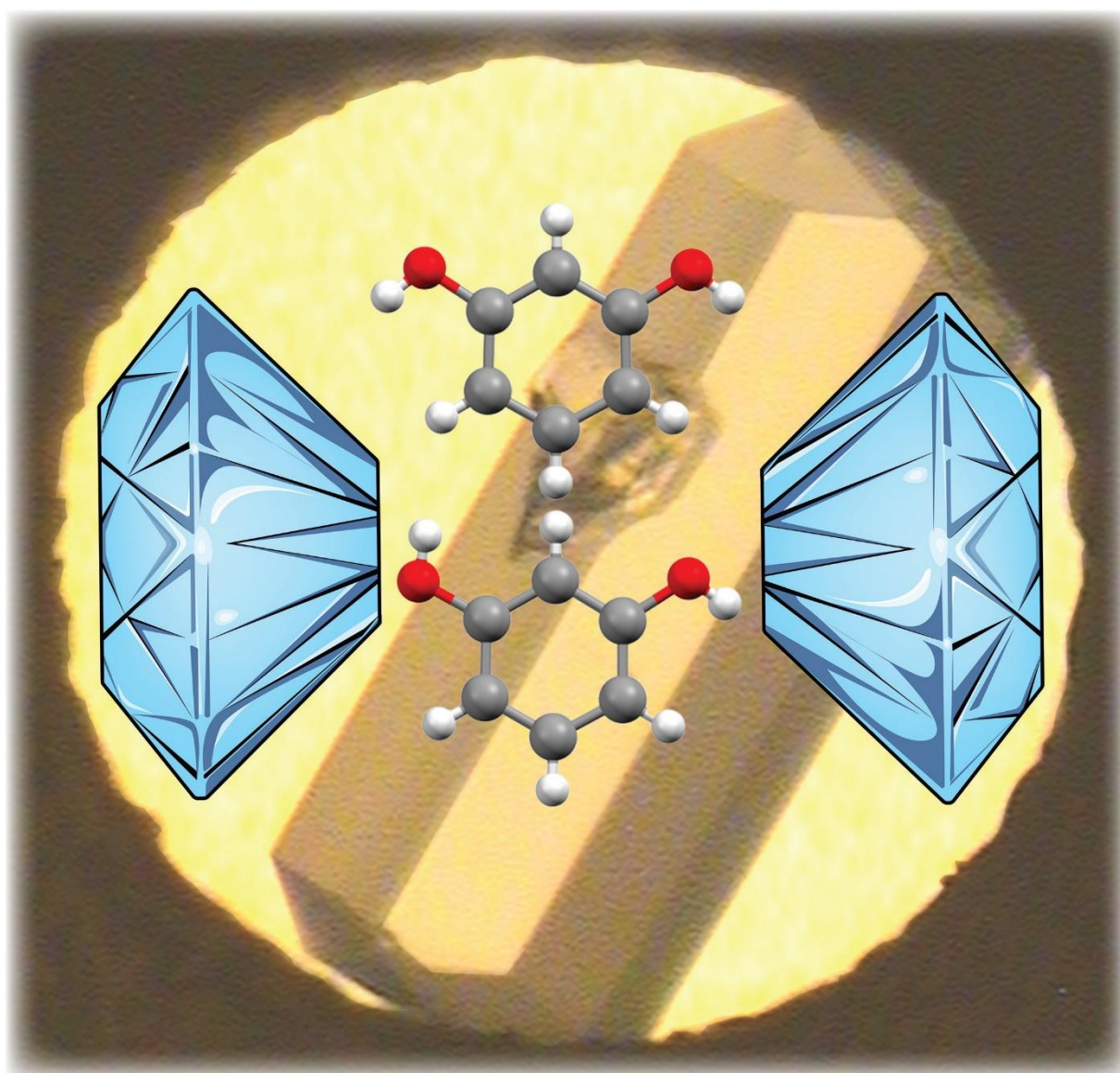
“Be less curious about people and more curious about ideas.”

-Maria Salomea Skłodowska-Curie (1867-1934)

CRYSTAL GROWTH & DESIGN

October 2019
Volume 19
Number 10
pubs.acs.org/crystal

INTEGRATING THE
FIELDS OF CRYSTAL
ENGINEERING AND
CRYSTAL GROWTH FOR
THE SYNTHESIS
AND APPLICATIONS
OF NEW MATERIALS



Acknowledgements

I would like to thank my supervisor Professor Andrzej Katrusiak for taking me on board in his group and giving me the opportunity to work in such an interesting and multidisciplinary field. His constant enthusiasm and encouragement have enabled me to find my feet and take pride in my work. I would also like to thank Prof. Piotr Pawluć for his support throughout these four years of my PhD program in all steps.

In addition, I would like to acknowledge Dr. Ewa Patyk-Kaźmierczak and Dr. Anna Olejniczak for having taught me everything they know and spending many hours with me at lab. Their friendship has been as indispensable as their knowledge and I would like to say, I'm grateful to have such amazing fellow labmates, thanks to which I have never felt homesick during my Ph.D. when I was far away from my family and my county.

I would like to dedicate this thesis to my father and mother, Hossein and Homma. Thank you for all your love, patience and sacrifice. A final thanks you to my favourite four: Hamid, Hasan, Elahe and Ida Moszczyńska who is my polish sister.

Last but not least, I am grateful for providing my scholarship to the EU European Social Fund, Operational Program Knowledge Education Development, grant POWR.03.02.00–00-I026/16.

Table of Contents

1 Introduction.....	1
1.1 Chemistry of resorcinol.....	1
1.2 Materials under high pressure.....	4
1.2.1 Diamond anvil cell and high-pressure X-ray diffraction experiments.....	5
1.2.2 Application of high-pressure techniques in pharmaceutical chemistry.....	10
1.2.3 Hydrogen-bonded solids under high pressure.....	12
1.3 Scope of the thesis.....	14
1.4 List of articles prepared within this thesis.....	16
1.5 Note on references to figures and tables.....	16
2 Experimental methods.....	17
2.1 Sample preparation for high-pressure X-ray diffraction experiments.....	17
2.2 Pressure calibration.....	18
2.3 Recovery of high-pressure polymorphs to ambient conditions.....	18
2.4 X-ray diffraction experiments.....	19
2.4.1 High-pressure single crystal X-ray diffraction measurements.....	19
2.4.2 Powder X-ray diffraction measurements.....	20
2.5 Data reduction, structure solution and refinement.....	20
3 Results and discussion.....	21
3.1 Transformation between resorcinol phases α and β	23
3.2 New solvates of resorcinol.....	24
3.3 Pure high-pressure polymorphs of resorcinol.....	28
3.4 Structural model of internal pressure.....	32
3.5 High-pressure polymorphs under ambient conditions.....	33
4 Conclusions.....	35
5 Bibliography.....	38
Appendix A: Summary.....	49
Appendix B: Summary in Polish (Streszczenie w języku polskim).....	51
Appendix C: Crystallographic data.....	54
Appendix D: Scientific articles.....	55
(R1) Pressure-Dependent Crystallization Preference of Resorcinol Polymorphs.....	55
(R2) Pressure-Promoted Solvation of Resorcinol.....	63
(R3) High-Pressure Polymorphs Nucleated and Stabilized by Rational Doping under Ambient Conditions.....	71

1 Introduction

1.1 Chemistry of resorcinol

Resorcinol (also known as resorcin, *meta*-dihydroxybenzene, 1,3-dihydroxybenzene, 1,3-benzenediol and 3-hydroxyphenol; Figure 1) is an organic compound naturally present in argan oil (Figure 1).¹ Due to its antibacterial properties, resorcinol is used in cosmetic and pharmaceutical products, for example in acne treatment.² It is also used in various organic syntheses, including those of pharmaceutical compounds,³⁻⁷ as well as in resins production.⁷ At ambient conditions resorcinol exists in the form of white crystallites (m.p. 384 K),⁸ has a bitter-sweet taste and faint, characteristic aromatic odour.⁷ Resorcinol is highly soluble in water, with the density of its water solution increasing approximately proportionally with the resorcinol concentration.⁹

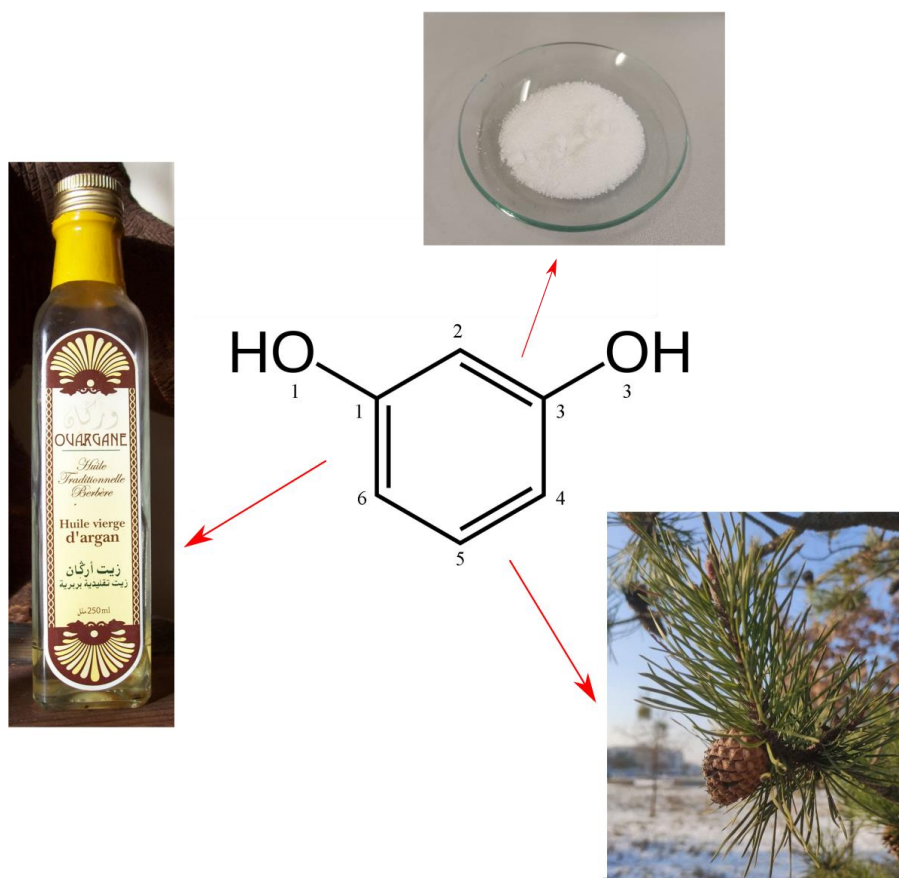


Figure 1. Structural formula of resorcinol with the atom numbers, a sample of resorcinol powder on a watch glass, a pine-tree branch, containing resorcinol and a bottle of argan oil.

The reactivity of resorcinol is related to the constitution of its molecule. The two hydroxyl groups located in *meta*-positions of the aromatic ring reinforce each other leading to the activation of the *ortho*- and *para*-positions (*i.e.* positions 2, 4, and 6 in the aromatic ring). Meanwhile, the 5th position in the benzene ring remains basically non-active.⁷

For the first time, resorcinol was synthesized in the laboratory in 1864.¹⁰⁻¹² However, it took 14 years to develop the process for resorcinol manufacturing. The process reported in 1878, based on the disulfonation of benzene and fusion of the disodium salt of benzenedisulfonic acid,¹³⁻¹⁵ is still used today in its modified form, as it offers an economical route for resorcinol synthesis.⁷ Although, other methods, besides disulfonation of benzene, have been developed over the years, presently only one (based on hydroperoxidation of *meta*-diisopropylbenzene) is commercially applied.⁷

Resorcinol is one of the first organic compounds for which polymorphism was observed, and according to the analysis of Cambridge Structural Database (CSD), it is the first organic compound for which the crystal structures of both polymorphs (α and β) were determined.^{16,17} In 1936, Robertson reported the crystal structure of polymorph α .¹⁶ Later, in 1938 Robertson and Ubbelohde recrystallized polymorph α at high temperature of *ca.* 347 K,¹⁷ obtaining crystals of polymorph β (having the symmetry of orthorhombic space group $Pna2_1$, the same as that of form α). Interestingly, the lower-temperature polymorph α is less dense than the high-temperature polymorph β . The counterintuitive density relation of resorcinol polymorphs and its solid-state properties have prompted a wide interest and investigations on this compound, with numerous studies of resorcinol by neutron¹⁸ and X-ray¹⁹ diffraction, proton NMR,¹⁹ Raman and IR spectroscopies,^{19,20,21} reported in recent years.

Besides polymorphs α and β of pure resorcinol, it is prone to co-crystallize with other compounds. In total, 77 structures of mono- and multi-component crystals of resorcinol are deposited in the CSD (version 2019.2.0). At this stage, it needs to be noted, that although constitution of resorcinol molecule makes it considerably rigid, the rotation of its hydroxyl groups is possible, allowing the hydrogen atoms in OH groups to assume different orientations. As a result, resorcinol molecules can be observed in the solid state in varied conformations, which are described by idealized descriptions: (i) *anti-anti*, (ii) *anti-syn*, and (iii) *syn-syn* (Figure 2). In fact, one of the differences between α and β polymorphs of resorcinol concerns the orientation of hydroxyl groups, with molecules having *anti-anti* and *anti-syn* conformation in forms α and β , respectively. Out of all 77 resorcinol-containing structures reported in CSD,

in 25 the molecules assume conformation *anti-anti*, in 22 *anti-syn*, and in 30 *syn-syn* (found exclusively in co-crystals). The conformational flexibility of hydroxyl groups plays a key role in molecular aggregation, leading to crystallization of different solid forms of resorcinol and its analogues, as the position of hydrogen atoms in OH groups affect the directions of the intermolecular hydrogen bonds.

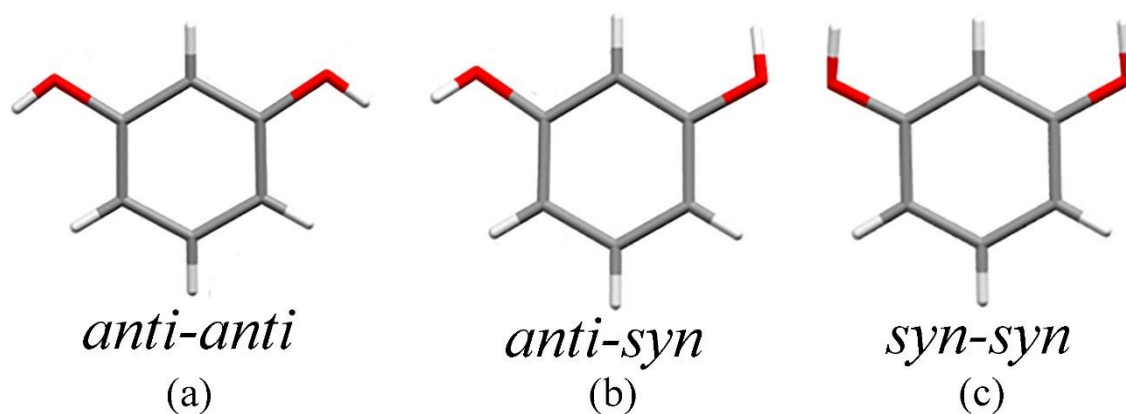


Figure 2. Different idealized conformations of resorcinol molecules: (a) *anti-anti*, present in polymorph α ; (b) *anti-syn*, present in polymorph β ; (c) *syn-syn*, present solely in co-crystals.

The exceptional density relation of polymorphs α and β and their identical space-group type, prompted high-pressure investigation of resorcinol crystals. The pressure-induced phase transition between form α and β was detected at 0.5 GPa by X-ray and Raman studies.^{22,23} However, the later study by Kichanov *et al.* has revealed somewhat lower pressure of the α -to- β phase transition at 0.4 GPa,¹⁹ and has confirmed that further compression of polymorph β to 5.6 GPa leads to second phase transition to form γ .^{19,24} Interestingly, rapid increase of pressure can suppress the α -to- β transformation, enabling phase transition from polymorph α to the second high-pressure polymorph (named δ) of the unknown symmetry above 3 GPa.^{19,24} In 2016, fifth polymorph of resorcinol, labelled ε , having the symmetry of orthorhombic space group $P2_12_12_1$, was discovered at ambient pressure.²⁵ This phase could only be obtained concomitant with polymorph β , by cooling the melted mixture of resorcinol and tartaric acid. In the same study Zhu *et al.* predicted the structure of yet another polymorph of resorcinol, of monoclinic space-group symmetry $P2_1$. However, so far this phase was not observed experimentally and therefore it was not labelled by a Greek letter but is referred to as polymorph $P2_1$ (after its postulated space group). Recently, as the part of the research presented in this thesis, a new high-pressure polymorph of resorcinol, form ζ , was discovered and is discussed in more detail in the *Results* section. Selected crystallographic information for polymorphs of resorcinol reported prior to this work are presented in Table 1.

Table 1. Selected crystallographic information of resorcinol polymorphs α , β , γ , ε and $P2_1$, discovered or postulated prior to this work.

<i>Phase</i>	α	β	γ	ε	$P2_1$
P (GPa)	0.0001	0.50	5.60	0.0001	0.0001
T (K)	298	298	298	298	298
Crystal system	Orthorhombic				Monoclinic
Space group	$Pna2_1$	$Pna2_1$	$Pnna$	$P2_12_12_1$	$P2_1$
Unit-cell ($\text{\AA}/^\circ$):					
<i>a</i>	10.550(3)	7.711(1)	7.3346*	17.900	9.380*
<i>b</i>	9.570(3)	12.611(2)	11.486(7)	10.568	5.466*
<i>c</i>	5.669(2)	5.379(1)	9.246(5)	5.722	5.529*
β	90	90	90	90	89.153*
Volume(\AA^3)	572.39(3)	523.1(2)	778.938*	1082.4	543.0*
Density (g/cm^3)	1.278	1.325	1.876	1.351	1.346
Z/Z'	4/1	4/1	8/1	8/2	4/2
Conformer	<i>anti-anti</i>	<i>anti-syn</i>	-	<i>anti-syn</i>	<i>anti-syn</i>
Reference	[16]	[17]	[19]	[25]	[25]

* For these cases the ESDs for the unit-cell parameters and volume were not included in the table, as they were not reported by the authors (polymorph γ) or the polymorph was not yet obtained experimentally (polymorph $P2_1$).

1.2 Materials under high pressure

The studies of materials under extreme pressure can reveal various interesting physical and chemical phenomena. Application of high pressure in geology and mineralogy enables the investigation of the processes taking place in the interiors of Earth and other planets.^{27,28} High-pressure techniques are widely used in search of new polymorphs^{29,30} and *pseudopolymorphs* (hydrates and other solvates)³¹ of chemical compounds. Their new solid forms can be obtained via recrystallization or isothermal compression. Extreme pressure is applied for investigation of phase transitions, including pressure-induced transformation of ambient-conditions gases and liquids into solid state,^{32,33} as well as solid-solid phase transitions.^{34,35} Previous reports has shown that various physical properties (*e.g.*, magnetic³⁶⁻³⁸ and thermal properties³⁹) can be affected by increased pressure. Moreover, high-pressure methods were successfully applied to induce chemical reactions in solid state, such as polymerization⁴⁰ or ionization.⁴¹ Recently, the development of computational techniques enabled charge-density studies at high pressure, providing new information on the pressure-induced effects in solids.⁴²⁻⁴⁴

1.2.1 Diamond anvil cell and high-pressure X-ray diffraction experiments

The origin of the high-pressure research as we know it can be dated back to the beginning of the 20th century, when Percy W. Bridgman developed a new approach to pressure-sealing, enabling carrying out experiments up to 7,000 atm.⁴⁵ Later modification of the technique, concerning the pumping system, expanded the pressure limit up to 2 GPa, while the development of the opposed-anvil device allowed to study solids in 5-10 GPa range.⁴⁵ Findings of Bridgman and use of diamonds for high-pressure devices^{46,47} ultimately led to inventing the diamond anvil cell (DAC) in 1958,^{48,49} which thanks to the contribution of other researchers over the years evolved into a versatile apparatus used today.⁵⁰

The crucial elements of the DAC are two parallel diamond anvils with flat culets, mounted on metal discs.⁵⁰ An example of the DAC, a modified Merrill-Bassett DAC,⁵¹ is shown in Figure 3. Different types of diamond anvils, such as brilliant cut anvils, Drukker anvils or Boehler-Almax anvils, are used in DACs.⁵⁰ The first type is historically the oldest, with anvils in the first DACs being gems confiscated from smugglers and donated by custom agents.⁵² The standard Drukker design⁵³ has simplified shape and increased table surface, while the Boehler–Almax anvil has conical crown that offers a superior mechanical stability by optimizing its support on the precisely matching tungsten carbide backing plate.⁵⁴ Depending on the pressure limit that needs to be reached, the size and shape of diamond anvils can vary. For achieving ultrahigh pressure, several features of diamond anvils need to be considered:⁵⁵

(i) The diamond anvil geometry. The higher-pressure limit can be reached with diamonds with single and double bevels (compared to no bevel diamonds). Recent studies have also shown that the limit can be increased even further for toroidal or double stage anvils.

(ii) The bevel diameter to flat culet diameter ratio, where the larger ratio values enable achieving higher pressure.^{55,56}

(iii) The bevel angles. For the single bevel diamonds, the angle in 7-8.5° range is most common, and highest pressure can be achieved for an angle of 8.5°, while for double bevelled anvils, the angle between 6 and 9° for the first bevel is usually considered optimal.

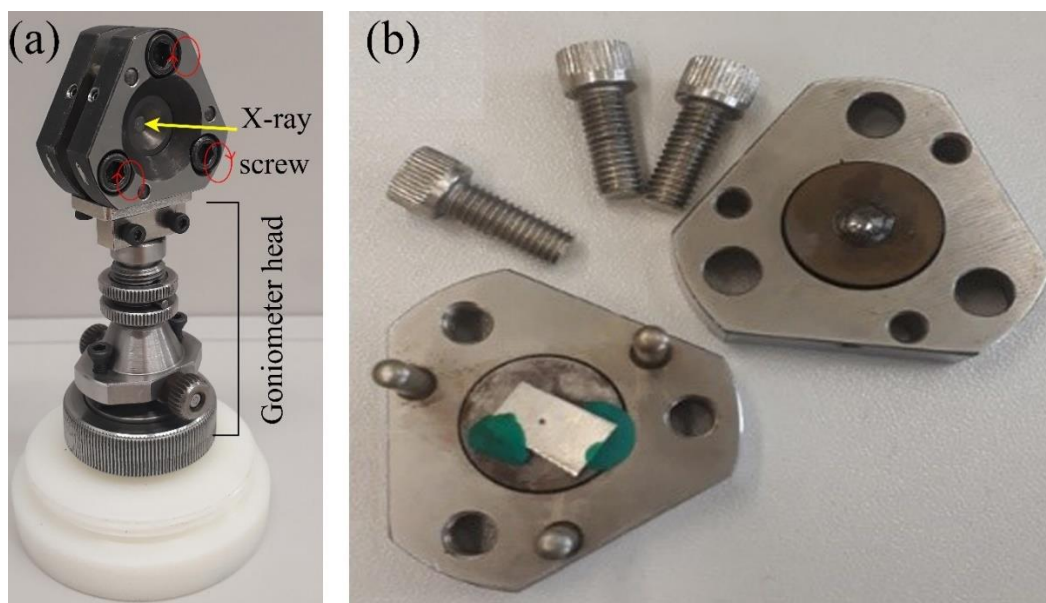


Figure 3. Picture of the modified Merrill-Bassett DAC: (a) mounted on the goniometer head, with the entry point for the X-ray incident beam marked with a yellow arrow, and the direction of the rotation of Allen screws indicated by red circular arrows; (b) opened and prepared for the sample loading, with gasket installed (supported on green modelling clay).

Between the diamond anvils of the DAC, a metal gasket with an opening is placed (Figure 4). The material of the gasket depends on several parameters, such as the pressure range, nature of the experiment, and reactivity of the sample and hydrostatic medium. For experiments under pressure exceeding 20 GPa, with use of high temperature, the rhenium or tungsten gaskets can be used.^{57,58} The amorphous boron composite gaskets can be used to eliminate X-ray diffraction peaks from the gasket for experiments up to 20 GPa, including high-temperature studies.⁵⁹ The Cu-Be gaskets can be implemented for magnetic measurements,⁶⁰ while for studies of reactive chemicals, gaskets lined with the inert metal such as gold can be used.⁶¹ For electrical measurements with DACs, insulated gaskets covered by MgO or alumina are implemented.⁶² The thickness of the gasket and the diameter of the opening can vary depending on the pressure range of the experiment, the size of diamonds culets, sample size, and the nature of the experiment.⁵⁰ Prior to the sample loading, the gasket is pre-indented in the DAC, which allows adjusting the thickness of the metal foil (affecting the dimensions of the chamber), strengthens the gasket material, and improves the sealing of the chamber.⁵⁰

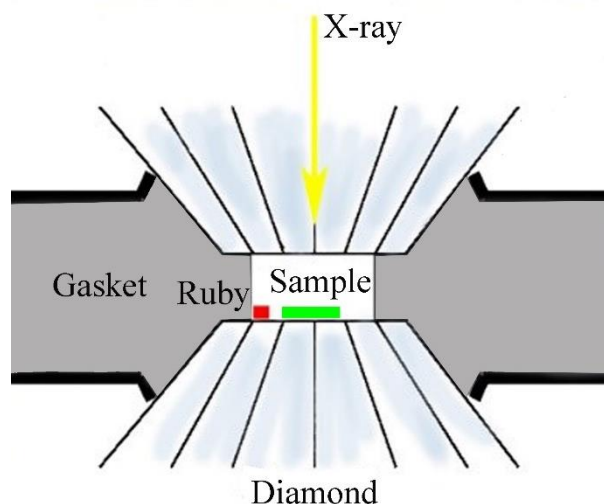


Figure 4. Schematic illustration of the DAC setup.

Two approaches for pre-indenting can be used. In the first one, the gasket is pre-indented and then an opening is drilled in the centre of the indentation. So-prepared gasket is then re-mounted in the DAC, keeping its initial orientation. For the second approach, the hole in the gasket is made first, the gasket is then centred in the DAC in respect to the diamond culets and the pre-indent is performed.⁵⁰ The hole in the gasket can be drilled with micro driller or spark eroding machine (Figure 5). Its size should be optimized in respect to the culet size, with the optimal radius of the opening being equal to, or smaller than, about half of the culet diameter.⁵⁰ Too big opening can lead to contact between the diamond anvils at higher pressure and their destruction and affects the pressure range that can be achieved. On the other hand, smaller holes, limit the sample size. When the diameter of the opening is decided, the limitations of the experimental techniques have to be considered as well. For example, for X-ray diffraction experiments, the hole should not be smaller than the size of the X-ray beam.

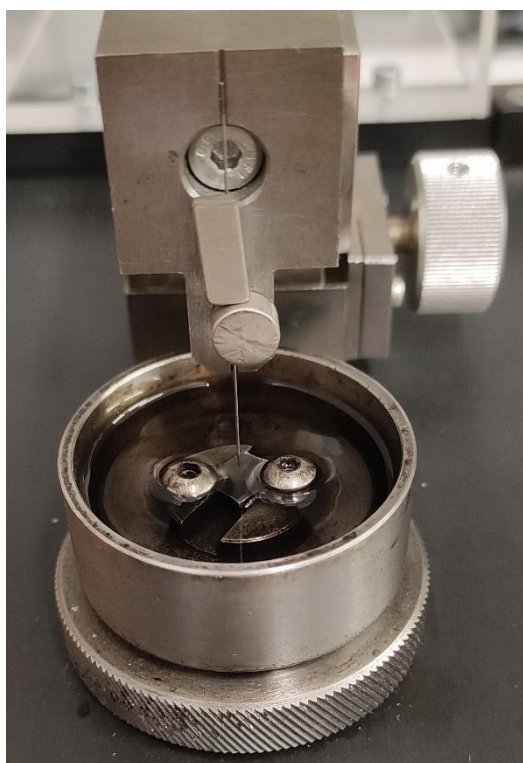


Figure 5. In-house made spark eroding machine used for gasket preparation.

The pressure inside the DAC is generated as a result of gasket deformation, affecting the size of the chamber filled with the sample and pressure transmitting medium (PTM). The deformation is caused by squeezing the gasket between diamond anvils.⁵⁰ In a modified Merrill-Bassett DAC the deformation is achieved by bringing the anvils closer together with the use of three Allen screws.⁵¹ To ensure the sample is under hydrostatic pressure, appropriate PTM that should not support any shear, needs to be selected. It needs to be noted that the melting line of fluids increases with pressure, eventually reaching the point when they solidify. Usually, as a result, the pressure inside the chamber becomes inhomogeneous and differential and shear stresses appear.⁶³ This in turn affects the quality and accuracy of the data and can result in appearance of ‘anomalies’ easy to misinterpret as new physical phenomena.⁶³ Therefore, the hydrostatic limit of the PTM is one of the properties that needs to be considered. Moreover, depending on the nature of the studied sample and the type of the experiment, the sample solubility in PTM, its reactivity, viscosity and the size of its molecules should be taken into account. A number of hydrostatic medias are used for high-pressure experiments, including both gases and liquids.⁶³⁻⁶⁵ Some examples of gaseous PTMs are nitrogen, helium and neon. Different hydrostatic limits have been reported for nitrogen in the literature, varying from approx. 3 GPa,⁶⁴ up to 10 or even 13 GPa, reported by Klotz *et al.*⁶³ and LeSar *et al.*,⁶⁶ respectively, with all being higher than the room temperature freezing pressure of nitrogen

equal approx. 2.4 GPa.⁶⁴ Meanwhile, at 300 K neon and helium solidifies above 4.8 and 12.1 GPa, respectively,⁶³ however, first signs of non-hydrostaticity does not appear up to 15 GPa for neon,⁶³ and good hydrostatic conditions can be maintained in helium up to 30-50 GPa, depending on the studied sample.⁶⁷ As the liquid PTMs, both pure compounds and mixtures are used. Isopropanol, methanol and glycerol, with reported hydrostatic limits of approx. 4.2,⁶⁴ 3.6⁶⁵ and 1.4 GPa,⁶⁴ respectively, are examples of single-component PTMs. Using mixtures of solvents as PTMs can offer an increased hydrostatic limit compared to the pure components (*e.g.* methanol:ethanol:water solution in 16:3:1 vol. ratio can be used up to ca. 10 GPa).⁶⁴ Non-polar liquid PTMs include silicon oil, Fluorinert™ and 7000 series Daphne oils. The silicone oils of 0.65 and 37 cSt viscosity, have hydrostatic limit of approx. 0.9 GPa),⁶⁴ while limits for Fluorinert™ vary depending on its type. For none of the pure Fluorinert™ FC-40, FC-70, FC-72 and FC-75 the hydrostatic properties are preserved above 1.2 GPa,⁶⁸ for FC-77 the limit is 1.5 GPa,⁶⁹ while the 1:1 mixture of FC-84:FC-87 maintain hydrostaticity up to 2.3 GPa.^{63,69} Daphne oil 7373 (mixture of olefin oligomers) solidifies at 2.2 GPa⁷⁰ and Daphne oil 7474 (composed mainly of mixture of 2,2,8,8-tetraalkylsilanes and silicon oils) have hydrostatic limit of 3.7 GPa at room temperature.^{63,71} Notably, the hydrostatic limit of Daphne 7474 can be increased by heating, with the limit reaching 6.5 GPa at 100 °C.⁶³

Compared to the routine single-crystal X-ray diffraction (SCXRD) experiment, the high-pressure SCXRD measurements carry some limitations. One of the issues concern data completeness, as construction of the DAC limits the access of the X-ray radiation to the sample crystal.^{50,72} This is especially notable for low-symmetry crystals. The completeness and quality of collected data can be improved by optimizing the experimental strategy, including:

(i) Orienting the crystal in a specific manner to ensure the highest possible coverage of the reciprocal lattice.⁷³

(ii) Merging of the data collected for several differently oriented crystals mounted in the DAC.⁷¹ Usually requiring use of the synchrotron radiation of a small beam, enabling individual data collection for the selected crystallite.⁴¹

(iii) Use of the radiation of a short wavelength.⁴²

Moreover, X-ray diffraction data, collected with the use of a DAC, need to undergo appropriate data treatment using specialistic software. The intensity of reflections should be corrected for Lorentz–polarization effects, DAC windows absorption and shadowing of the sample crystal by the gasket.⁵⁰

1.2.2 Application of high-pressure techniques in pharmaceutical chemistry

One of the phenomena explored extensively in pharmaceutical industry, is polymorphism and *pseudopolymorphism* of Active Pharmaceutical Ingredients (APIs).⁷⁵ Polymorphs of the same compound (including APIs) can differ in their physicochemical properties,⁷⁶⁻⁷⁸ which in turn can affect their bioavailability, processability and storage.⁷⁸ Some of the properties considered during the selection of an appropriate solid form for the final drug product are the solubility and stability. Moreover, search for new forms of APIs can be important from the intellectual property point of view, as (depending on the region) methods for crystallization of polymorphs and *pseudopolymorphs* can be patented if they meet criteria for patent eligibility (*i.e.* non-obviousness, utility and novelty).⁷⁹

Investigation of polymorphism of APIs focuses not only on finding the forms best suited to be used in a drug product (*i.e.* being stable, soluble, and having high bioavailability), but also to understand the polymorphic landscape of the compound.⁷⁸ During manufacturing and storage, APIs can be exposed to mechanochemical treatment,⁸⁰ as well as varied temperature,⁸¹ pressure⁸² and humidity conditions.⁸³ Therefore, it is advisable to learn about any possible transformations that can occur, as they may unfavourably affect the properties of the final drug product.^{84,85}

In this context the application of high-pressure techniques has dual use. Firstly, it can be used as a means for the discovery of new crystal forms (polymorphs,⁸⁶ *pseudopolymorphs*^{87,88} and co-crystals⁸⁹), and it can be applied for the investigation of the pressure stability of the solid forms of APIs.⁹⁰ The latter is especially important, as APIs can be exposed to non-ambient pressure at several stages of drug processing, such as milling⁸² or compaction.⁹¹ The milling is used to reduce the particle size to improve the dissolution rate by increasing the surface area of solids.⁹² During this step, the material is exposed to stress and as a result phase transitions can occur.⁹³ One of the examples is phenylbutazone, that undergoes phase transition during the grinding, however, this process is strongly temperature dependent.^{94,95} Other cases reported in the literature, concern less stable polymorphs of chloramphenicol palmitate⁹⁶ and famotidine⁹⁷ that have been transformed to more stable phases by grinding. The compaction takes place during the tablet production, when pressure is applied to transform the powder into cohesive compact.⁹⁸ Previous reports has shown that compaction of a number of APIs can lead to transformations in the solid state, such as phase transitions between polymorphs (*e.g.*, caffeine, sulfabenzamide and maprotiline hydrochloride),⁹⁹ desolvation (*e.g.*, N,N-dimethyl acetamide

and N,N-dimethyl formamide solvates of celecoxib)¹⁰⁰ or amorphization and crystal disordering (*e.g.*, theophylline, nitrofurantoin and amlodipine besylate investigated under compaction pressure in 100-1000 MPa range).¹⁰¹

The application of DAC enables study of APIs under high-pressure in a small scale. The first APIs which have been investigated with the use of DAC¹⁰² are acetaminophen, an analgesic, better known as paracetamol,¹⁰³ and phenacetin.¹⁰⁴ The experiments were carried out under pressure of up to 4 GPa and have revealed the anisotropic distortion of the crystal structure of the investigated crystals. In the follow-up study from 2002, two paracetamol polymorphs, monoclinic form I of $P2_1/n$ symmetry and a metastable orthorhombic polymorph (form II, crystallizing in $Pcab$ space group), were investigated under high pressure.¹⁰⁵ It was revealed that despite the differences in their crystal structures (Figure 6), both polymorphs have very similar bulk compressibility, however, they differ in the anisotropy of the structural distortion. In this high-pressure study, the pressure-induced transformations between polymorphs I and II were also investigated, but the results were poorly reproducible and depended on the applied experimental procedure. No phase transition from form I to II was observed for single crystals up to 4 GPa, while a partial, irreversible, conversion was detected for powder sample. The transformation from polymorph II to I was induced by grinding, while hydrostatic compression of the powder of form II led to some structural changes evidenced in the powder X-ray diffraction (PXRD) pattern. However, at that time it was not possible to reliably determine the cause. The subsequent high-pressure studies of paracetamol have led to the discovery of its dihydrate at 1.1 GPa⁸⁷ and 1:1 methanol solvate at 0.62 GPa.⁸⁸

Until today, the large number of APIs such as amino acids,¹⁰⁶⁻¹⁰⁸ ibuprofen,¹⁰⁹ and urea.¹¹⁰⁻¹¹² have been studied under high pressure, using both recrystallization¹⁰⁹ and compression¹⁰⁶⁻¹⁰⁸ protocols. Previous studies were aimed at finding new polymorphic,¹¹³ and *pseudopolymorphic* forms,⁸⁶ investigating the pressure stability of APIs,⁹⁰ or determining the pressure-temperature diagrams.¹¹⁰

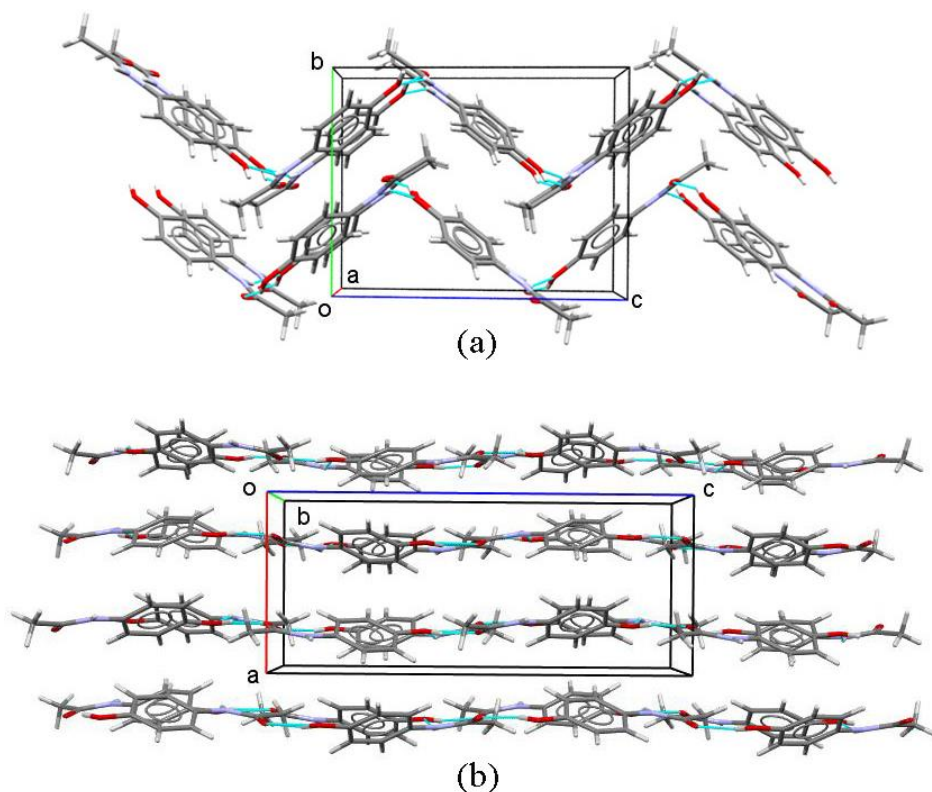


Figure 6. Autostereogram¹¹⁴ of the molecular packing in (a) monoclinic paracetamol (phase I), and (b) orthorhombic paracetamol (phase II), both at ambient conditions, shown along [100] and [010] directions, respectively. The OH...O hydrogen bonds are marked in cyan.

1.2.3 Hydrogen-bonded solids under high pressure

The intermolecular interactions play crucial role in Nature. They regulate many biological processes such as molecular recognition,^{115,116} protein folding¹¹⁷ and transcription of RNA and DNA.¹¹⁸ They govern properties of water—the most ubiquitous substance on Earth,¹¹⁹ and are important from the solid-state physic perspective, as they affect structure¹²⁰ and properties of materials.^{121,122} Among the intermolecular interactions, hydrogen bonds are one of the most important ones.¹²³

Thy hydrogen bond is defined by IUPAC as “(...) *an attractive interaction between a hydrogen atom from a molecule or a molecular fragment X–H in which X is more electronegative than H, and an atom or a group of atoms in the same or a different molecule, in which there is evidence of bond formation*”.¹²⁴ External conditions, such as pressure and temperature, can affect hydrogen bonds in solid state.¹²⁵⁻¹²⁷ Pressure is known to modify the geometry (*e.g.* the bond length and X–H...Y angle)^{128,129} and energy¹³⁰ of hydrogen bonds. Exposure to high pressure can also lead to formation or breaking of the H-bonds (for example during pressure-induced phase transitions).^{131,74} Moreover, hydrogen bonds can become

disordered¹³² under pressure. A number of reports on the effects of pressure on hydrogen bonding pattern can be found in the literature.¹³³ One of the examples is the high-pressure study of carbohydrates, which crystals are governed by O–H···O hydrogen bonds. It was observed for (+)-sucrose,⁷⁴ α -D-glucose¹³⁴ and β -D-mannose,¹³⁵ that changes in molecular orientation during pressure-induced phase transitions are accompanied by the significant rearrangement of the O–H···O H-bonding patterns, in some cases leading to lowering the number of such hydrogen bonds in high-pressure phase.¹³⁴ Moreover, the number of weak hydrogen bonds, C–H···O, increases and they become shorter with pressure, showing their increased role in supporting the crystal structure.

Another example of a study of crystalline material governed by hydrogen bonds under pressure is investigation of urea crystals, for which first compressibility measurements were performed already in 1916 by Bridgman.¹¹⁰ It was reported that the ambient-conditions tetragonal phase I (space group $P\bar{4}2_1m$) transforms into orthorhombic phase III (space group $P2_12_12_1$) at 0.48 GPa, and another transformation occurs at 2.8 GPa, when form III undergoes phase transition to phase IV (space group $P2_12_12_1$).¹¹² The most significant change in the hydrogen bonding pattern accompany the I-to-III phase transition, when one of the hydrogen bonds is broken and dimensions of others change drastically. As a result, the oxygen atom of the carbonyl group is bonded only to two neighbouring urea molecules via three N–H···O hydrogen bonds, instead of being fourfold coordinated to three molecules (Figure 7).¹¹² Interestingly, the second phase transition to phase IV leads to restoring H-bonding pattern alike the one observed at ambient conditions, with carbonyl oxygen being involved in four hydrogen bonds of the dimensions similar to those observed in phase I (Figure 7).¹¹²

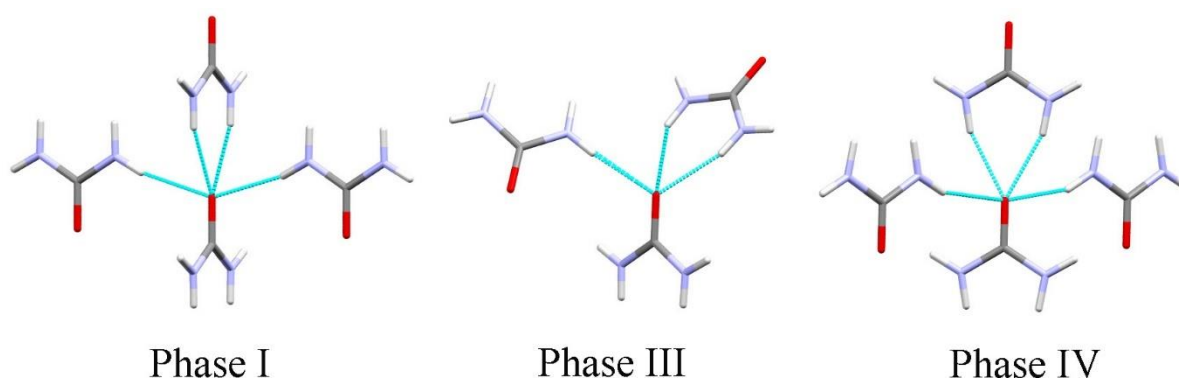


Figure 7. Coordination of the carbonyl oxygen in urea phases I, III and IV. The hydrogen bonds are indicated by the dashed cyan lines.

1.3 Scope of the thesis

The aim of the Ph.D. thesis was to investigate the behaviour of resorcinol crystals under extreme pressure, and to test a method for the recovery of high-pressure polymorphs at ambient conditions (one of the main challenges of high-pressure research). My original contribution to knowledge includes discovery of new polymorph and *pseudopolymorphs* of resorcinol, improvement of the understanding of the pressure-induced phase transitions of resorcinol and providing new information on pressure stability of novel and previously reported crystal forms of this compound. Moreover, I successfully crystallized high-pressure polymorphs of imidazole and its derivatives at ambient conditions using concept of the doping pressure.

For the study of polymorphism and *pseudopolymorphism* of resorcinol, a series of high-pressure experiments with the use of the DAC was performed, including isochoric and isothermal recrystallizations. This research led to several discoveries concerning resorcinol crystals:

- (i) It was shown that polymorphs α and β can be compressed up to 4.0 GPa with no signs of phase transitions.
- (ii) The structural features of polymorph α of resorcinol destabilizing it at high pressure were identified.
- (iii) The differences in conformation and H-bonding patterns of polymorphs α and β were analysed.
- (iv) Polymorph ϵ was crystallized under high pressure and its pressure stability was assessed.
- (v) New high-pressure polymorph ζ was discovered and its structure was determined.
- (vi) Three novel solvates of resorcinol: a monomethanol, monohydrate and duotrihydrate, were crystallized under pressure. Their crystal structures were solved and experimental conditions leading to their formation were established.

New crystal forms of resorcinol crystallized in this study were analysed in terms of packing, H-bonding patterns and molecular conformation.

For the recovery of high-pressure polymorphs, a concept of doping pressure was tested for resorcinol, and several chemical compounds known to have high-pressure polymorphs: imidazole, benzimidazole, and 2-methylbenzimidazole. While milling of studied compounds with dopants in variable weight ratios did not lead to obtaining high-pressure polymorphs at ambient conditions, mixing followed by melting and cooling led to following results:

- (i) The ϵ polymorph of resorcinol, concomitant with form β was obtained in different ratios when D-, L-, and DL-tartaric acid (in 15 wt % ratio), 2-methylbenzimidazole (in 15 and 25 wt % ratios), and 5,6-dimethylbenzimidazole (in 25 wt % ratio) were used as dopants. The highest amount of ϵ polymorph (90%) was obtained for DL-tartaric acid, and smallest (23%) for 2-methylbenzimidazole (at 15 wt % ratio).
- (ii) For imidazole, the high-pressure form β concomitant with ambient-conditions phase α , was obtained when benzimidazole and 2-methylimidazole (both at 25 wt % ratio) were used as dopants.
- (iii) The high-pressure polymorph β of benzimidazole, was obtained in 100% yield when 2-methylbenzimidazole in 5 wt % ratio was used as a dopant. Meanwhile, the use of 2-methylbenzimidazole and 5,6-dimethylbenzimidazole in 15 wt % ratio led to crystallization of form β and ambient-conditions form α , however, the ratio of high-pressure polymorph was high, *i.e.* 95 and 87%, respectively.
- (iv) Experiments with 2-methylbenzimidazole, led to successful crystallization of high-pressure β form when 5,6-dimethylbenzimidazole in 15 and 25 wt % ratios were used as dopant. The resultant samples contained small amounts of the ambient-conditions polymorph α (*i.e.* 23 and 18%, respectively).

The results presented in the Ph.D. thesis have been published in a series of three papers (labelled R1-R3, included in Appendix D), and are discussed in detail in the *Results* section. The findings presented in the thesis, and enclosed publications, not only provide new information about crystal forms of resorcinol, an important organic compound of various applications, but also allow to better understand the relationship between its polymorphs and *pseudopolymorphs* under high-pressure conditions. I have also shown that the doping pressure concept can be employed for recovery of high-pressure polymorphs at ambient conditions for a series of selected chemical compounds, with the success rate strongly dependant on the dopant and its ratio.

1.4 List of articles prepared within this thesis

(R1)

F. Safari, A. Olejniczak, A. Katrusiak,

Pressure-Dependent Crystallization Preference of Resorcinol Polymorphs,
Cryst. Growth Des. **2019**, *19*, 5629–5635.

DOI: 10.1021/acs.cgd.9b00610

(R2)

F. Safari, A. Olejniczak, A. Katrusiak.

Pressure-Promoted Solvation of Resorcinol.
Cryst. Growth Des. **2020**, *20*, 3112–3118.

DOI: 10.1021/acs.cgd.9b01732

(R3)

F. Safari, A. Katrusiak.

High-Pressure Polymorphs Nucleated and Stabilized by Rational Doping under Ambient Conditions.

J. Phys. Chem. C **2021**, *42*, 23501–23509.

DOI: 10.1021/acs.jpcc.1c07297

1.5 Note on references to figures and tables

When figures and tables included in the enclosed manuscripts are referenced, they are preceded by the label assigned to the publication (*i.e.* R1, R2 or R3). For example, Figure 1 from paper R1 is referenced as Figure R1-1.

2 Experimental methods

2.1 Sample preparation for high-pressure X-ray diffraction experiments

In this thesis, for all high-pressure experiments, a modified Merrill-Bassett DAC, with brilliant cut diamonds of 680 μm culet diameter, mounted on steel discs, and enabling reaching pressure of up to 10 GPa, was used. Two types of experiments were performed: (i) isochoric recrystallization under pressure and (ii) isothermal compression. The DAC preparation before the sample loading was the same for both methods. A steel gasket (200 μm thick), with an opening of approx. 350 μm in diameter, was placed on the lower diamond anvil and its position was secured with the modelling clay. Gasket was then centred, ensuring central position of the opening in respect to the diamond culets, and was pre-indented by slightly squeezing it in the DAC. In the next step, several tiny ruby chips used for pressure measurement, were placed in the opening of the gasket.

For the isochoric method, DAC was loaded with either solution of studied compound (in various concentrations), or several crystals obtained at ambient conditions covered with the saturated solution (acting also as a PTM). After achieving the desirable pressure, the single crystals suitable for X-ray diffraction experiments were obtained by dissolving the sample by heating and subsequent cooling of the DAC. For the experiments where only solution was loaded in the DAC, the recrystallization stage had to be preceded by crystallization of the sample by increasing the pressure. In isothermal method, two approaches were applied. In the first one, a single crystal of sufficient quality and size obtained at ambient conditions was loaded in the DAC alongside cotton fibre (used to prevent the sample crystal movement during the experiment). It was then covered with saturated PTM, and crystal was isothermally compressed. Alternatively, single crystal was obtained *in situ* in DAC via isochoric recrystallization, by heating and cooling, and then compressed isothermally. In the second approach, the DAC was loaded with water, methanol, MeOH:H₂O (in 4:1 vol. ratio) or MeOH:EtOH:H₂O (in 16:3:1 vol. ratio) solutions of studied compound in various concentrations, and then crystallization was induced by the pressure increase. As a result, several crystals or polycrystalline mass were obtained and then recrystallized as one single crystal by oscillating the pressure.

2.2 Pressure calibration

The pressure inside the DAC was measured with ruby fluorescence method,^{136,137} based on the shift of R1 line. The measurement was performed with BETSA PRL microscope equipped in Photon Control spectrophotometer affording the accuracy of 0.02 GPa (Figure 8a). The online pressure calculator provided by Kantor¹³⁸ was used to calculate the pressure using the pressure dependence of the ruby shift established by Dewaele *et al.*¹³⁹

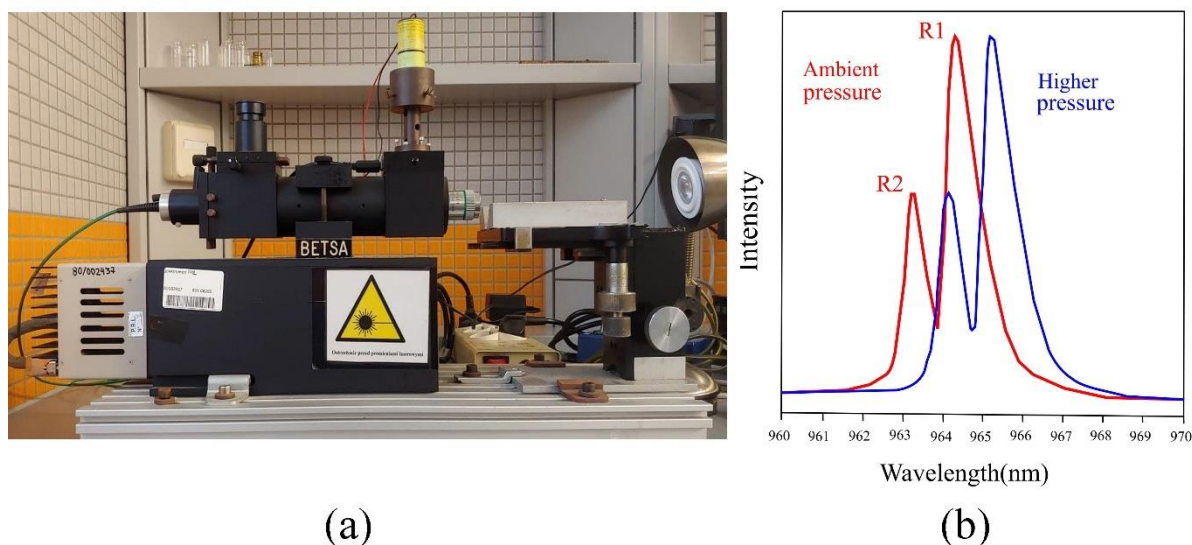


Figure 8. (a) BETSA PRL microscope with Photon Control spectrophotometer, and (b) ruby fluorescence spectra for ambient and high pressure, shown as red and blue lines, respectively.

2.3 Recovery of high-pressure polymorphs to ambient conditions

In order to reproduce the high-pressure polymorphs of selected chemical compounds at ambient conditions, a rational doping by compounds with molecules larger than those of the host was performed. Resorcinol, imidazole, benzimidazole, and 2-methylbenzimidazole were selected as the host compounds, while L-, D- and DL-tartaric acid, as well as 2-methylbenzimidazole, and 5,6-dimethylbenzimidazole were used as dopants. Two approaches were applied for the experiments. In the first approach, ambient pressure phases of the host were mixed with the dopants at 5, 15 and 25 wt % ratios by grinding, and then recrystallized by melting and subsequent freezing of the mixture (following the procedure previously reported by Zhu *et al.*²⁵ for the mixture of α -resorcinol and tartaric acid). Both, mixtures and reference samples, were melted on the thermal stage mounted on the microscope and then left

for cooling to allow crystallization. In the second approach, 4.1 mg of the ambient-pressure polymorphs of host compounds were milled with the dopants at 5, 10, 15, 20, and 25 wt % ratios, using an MM 400 mill equipped in steel containers (Figure 9). The milling was performed for 4h, using several steel balls and frequency of 30 Hz. Samples obtained with both approaches, were then investigated with powder X-ray diffraction (PXRD) methods, and qualitative and quantitative analysis of PXRD patterns was performed to establish their polymorphic composition.

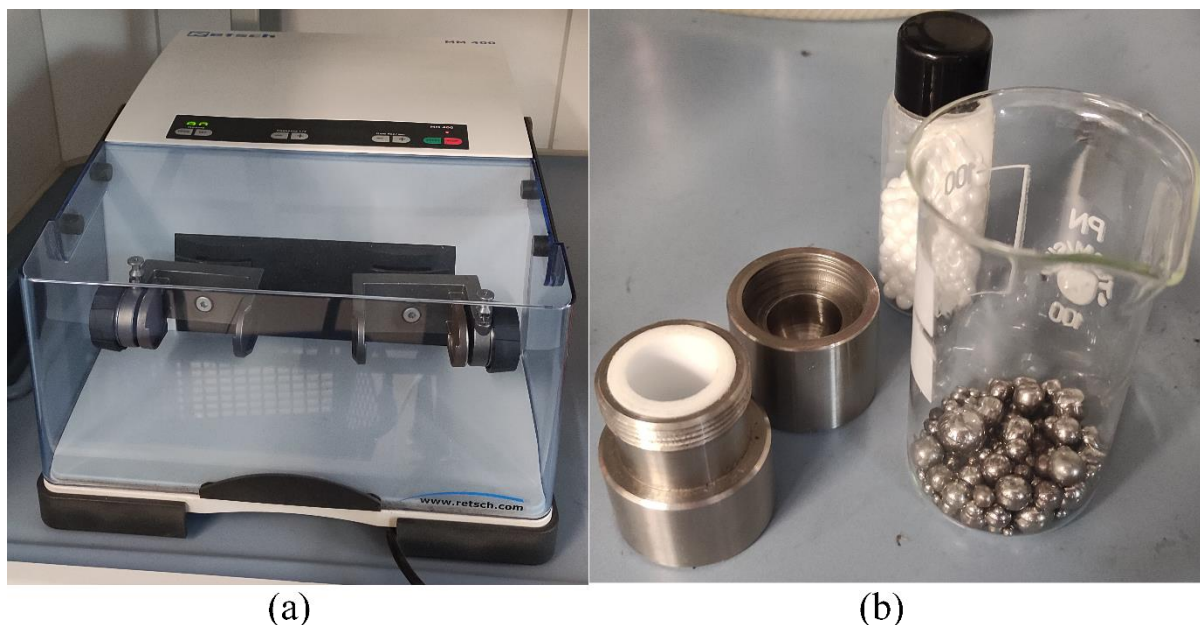


Figure 9. (a) The mixer Mill MM 400 and (b) steel container alongside agate and steel balls placed in two beakers.

2.4 X-ray diffraction experiments

2.4.1 High-pressure single crystal X-ray diffraction measurements

High-pressure X-ray diffraction experiments were performed with four-circle KUMA KM4 CCD diffractometer, with $\text{MoK}\alpha$ radiation source ($\lambda = 0.71073 \text{ \AA}$). The diffractometer setup was prepared according to the requirements of the high-pressure experiments *i.e.* the beam stop position, and collimator were adjusted in order to ensure sufficient space for the DAC. The DAC was centred using gasket shadowing method.¹⁴⁰ A specially prepared run list was used for all experiments, to ensure collection of as complete data as possible.

2.4.2 Powder X-ray diffraction measurements

For the powder X-ray diffraction (PXRD) measurements a Bruker D8 diffractometer operating in the θ - 2θ geometry and equipped in a Johansson monochromator, λ ($\text{CuK}\alpha_1$) = 1.54060 Å radiation, and a LynxEye silicon-strip detector, was used.

2.5 Data reduction, structure solution and refinement

CrysAlis Pro¹⁴¹ software was used for single-crystal X-ray data collection, the UB-matrix determination, absorption correction and data integration. The structures were solved by direct methods using ShelXS¹⁴² and refined using least-squares method with ShelXL¹⁴³ (both implemented in OLEX2¹⁴⁴ program). Hydrogen atoms were localized at idealized positions based on the molecular geometry and were assigned isotropic thermal parameters depending on the equivalent displacement parameters of their carriers ($1.2U_{\text{eq}}$ and $1.5U_{\text{eq}}$ for the C- and O-atoms, respectively). For the refinement of the rotating hydroxyl groups, instruction AFIX 147 was applied for the hydrogen atoms, to allow changes in the C-C-O-H torsion angle. Where appropriate and necessary, RIGU and ISOR restraints were used, and C-C and C-O bond lengths were restrained to 1.54 and 1.43 Å, respectively, using DFIX instruction. The O-H bond lengths of hydroxyl groups were set at 0.82 Å, and C-H bonds at 0.97 Å and 0.98 Å for methylene and methine groups, respectively.

3 Results and discussion

Polymorphism of organic compounds was discovered in 1832 by Wöhler and Liebig for benzamide.¹⁴⁵ The discovery of polymorphism of resorcinol by Robertson in 1936 and the subsequent determination of the structures of polymorphs α and β ^{16,17} can be classified to these cases of scientific results, which provide a plentiful of new information, but at the same time these results generate even more new questions. It is important that the structural determinations of resorcinol polymorphs were the first ones in the history of the research on polymorphism of organic compounds. Hence the expectations were high for the elucidation of the structural background behind the occurrence of polymorphs in general. Meanwhile, it was established that both α - and β -resorcinol despite the same orthorhombic space group type $Pna2_1$ have quite different structures. In the 1930s, crystallographers and even organic chemists were experts in deriving the class symmetry from crystal morphology habits. So, they knew then that generally the symmetry of polymorphs is in most cases different. However, the case of resorcinol determined that the space-group type can be the same – to my knowledge at these times no other such evidence of identical space groups for polymorphs were known. Another intriguing information about resorcinol revealed by Robertson and Ubbelohde in the 1930s was that the conformation of molecules in polymorphs α and β was different, *anti-anti* and *anti-syn* respectively. In fact, term 'conformational polymorphs' was pinned much later by Bernstein and Hagler for 2,2,4,4',6,6'-hexanitroazobenzene.¹⁴⁶ However, it was resorcinol that showed for the first time that molecules can assume different conformations in crystals. That result also indicated that molecular conformation can be flexible in crystals. In the other words, it showed that the conformer of lowest energy is not necessarily stabilized in the crystal structure. Another counterintuitive finding connected to resorcinol was that the density of low-temperature phase α is lower than the density of high-temperature phase β . Presently one can regard this result as the indication of the anomalous properties of the structures where the cohesion forces are dominated by directional forces, such as O–H \cdots O hydrogen bonds or an indication about the possible kinetic polymorph. The clearly defined transition from resorcinol α to β at 360 K on heating, with the hysteresis exceeding 100 K on cooling, strongly supported the approach that these are thermodynamic phases of resorcinol. Thus, the polymorphs of resorcinol for years were the flag examples of the polymorphism of molecular crystals on one hand, while on the other hand this compound was avoided in the discussion of polymorphs due

to its exemption from typical behaviours associated with most of polymorphs. This incited further structural studies of resorcinol polymorphs, including one of pioneering neutron diffraction measurements.¹⁸ Also other methods were employed for investigating the polymorphism of resorcinol, mainly spectroscopic and theoretical studies.^{19-21,24} In 2011, Kichanov *et al.*¹⁹ reported a systematic series of high-pressure X-ray and neutron diffraction as well as NMR solid-state spectroscopy studies on resorcinol polymorphs α and β . The NMR study revealed the α -to- β transition at about 0.5 GPa at 300 K.¹⁹ However, in the X-ray and neutron-diffraction experiments, the powder sample of polymorph β could be compressed to 5.6 GPa then it transformed to a phase labelled γ . Its space-group symmetry was assigned as *Pnna*, but the structure was not solved. The compression of phase γ starts transition to amorphous phase about 10.5 GPa.¹⁹ Meanwhile, Raman spectroscopy has revealed a phase transition from β to a new phase δ at 2.5 GPa. However, the space group symmetry nor the structure of phase δ were not reported.²⁴ Thus the NMR-spectroscopy and neutron diffraction results were significantly inconsistent. The former demonstrated the transition of phase α to phase β at 0.5 GPa, and the latter showed an exceptional stability of both phase α and β up to 4 GPa.

In 2016, Zhu *et al.*²⁵ announced the discovery of a new ambient-pressure resorcinol phase ε . Its structure was solved basing on the X-ray powder diffraction measurements and structure-prediction calculations. The space-group symmetry of the ε -phase is *P2₁2₁2₁*. Phase ε was obtained by freezing the molten mixture of resorcinol with tartaric acid. In fact, all the samples obtained in this way were the mixtures of β - and ε -resorcinol with tartaric acid in different ratios. Most importantly, no pure ε -resorcinol (*i.e.* without the presence of β -resorcinol) were obtained.

A significant information about ε -resorcinol was its structure. It was puzzling to us, particularly in the context of ‘reverse’ density higher for the high-temperature phase β . The density of ε -resorcinol was higher than those of phases α and β . This information motivated us to undertake further experiments on resorcinol. We have reported our results in three papers dedicated to this fascinating compound. These results are described in the following five sections below.

3.1 Transformation between resorcinol phases α and β

It appeared quite natural, according to the wide literature on resorcinol, that under high pressure the low-density phase α would transform to the high-density phase β . However, our experiments did not reproduce this expected scenario, in accordance to the neutron-diffraction results reported by Kichanov *et al.*¹⁹ and contrary to their own NMR-spectroscopy results.¹⁹ solid-state NMR study of resorcinol α showed its transformation to resorcinol β at about 0.5 GPa. In our single crystal X-ray diffraction study on resorcinol α , we assumed that the persistence of phase α can be connected to the different networks of O–H \cdots O hydrogen bonds, and this network of polymorphs α , without sufficient activation, can be over pressurized into the stability region of polymorph β (Figure R1-2). It should be noted that the sites of all hydroxyl H atoms in polymorph α are coupled and the H-site change in any one of the hydrogen bonds from O–H \cdots O to O \cdots H–O would trigger the analogous changes of all H-sites in the structure.

Hydrogen bonds between hydroxyl groups can be considered as bistable H-bonds, similarly as those in H₂O ice I_h. However, in ice I_h the O \cdots O \cdots O angles are close to the ideal tetrahedral angle of 109.3°, so both sites of the H atom, O–H \cdots O and O \cdots H–O, are equally likely.¹⁴⁷ It was shown for orthoboric acid H₃BO₃ that the H sites are coupled to the molecular orientation and that on the H-donor site the B–O \cdots O' angle is significantly smaller than the O \cdots O'–B' angle on the H-acceptor site of the H-bond.^{148,149} Therefore, the stability of H-bonded network depends both on the H-sites in the O–H \cdots O hydrogen bonds and on the molecular orientations. The molecular orientations can be strongly changed by high pressure, and we have analysed the changes of the H-bonds dimensions in polymorph α as a function of pressure.

Resorcinol molecules are in the *anti–anti* configuration in polymorph α ($Z'=1$) and there are two independent hydrogen bonds: O1–H \cdots O3 and O3–H \cdots O1. Consequently, in all the H-bonds the hydroxyl H-atoms is in the *anti*-position. We observed that at ambient conditions angles C1–O1_{anti} \cdots O3'_{syn} and C3–O3_{anti} \cdots O1''_{syn} are approximately equal to 115°, and as expected angles O1_{anti} \cdots O3'_{syn}–C3' and O3_{anti} \cdots O1''_{syn}–C1'' are larger, of 132.5° and 117.4°, respectively (Figure R1-8). Our high-pressure structural determinations have shown that angles C \cdots O_{anti}–O'_{syn} hardly depend on pressure and at 2.5 GPa they are reduced by about mere 0.3°. In contrast, the pressure dependence of angles O1_{anti} \cdots O3'_{syn}–C3' and O3_{anti} \cdots O1'_{syn}–C1' is much stronger and at 2.5 GPa they are reduced by over 12° and over 6°, respectively. This strong reduction ‘inverts’ the C–O3_{anti} \cdots O1'_{syn} and O3_{anti} \cdots O1'_{syn}–C1' angles, as at about

0.3 GPa the latter angle becomes smaller than the first one. Thus, for this specific bond O3–H3···O1 high pressure above 0.3 GPa destabilizes the H atoms, however the whole H-bonded network is stabilized by the other H-bond O1–H1···O3', for which the angular dimensions continue to stabilize the H1 site.

It should be noted that while the destabilizing effect of angular dimensions of bond O3–H···O1' increases with pressure above 0.3 GPa, the stabilizing effect of bond O1–H1···O3' decreases (Figure R1-8) and at 2.5 GPa the destabilizing difference (between angles C3–O3_{anti}···O1_{syn} and O3_{anti}···O1'_{syn}–C1', of about 5°) approaches the stabilizing difference (between angles C1–O1_{anti}···O3'_{syn} and O1_{anti}···O3'_{syn}–C3_{anti}, of about 6°). These structural dimensions clearly indicate that the structure aims at a transformation.

At the same time the higher pressure increases the work contribution to Gibb's energy, $p\Delta V$, where ΔV is the volume difference $V_\alpha - V_\beta$ of polymorphs α and β , respectively. It remains favourable for polymorph β in all pressure range investigated, to 2.5 GPa at least (Figure R1-6). Another aspect of the pressure-induced changes is that their derivatives $\delta(\text{angles})/\delta p$ and $\delta V/\delta p$ (also $\delta\Delta V/\delta p$) diminish with pressure. It indicates that the hysteresis of this strongly first-order phase transition can extend to several GPa. Indeed, for ideal resorcinol α single crystals they could be compressed to 2.5 GPa with no signs of deterioration of their quality (Figure R1-3). On the other hand, the fine powder prepared for the solid-state NMR studies could be composed of tiny grains defected on grinding, and these defects could facilitate the transition to phase β about 0.5 GPa. In order to avoid the effect of the sample preparation and handling, in my further studies I have chosen the method of *in situ* recrystallization of resorcinol under pressure, which led to new surprising results described in articles R2 and R3. With regard to the same space-group symmetry type of polymorphs and, I have found no apparent structural relations between differently arranged molecules in different conformations and differently H-bonded into different patterns (Figure R1-5).

3.2 New solvates of resorcinol

Our plan to investigate the stability regions of resorcinol phases by the method of *in situ* recrystallizations, as described at the end of subsection 3.1, was initially hampered by the formation of hydrates. Although we were primarily interested in the polymorphs of pure resorcinol, the discovery of so-far unknown hydrates of such a thoroughly studied compound

was interesting by itself and we attempted to understand the reason for their high-pressure stabilization.

Formation of solvates can be advantageous in pharmaceutical and agriculture industries because the solvation of bioactive compounds can improve their properties, such as solubility and bioaccessibility. There are many organic compounds which preferably form anhydrate from aqueous solutions and resorcinol behaves in this way at normal conditions. Presently, there are 121 multicomponent structures of resorcinol with different compounds deposited in the Cambridge Structure Database (version 1.23), but none of them is a hydrate. Therefore, the *in situ* recrystallizations of resorcinol from the aqueous and methanol solutions under high pressure appeared as a very interesting subject by itself. It is known from the literature that the high-pressure conditions promote the formation of solvates. For example, the high-pressure recrystallization of thiourea yields its monohydrate between 0.5 GPa and 0.7 GPa and duotritohydrate between 0.7 and 1.0 GPa, which were unknown at ambient conditions.¹⁵⁰ Similar preference to form hydrates was observed for selenourea.¹⁵¹

According to our experiments, the monohydrate of resorcinol, space group $P2_12_12_1$, can be obtained by isothermal crystallization method at 0.80 GPa. However, after increasing pressure to 0.93 GPa and after several hours, the thin layer of tiny crystals of resorcinol duotritohydrate, $3C_6H_4(OH)_2 \cdot 2H_2O$, space group $C2/c$ (Figure R2-2, Figure 10) covered the surface of the monohydrate crystal. This was a very strange result, because in most of our *in situ* crystallizations the obtained crystals had clear faces, like those of initially obtained resorcinol monohydrate. But a slight increase of pressure produced a ‘frosted’ layer on its surface. After several attempt to confirm these results, we observed that the monohydrate crystals are metastable with respect to the duotritohydrate and when the ‘passivation’ layer of $3Res \cdot 2H_2O$ crystals is formed, it protects the monohydrate from dissolution (Figure R2-2). This passivation layer can be easily dissolved by gentle heating and then single crystals of duotritohydrate grow at the cost of dissolving monohydrate crystals. To our knowledge this is the first description of such a passivation layer in organic compounds.

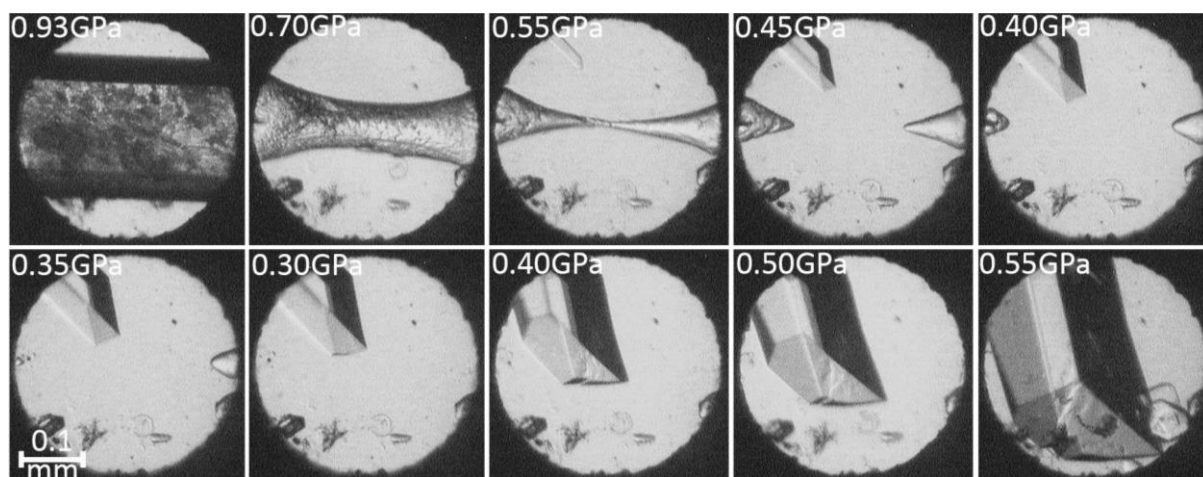


Figure 10. Isothermally crystallized monohydrate $C_6H_4(OH)_2 \cdot H_2O$ at 297 K up to 0.80 GPa and then covered by tiny crystals of duotritohydrate $3C_6H_4(OH)_2 \cdot 2H_2O$ at 0.93 GPa. Then, after releasing pressure to 0.7 GPa the monohydrate starts to dissolve while the single crystal of duotritohydrate grows. A ruby chip for the pressure calibration lies at the top-left quadrant of the DAC chamber.

In the crystal structure of $Res \cdot H_2O$, water molecules are surrounded by resorcinol molecules by forming hydrogen bonds to four hydroxyl groups (Figure 11). In the monohydrate structure all the hydrogen bonds bind water and resorcinol molecules, while no water \cdots water or resorcinol \cdots resorcinol bonds are present (Figures R2-5 and R2-6).

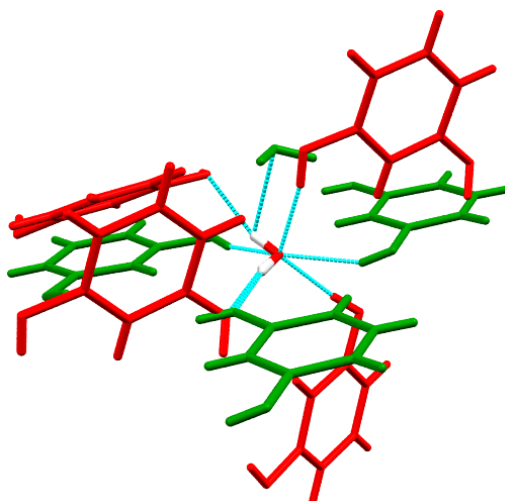


Figure 11. H-Bonded neighbors around the exactly superimposed central molecule of water in $Res \cdot H_2O$ (red) and in $3Res \cdot 2H_2O$ (green). H-Bonds are indicated in cyan.

The crystal structure of $3Res \cdot 2H_2O$ strongly differ from the monohydrate, as it can be seen in Figure R2-6. In $3Res \cdot 2H_2O$, there are two independent molecules of resorcinol ($Z'=1+1/2$)

which are labelled A (conformer *syn-syn* located in general position) and B (disordered conformer *anti-anti* located on an inversion centre). The water molecule lies in a general position. Contrary to the monohydrate structure, there is one $\text{H}_2\text{O}\cdots\text{H}_2\text{O}$ hydrogen bond besides three hydrogen bonds to resorcinol molecules A; in addition, molecule A is H-bonded to one molecule B which in turn is H-bonded to another molecule A. The H-bonding pattern is shown in Figure R2-6 (*cf.* Table R2-S3).

Several different types of disorder in resorcinol molecules were reported. For example, in hexamine¹⁵² and bis(5-ferrocenylpyrimidine)¹⁵³ co-crystallized with resorcinol, disordered molecules are in *anti-anti* configuration while in co-crystal with N-phthaloyl glycine¹⁵⁴ the *syn-syn* conformer is present. In the $3\text{Res}\cdot 2\text{H}_2\text{O}$ structure the benzene ring with its half-occupied sites of hydroxyl group shows the disorder.

In order to find possible reasons of metastability of resorcinol monohydrate in the presence of duotritohydrate, we compared the hydrogen-bonding networks in both these structures. One of the $\text{O}-\text{H}\cdots\text{O}$ bonds in the monohydrate is much longer, of nearly 3 Å (Figure R2-8), than other hydrogen bonds in these hydrates and in pure resorcinol (between 2.65 and 2.85 Å). It appears that in the monohydrate a steric hindrance interferes with the formation of one of the H-bonds which destabilizes the $\text{Res}\cdot\text{H}_2\text{O}$ structure. In the presence of nucleated $3\text{Res}\cdot 2\text{H}_2\text{O}$, the resorcinol and water molecules are capable of more efficient crystal packing. The calculation of the energy of cohesion forces in resorcinol polymorphs α and β as well as in monohydrate and duotritohydrate is consistent with the observed experimental observations that at normal conditions resorcinol α is obtained. The monohydrate is less stable, but it is obtained in accordance with the Oswald rule of stages. Above about 0.2 GPa the duotritohydrate becomes most favoured and its rapid precipitation on the surface of the monohydrate preserves this crystal from dissolving. When this passivation layer is dissolved the unprotected monohydrate crystal is dissolved too, while the $3\text{Res}\cdot 2\text{H}_2\text{O}$ crystal grows. These experimental and theoretical calculations are schematically illustrated in Figure R2-10.

I performed also other high-pressure crystallizations aimed at obtaining other new solvates of resorcinol. The isochoric recrystallization from the methanol solution yielded above 0.4 GPa the methanol solvates, $\text{Res}\cdot\text{CH}_3\text{OH}$. It is isostructural with resorcinol monohydrate (*cf.* Table R2-1 and Figures R2-5 and R2-7). The structural determinations at 0.49 GPa and 0.70 GPa revealed that the crystal is built of resorcinol and methanol molecules H-bonded into ribbons propagating along [010].

The molecular volume is an important factor for the stability of crystals under high pressure. As shown in Figure R2-9, the molecular volumes of both hydrates of resorcinol and of the methanol solvate Res·CH₃OH are somewhat smaller than the sums of volumes of the stoichiometric amounts of pure resorcinol polymorph β (stable in the investigated range of pressure), added to the volume of solvent molecules under the appropriate pressure (Figure R2-10).¹⁵⁵ These calculations show that the system of resorcinol and solvent molecules assume the lowest volume under pressure.

3.3 Pure high-pressure polymorphs of resorcinol

While the puzzling features of resorcinol polymorphs α and β remained unsolved, new phases δ and γ were found under high pressure,^{19,24} but their structures were not solved. Soon later, Kahr's group²⁵ reported the structure of a new polymorph ε . It was obtained by freezing the molten mixture of resorcinol with tartaric acid. The discovery of polymorph ε could not be reconciled with the phase diagram postulated for pure resorcinol (article R1), where only two phases were indicated up to 1 GPa. Therefore, we have undertaken the systematic search by isothermal and isochoric recrystallizations from different solutions of different concentrations. The solvate crystals obtained in this way were described above in chapter 3.2 and in article R2. The recrystallization from different solutions under pressure up to 1.0 GPa yielded resorcinol polymorphs α , β , ε and ζ , as well as the solvates discussed in section 3.3 (Table 2).

Table 2. Conditions of *in situ* high-pressure recrystallizations of resorcinol polymorphs and solvates performed within my project and those reported in the literature.

Initial form, concentration of solution % *	Crystallization type, <i>p/T</i> range	Time required (h)	Obtained polymorph	Morphology	Reference number
1. Saturated in H ₂ O (58%) in MeOH (60%) or EtOH (60%) 2. Pure α -Res 3. Pure α -Res	1. Evaporation 0.1 MPa 2. Isothermal compression 0.1 MPa-0.5 GPa, 300 K 3. Isothermal compression, 0.1 MPa-4 GPa, 300 K	1. 2 h	α	Plates	16,17,19,R1
1. Saturated in H ₂ O (58%) in MeOH (60%) or EtOH (60%) at 363K 2. Pure α -Res	1. Crystallization of polymorph α at 0.1MPa/363K 2. Isothermal compression 0.5GPa/363K	1. 1 h 2. 2 h	β	Plates	17,23
Pure β -Res	Isothermal compression of polymorph β , 5.6GPa/296K	N/A	γ	N/A	19
Pure β -Res	Isothermal compression of polymorph β at 2.5GPa	N/A	δ	N/A	24
1. H ₂ O: MeOH (1:1 vol.) solution 30% 2. H ₂ O solution 25%	1. Isochoric, 0.56GPa/ 373-296K, 2. Isothermal, 0.2 GPa/296 K	1. 2 h 2. 1.5 h	ϵ	Needles	R3
H ₂ O: MeOH: EtOH (1:16:3 vol.) solution 45%-55%	Isochoric, 0.70 GPa/ 490-296 K	3 h	ζ	Needles	R3
H ₂ O solution \approx 50%	Isothermal, 0.8 -0.93 GPa/296 K	1.5 h	Res·H ₂ O	Plates	R2
H ₂ O solution \approx 50%	Isothermal, 0.55-0.93 GPa/296 K	5.5 h	3Res·2H ₂ O	Prisms	R2
MeOH solution \approx 50% \approx 30%	Isochoric, 0.49 GPa/3 63-296 K, Isothermal 0.7 GPa/296 K	2 h	Res·CH ₃ OH	Plates	R2

*Concentration of resorcinol in the solution is $M_{\text{res}}/M_{\text{solution}}$, estimated from the size of the resorcinol crystal and volume of the DAC chamber filled with the solvate.

We tried to find the effect of concentration of resorcinol, temperature, pressure and different solvent (methanol, ethanol, water and their various mixtures) on the polymorph/solvate nucleation. Isothermal and isochoric crystallizations were performed to obtain high-quality single crystals suitable for X-ray diffraction studies; moreover, we investigated the stability of the obtained crystal forms by observing their decompression through a microscope. All the *in situ* recrystallizations described above, allowed us to repetitively obtain any of four polymorphs α , β , ε and ζ of pure resorcinol in the pressure region up to 1.20 GPa (Table R3-1).

We obtained the high-quality single crystals of polymorph ε by both isochoric and isothermal method between 0.20 and 0.70 GPa (Figures R3-S1, R3-S2). However, all our efforts to recover the single crystal of polymorph ε to ambient conditions failed. We observed that polymorph ε crystals crushed into small pieces below 0.20 GPa due to the strain induced by the first-order phase transition to polymorph α , according to all PXRD study on the sample kept below 0.20 GPa in the DAC and for the powder recovered to ambient conditions. This our systematic observation that polymorph ε is unstable below 0.2 GPa contrasted with the discovery of polymorph ε by Zhu *et al.*²⁵ who performed their experiments at ambient pressure. The polymorph ε was obtained from 50:50 methanol:water solution, thus the single crystals of polymorph ε could be compressed to about 1 GPa when water freezes off. Indeed, the crystals crushed at higher pressure, but the *in situ* PXRD measurements confirmed that the tiny fragment are still in the ε phase (Figures R3-S1, R3-S2).

All our recrystallizations from the resorcinol solution in the H₂O:MeOH:EtOH (1:16:3 vol.) mixture above 0.70 GPa led to the formation of a new polymorph ζ (Figure R3-S3). It indicates that polymorph ε is stable from 0.20 up to 0.70 GPa and that polymorph ζ is the stable phase under still higher pressure.

This result is consistent with the molecular volume of polymorph ε , smaller than those of polymorphs α and β up to 1.0 GPa (Table R3-1, Figure R3-3). Polymorph ζ is still denser than polymorph ε above 0.70 GPa, which agree with recrystallization above 0.7 GPa. The microscopic observations and SCXRD/PXRD results are illustrated in Figures R3-3, R3-S4.

The Gibbs free energy and p - T phase diagram outlined by us, which have been based on our recrystallization experiments, when confronted with other experimental reports on the compression of polymorphs α and β to 5.6 GPa with no sign of transformation,^{19,24} show that the O–H···O hydrogen bonding networks in these crystals strongly stabilize the polymorphs (Figure 12). In this respect, when taking into account such a wide pressure hysteresis of several

GPa, our study agrees with the previous studies on polymorphs α and β . However, the instability of our polymorph ε samples at 0.2 GPa clearly required a further investigation and explanation.

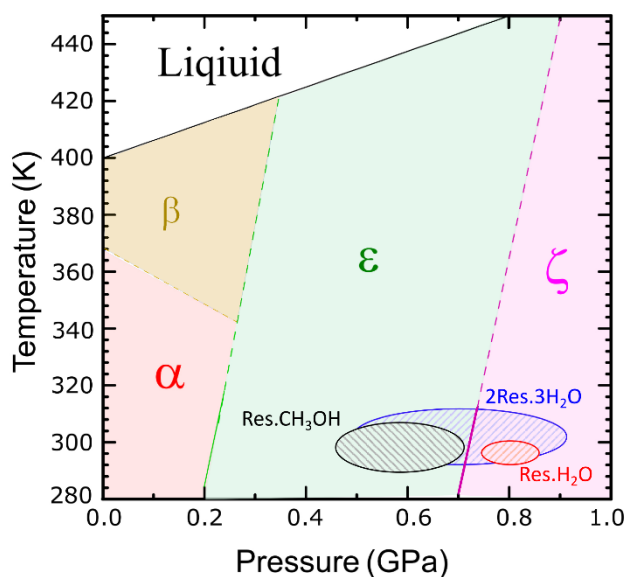


Figure 12. Preference p/T diagram for resorcinol polymorphs and solvates showing the conditions where these different resorcinol forms were obtained. The uniform fields of pastel colours mark the p/T regions where polymorphs of pristine resorcinol were obtained, whereas the hatched ovals indicate the regions where Res·H₂O (red), 3Res·2H₂O (blue) and Res·CH₃OH (black) solvates formed.

We regard the discovery of polymorph ζ as a valuable additional information about resorcinol, and particularly its structure, interactions, aggregation of molecules and their conformational properties. This polymorph ζ is the only centrosymmetric structure of resorcinol (space group $P2_1/c$) determined so far and the only resorcinol structure where molecules are hydrogen bonded into layers, which contrasts with the 3-dimensional H-bonded networks in other resorcinol polymorphs (Figures R3-S6, R3-S8). In polymorph ζ the conformations of two independent molecules are similar to those in polymorphs β and ε : one of torsion angles C2–C1–O1–H and C2–C3–O3–H is close to $\pm 150^\circ$ and the other to about 10° (Table R3-1). It shows that the conformation of resorcinol molecules significantly diverts from idealized values of torsion angles C2–C–O–H equal to 180° and 0° , described as *anti* and *syn* conformations, respectively. On the other hand, the values of torsion angles C2–C–O–H correlate with the torsion angles C2–C–O \cdots O', where the prime indicates the acceptor O-atom in the hydrogen-bonded molecule. This correlation shows that the molecular conformation in resorcinol polymorphs strongly depends on their crystal packing. However,

there are no easy paths for the molecules to change their arrangements and aggregation topologies by the way of solid-solid phase transitions. This combination of the molecular conformation, H-bonding pattern and the crystal packing is the reason of large hysteresis of transformations between resorcinol phases, which for decades hampered the detection of polymorphs ε and ζ .

3.4 Structural model of internal pressure

The discovery of polymorph ε in the frozen melt of resorcinol mixed with D-tartaric acid (D-Ta) initially appeared contradictive to our observation that polymorph ε is unstable below 0.2 GPa. However, we have noted that Zhu *et al.*²⁵ obtained polymorph ε only in its mixtures of with D-tartaric acid and with other resorcinol polymorphs, but no pure resorcinol ε . This led us to the conclusion that the crystallization of mixed compounds results in their doping, which stabilizes the high-pressure polymorph at ambient conditions. Therefore, we have worked out the model and formula for explaining how tartaric acid acting as a dopant can generate internal strain mimicking the external compression. Under such an internal compression polymorph ε was formed. According to this model, the dopant molecules (Figures R3-6) embedded in the host structure built of somewhat smaller molecule (Figure R3-6a), generate the internal doping pressure (p_d). In the structure where the isolated dopant molecules are on average separated by n host molecules, the dopant-to-host molar ratio (c_d) is:

$$c_d = [(n+1)^3 - 1]^{-1} \quad (\text{R3-1})$$

Therefore, the molar ratio equal to 1:7 (14.3% dopant) can be obtained for average separation $n=1$, $n=2$ gives a ratio of 1:26 (3.8%), $n=3$ gives a ratio of 1:80 (1.25%), *etc.* for the large member of host molecules (n), the c_d value approximates the molar concentration of the dopant in the mixture, equal to $(n+1)^{-3}$. Consequently, the internal doping pressure can be determined by Equation R3-2,

$$p_d = K_o \cdot c_d \cdot \delta V / V_o \quad (\text{R3-2})$$

In this formula, K_o is the bulk modulus describing the compression of the pure host crystal and the doped crystal; when assuming the spherical shape and isotopic interactions of all molecules, δV is the difference between the molecular volumes of the dopant and host compounds $\delta V = (V_d - V_o)$, and V_o is the molecular volume of the pure host compound, while the

effects of mismatched directional interactions, conformational flexibility *etc.* are neglected; it is also assumed that isolated dopant molecules are embedded in the host lattice.

We found that the method of crystallization strongly affects the type of solid mixture. In other words, the aggregation shown in Figures R3-6b and R3-6c is more favoured by the slow crystallization, while the quick quenching of molten mixture causes the kinetic crystallization, which generates the random distribution of isolated dopant molecules in the host lattice (Figure R3-6a). The quick and kinetic quenching of the melt can also result in thin films or amorphized portions of the dopant in the sample, which is difficult to detect by PXRD. When several types of solidification occur in the frozen melt, the actual concentration of isolated dopant molecules in the obtained solid solution is smaller than the ratio of mixed components. We tried to increase the homogeneity of the dopant distribution by milling the dry samples. However, our results of the milling experiments show that the milling alone, without melting, is very unlikely to produce high-pressure phases. In order to obtain the required concentration of the dopant, the host crystals in the process of milling would have to cleave along every second or third layer. We have fully confirmed that the positive results of our melting-and-freezing experiments could not be reproduced in our milling experiments on mixing resorcinol with various dopants.

The dopant molecules larger than resorcinol generate local pressure in the liquid solution of molten host and dopant. In the crystal form, the large dopant molecules exert pressure on their environment and generate internal pressure. This internal pressure can be sufficient to induce formation of the high-pressure polymorph (Figure R3-7). Consequently, the high-pressure polymorph ε is stabilized at ambient conditions.

3.5 High-pressure polymorphs under ambient conditions

In order to confirm the concept of doping pressure we have tested the resorcinol and several imidazole derivatives, for which high-pressure phases were previously reported.¹⁵⁶⁻¹⁵⁸ According to the molecular volume, we chose the suitable dopant compound, larger than the host molecules. The volume of tartaric acid molecules is only approximately 5% larger than that of resorcinol. It can be assumed that the mismatched interactions of the dopant molecules with the crystal environment can cause additional strain. We identified the polymorphs present in the sample by comparing the PXRD patterns and the quantities of the components were calculated from the intensities of reflections (Figures from R3-S11 to R3-S26). For example,

the frozen mixture of resorcinol and 15% (wt.) of DL-Ta yielded both polymorph ϵ and β . The presence of polymorph β was expected, because at 0.1 MPa its stability temperature region is below the melting point (Tables R3-3 and R3-S6). The results of our calculations of internal pressure according to Equation R3-2 are summarized in Table R3-3 (detailed in Tables R3-S4, R3-S5 and R3-S6). We have performed analogous experiments for imidazole, benzimidazole and its derivatives. We chose these compounds because their high-pressure polymorphs were found below 1 GPa.¹⁵⁶⁻¹⁵⁸ In the experiment of mixing benzimidazole (BzIm) with 5% 2-methylbenzimidazole (dM-BzIm), we obtained a 100% yield of doped BzIm polymorph β (the high-pressure phase). This doped β -BzIm sample was stable for at least several months. In case of 2-methylbenzimidazole (M-BzIm) doped with 5% 5,6-dimethylbenzimidazole (dM-BzIm), the internal pressure estimated by Equation R3-2 is lower than the pressure required for obtaining the high-pressure phase and this result is also consistent with our experimental results obtained at ambient conditions, because no traces of the high-pressure polymorph β of M-BzIm were detected (Table R3-4).

4 Conclusions

My Ph.D. thesis has shown that resorcinol certainly belongs to this group of organic compounds which confirm McCrone's famous statement "*...that every compound has different polymorphic forms, and that, in general, the number of forms known for that compound is proportional to the time and money spent in research on that compound*".¹⁵⁹ Over one and half centuries after the first syntheses of resorcinol and intensive research on this important compound, I have revealed yet another polymorph and solvates of resorcinol under pressure. From the perspective of high pressure, I was able to review the properties of resorcinol and explain its strange behaviour.

I have shown that the application of high pressure can provide access to new phases of resorcinol, which reveal new information about this intriguing compound. Moreover, the transformations of resorcinol phases suggested a general method of stabilizing high-pressure polymorphs at normal conditions.

The compression of polymorph α identified several structural features which destabilize its structure. Apart from the volume difference which favours polymorph β , high pressure destabilizes the hydrogen bonds between hydroxyl groups by reversing the angular dimensions (angles C–O \cdots O' and O \cdots O'–C') on the H-donor and H-acceptor sites. The transformation between phases α and β changes the conformation of molecules, the H-bonding network, and the transitional symmetry (*i.e.* the unit-cell dimensions), but the space group type remains the same.

While explaining the high-pressure forms of resorcinol, I have also obtained its three new solvates: resorcinol monohydrate Res·H₂O, duotrihydrate 3Res·2H₂O, and mono-methanol solvate Res·CH₃OH. Although these high-pressure solvates are unstable at ambient conditions, they show that hydrogen bonds O–H \cdots O in conjunction with the molecular conformation play an important role in the formation of the high-pressure structures. For the well-defined geometrical dimensions of hydrogen bonds O–H \cdots O it was possible to identify interactions responsible for low stability of monohydrate Res·H₂O. It is metastable, because its disadvantageous molecular arrangement hampers the formation of one of hydrogen bonds O–H \cdots O (it is much longer than its counterparts despite the high-pressure conditions). In contrast with the general assumption that high pressure eliminates orientational disorder of molecules in the crystal, and despite the considerable orientational disorder of one of two

independent resorcinol molecules, the duotrihydrate is more stable than monohydrate Res·H₂O. The independent molecules in duotrihydrate ($Z'=1+1/2$), assume either *syn-syn* or *anti-anti* conformation, while in the other two solvates only the *syn-anti* conformation is present.

Our exploration of high-pressure regions of the phase diagram of pure resorcinol led us to two high pressure polymorphs in different ranges of pressure: polymorph ϵ above 0.20 GPa and a new polymorph ζ above 0.70 GPa. This result was surprising, because polymorphs α and β can be compressed, without melting or dissolving the crystals, up to 4 GPa with no signs of transitions to other forms. Moreover, polymorph ϵ was discovered by Zhu. *et al.*²⁵ in 2016 at ambient pressure, when resorcinol was frozen of its molten mixture with tartaric acid. This observation led us to the general method of stabilizing high pressure polymorphs at ambient conditions by doping a compound with another one with larger molecules. This generates internal strain around the larger dopant molecules exerted on the host compound, which is similar in effects to the external compression. We have shown that our method is quite general and that it can be applied to other compounds, such as imidazole and its derivatives, for which we could stabilize by the rational doping their high-pressure polymorphs under ambient conditions. Moreover, we have devised the molecular-scale model of the structural effects of doping and its connection to the internal strain. By using this model, we have derived equations allowing the quantitative description of the internal strain mimicking the effect of external pressure. The results of our experiments on doping crystals well agree with the pressure value calculated according to our Equation R3-2. These results are quite important because they provide a method of stabilizing the high-pressure polymorphs at normal conditions. Naturally, these are preliminary results obtained for a selected series of organic compounds and further studies are required. However, undoubtedly this method of rational doping proved valid for several compounds, and it opens a new alley for obtaining new materials reaching out to the high-pressure regions of phase diagrams. For example, new forms of active pharmaceutical ingredients (APIs) can be sought in the search for their better performance. It can be envisaged, that the method of rational doping will bring about new practical applications in the future.

Another conclusion of my research is that the hydrogen-bonded structures can display exceptionally wide hysteresis. This feature can have significant consequences for the crystal chemistry and engineering of numerous chemical compounds. It may mean that indeed, consistently with McCrone's statement, there are many unknown polymorphs 'waiting' for their discovery. High pressure provides a convenient method for exploring the phase diagrams

of chemical compounds and the preference diagrams of their mixtures. Undoubtedly, all these unknown forms, very many of them, are there, with their exceptional properties, which can be ideal for practical applications.

5 Bibliography

- (1) Tahrouch, S.; Rapior, S.; Bessière, J.-M.; Andary, C. Les Substances Volatiles DeArgania Spinosa (Sapotaceae). *Acta Bot. Gallica* **1998**, *145*, 259–263. DOI: 10.1080/12538078.1998.10516305.
- (2) Decker, A.; Graber, E. M. Over-the-Counter Acne Treatments: A Review. *J. Clin. Aesthet. Dermatol.* **2012**, *5*, 32–40.
- (3) Kashapov, R.; Razuvayeva, Y.; Ziganshina, A.; Sergeeva, T.; Lukashenko, S.; Sapunova, A.; Voloshina, A.; Kashapova, N.; Nizameev, I.; Salnikov, V.; Ziganshina, S.; Gareev, B.; Zakharova, L. Supraamphiphilic Systems Based on Metallosurfactant and Calix[4]Resorcinol: Self-Assembly and Drug Delivery Potential. *Inorg. Chem.* **2020**, *59*, 18276–18286. DOI: 10.1021/acs.inorgchem.0c02833.
- (4) Cheng, B.; Wang, W.; Niu, X.; Ren, Y.; Liu, T.; Cao, H.; Wang, S.; Tu, Y.; Chen, J.; Liu, S.; Yang, X.; Chen, J. Discovery of Novel and Highly Potent Resorcinol Dibenzyl Ether-Based PD-1/PD-L1 Inhibitors with Improved Drug-like and Pharmacokinetic Properties for Cancer Treatment. *J. Med. Chem.* **2020**, *63*, 15946–15959. DOI: 10.1021/acs.jmedchem.0c01684.
- (5) Cannon, J. G.; Pease, J. P.; Hamer, R. L.; Ilhan, M.; Bhatnagar, R. K.; Long, J. P. Resorcinol Congeners of Dopamine Derived from Benzocycloheptene and Indan. *J. Med. Chem.* **1984**, *27*, 186–189. DOI: 10.1021/jm00368a014.
- (6) Bracher, M.; Swistak, J.; Noser, F. Studies on the Potential in Vivo Induction of Sister-Chromatid Exchanges in Rat Bone Marrow by Resorcinol. *Mutat. Res. Lett.* **1981**, *91*, 363–369. DOI: 10.1016/0165-7992(81)90016-6.
- (7) Durairaj, R. B. *Resorcinol Chemistry, Technology and Applications*. Springer-Verlag Berlin, Germany, 2005. DOI: 10.1007/3-540-28090-1.
- (8) *CRC Handbook of Chemistry and Physics 78th Edition*, 78th ed.; Lide, D. R., Frederiske, H. P. R., Eds.; CRC Press: Boca Raton, FL, USA, 1997.
- (9) Seidell, A. *Solubilities of Organic Compounds*. D. Van Nostrand Co **1941**, *11*, 189–223.
- (10) Denselben. Ueber einen neuen, dem Orcin homologen Körper. *Ann. Chem. Pharm.* **1864**, *130*, 354–359. DOI: 10.1002/jlac.18641300309.
- (11) Scheeline, H. “Dihydroxybenzenes”. *SRI Process Economics Program* **1972**, No. 79.
- (12) Schmiedel, K.; Decker, D. “Resorcinol”. *Ullmann’s Encycl. Ind. Chem* **2000**, A23, 111.
- (13) Binschedlar, L.; Busch, Y. *Chem. Ind.*, **1878**, 370.
- (14) Binschedlar, L.; Busch, Y. *Mon. Scientif* **1878**, 1168.
- (15) Holter, S., Dressler, H. Paper Presented at the American Institute of Chemical Engineers. Denver, CO **1988**.
- (16) Robertson, J. M. The Structure of Resorcinol a Quantitative X-Ray Investigation. *Proc. R. Soc. Lond. A* **1936**, *157*, 79–99. DOI: 10.1098/rspa.1936.0181.
- (17) Robertson, J. M.; Ubbelohde, A. R.; Bragg, W. H. A New Form of Resorcinol. I. Structure Determination by X-Rays. *Proc. Math. Phys. Eng. Sci.* **1938**, *167*, 122–135. DOI: 10.1098/rspa.1938.0122.

- (18) Bacon, G. E.; Curry, N. A. A Study of α -Resorcinol by Neutron Diffraction. *Proc. R. Soc. Lond. A* **1956**, *235*, 552–559. DOI: 10.1098/rspa.1956.0105.
- (19) Kichanov, S. E.; Kozlenko, D. P.; Bilski, P.; Wąsicki, J.; Nawrocik, W.; Medek, A.; Hancock, B. C.; Lukin, E. V.; Lathe, C.; Dubrovinsky, L. S.; Savenko, B. N. The Polymorphic Phase Transformations in Resorcinol at High Pressure. *J. Mol. Struct.* **2011**, *1006*, 337–343. DOI: 10.1016/j.molstruc.2011.09.029.
- (20) Trivedi, M. K.; Branton, A.; Trivedi, D.; Nayak, G.; Singh, R.; Jana, S. Characterisation of Physical, Spectral and Thermal Properties of Biofield Treated Resorcinol. *Org. Chem. Curr. Res.* **2015**, *3*, 4. DOI: 10.4172/2161-0401.1000146.
- (21) Deb, S. K.; Rekha, M. A.; Roy, A. P.; Vijayakumar, V., V.; Meenakshi, S.; Godwal, B. K. Raman-Scattering Study of High-Pressure Phase Transition and Amorphization of Resorcinol. *Phys. Rev. B Condens. Matter* **1993**, *47*, 11491–11494. DOI: 10.1103/physrevb.47.11491.
- (22) Sharma, S. M.; Vijayakumar, V.; Sikka, S. K.; Chidambaram, R. High Pressure Phase Transitions in Organic Solids I: $\alpha \rightarrow \beta$ Transition in Resorcinol. *Pramana - J Phys* **1985**, *25*, 75–79. DOI: 10.1007/bf02847646.
- (23) Ebisuzaki, Y.; Askari, L. H.; Bryan, A. M.; Nicol, M. F. Phase Transitions in Resorcinal. *J. Chem. Phys.* **1987**, *87*, 6659–6664. DOI: 10.1063/1.453401.
- (24) Rao, R.; Sakuntala, T.; Godwal, B. K. Evidence for High-Pressure Polymorphism in Resorcinol. *Phys. Rev. B* **2002**, *65*, 054108-054116-. DOI: 10.1103/PhysRevB.65.054108.
- (25) Zhu, Q.; Shtukenberg, A. G.; Carter, D. J.; Yu, T.-Q.; Yang, J.; Chen, M.; Raiteri, P.; Oganov, A. R.; Pokroy, B.; Polishchuk, I.; Bygrave, P. J.; Day, G. M.; Rohl, A. L.; Tuckerman, M. E.; Kahr, B. Resorcinol Crystallization from the Melt: A New Ambient Phase and New “Riddles.” *J. Am. Chem. Soc.* **2016**, *138*, 4881–4889. DOI: 10.1021/jacs.6b01120.
- (26) Safari, F.; Katrusiak, A. High-Pressure Polymorphs Nucleated and Stabilized by Rational Doping under Ambient Conditions. *J. Phys. Chem. C Nanomater. Interfaces* **2021**, *125*, 23501–23509. DOI: 10.1021/acs.jpcc.1c07297.
- (27) Mao, H. K.; Hemley, R. J. New Windows on the Earth's Deep Interior. In *Ultra-high-Pressure Mineralogy: Physics and Chemistry of the Earth's Deep Interior*. *Rev. Min* **1998**, *37*, 1–32.
- (28) Hemley, R. J.; Mao, H. K. New Windows on Earth and Planetary Interiors. *Mineral. Mag.* **2002**, *66*, 791–811.
- (29) Patyk-Kaźmierczak, E.; Kaźmierczak, M. A New High-Pressure Benzocaine Polymorph-towards Understanding the Molecular Aggregation in Crystals of an Important Active Pharmaceutical Ingredient (API). *Acta Crystallogr., Sect. B: Struct. Sci., Cryst. Eng.Mater.* **2020**, *76*, 56–64. DOI: 10.1107/S2052520619016548.
- (30) Marciniak, J.; Bąkiewicz, J.; Dobrowolski, M. A.; Dziubek, K. F.; Kaźmierczak, M.; Paliwoda, D.; Rajewski, K. W.; Sobczak, S.; Stachowicz, M.; Katrusiak, A. Most Frequent Organic Interactions Compressed in Toluene. *Cryst. Growth Des.* **2016**, *16*, 1435–1441. DOI: 10.1021/acs.cgd.5b01538.
- (31) Zielinski, W.; Katrusiak, A. Pressure-Induced Preference for Solvation of 5,6-Dimethylbenzimidazole. *CrystEngComm* **2016**, *18* (18), 3211–3215. DOI: 10.1039/c6ce00419a.

- (32) Podsiadło, M.; Olejniczak, A.; Katrusiak, A. A New Ethane Polymorph. *Cryst. Growth Des.* **2017**, *17*, 228–232. DOI: 10.1021/acs.cgd.6b01474.
- (33) Oswald, I. D. H.; Allan, D. R.; Motherwell, W. D. S.; Parsons, S. Structures of the Monofluoro- and Monochlorophenols at Low Temperature and High Pressure. *Acta Cryst. B* **2005**, *61*, 69–79. DOI: 10.1107/S0108768104030617.
- (34) Zakharov, B. A.; Boldyreva, E. V. A High-Pressure Single-Crystal to Single-Crystal Phase Transition in DL-Alaninium Semi-Oxalate Monohydrate with Switching-over Hydrogen Bonds. *Acta Cryst. B* **2013**, *69*, 271–280. DOI: 10.1107/S2052519213011676.
- (35) Novelli, G.; Maynard-Casely, H. E.; McIntyre, G. J.; Warren, M. R.; Parsons, S. Effect of High Pressure on the Crystal Structures of Polymorphs of L-Histidine. *Cryst. Growth Des.* **2020**, *20*, 7788–7804. DOI: 10.1021/acs.cgd.0c01085.
- (36) Irie, K.; Shibayama, K.; Mito, M.; Takagi, S.; Ishizuka, M.; Lakin, K.; Oakley, R. T. High-Pressure Dc Magnetic Measurements on a Bisdiselenazolyl Radical Ferromagnet Using a Vibrating-Coil SQUID Magnetometer. *Phys. Rev. B.* **2019**, *99*, 014417–014425. DOI: 10.1103/physrevb.99.014417.
- (37) Handzlik, G.; Sieklucka, B.; Tomkowiak, H.; Katrusiak, A.; Pinkowicz, D. How to Quench Ferromagnetic Ordering in a CN-Bridged Ni(II)-Nb(IV) Molecular Magnet? A Combined High-Pressure Single-Crystal X-Ray Diffraction and Magnetic Study. *Magnetochemistry* **2019**, *5*, 33–44. DOI: 10.3390/magnetochemistry5020033.
- (38) Yasuda, N.; Okamoto, M.; Shimizu, H.; Fujimoto, S.; Yoshino, K.; Inuishi, Y. Pressure-Induced Antiferroelectricity in Ferroelectric CsH₂PO₄. *Phys. Rev. Lett.* **1978**, *41*, 1311–1314. DOI: 10.1103/physrevlett.41.1311.
- (39) Faraji, S.; Allaei, S. M. V.; Amsler, M. Thermal Conductivity of CaF₂ at High Pressure. *Phys. Rev. B.* **2021**, *103*, 134301–09. DOI: 10.1103/physrevb.103.134301.
- (40) Friedrich, A.; Collings, I. E.; Dziubek, K. F.; Fanetti, S.; Radacki, K.; Ruiz-Fuertes, J.; Pellicer-Porres, J.; Hanfland, M.; Sieh, D.; Bini, R.; Clark, S. J.; Marder, T. B. Pressure-Induced Polymerization of Polycyclic Arene-Perfluoroarene Cocrystals: Single Crystal X-Ray Diffraction Studies, Reaction Kinetics, and Design of Columnar Hydrofluorocarbons. *J. Am. Chem. Soc.* **2020**, *142*, 18907–18923. DOI: 10.1021/jacs.0c09021.
- (41) Casati, N.; Macchi, P.; Sironi, A. Hydrogen Migration in Oxalic Acid Di-Hydrate at High Pressure? *Chem. Commun.* **2009**, *19*, 2679–2681. DOI: 10.1039/b823458b.
- (42) Casati, N.; Genoni, A.; Meyer, B.; Krawczuk, A.; Macchi, P. Exploring Charge Density Analysis in Crystals at High Pressure: Data Collection, Data Analysis and Advanced Modelling. *Acta Cryst. B* **2017**, *73*, 584–597. DOI: 10.1107/s2052520617008356.
- (43) Casati, N.; Kleppe, A.; Jephcoat, A. P.; Macchi, P. Putting Pressure on Aromaticity along with *in Situ* Experimental Electron Density of a Molecular Crystal. *Nat. Commun.* **2016**, *7*, 10901–10910. DOI: 10.1038/ncomms10901.
- (44) Gajda, R.; Stachowicz, M.; Makal, A.; Sutula, S.; Parafiniuk, J.; Fertey, P.; Woźniak, K. Experimental Charge Density of Grossular under Pressure - a Feasibility Study. *IUCrJ* **2020**, *7*, 383–392. DOI: 10.1107/S2052252520001955.
- (45) McMillan, P. F. Pressing on: The Legacy of Percy W. Bridgman. *Nat. Mater.* **2005**, *4*, 715–718. DOI: 10.1038/nmat1488.
- (46) Lawson, A. W.; Tang, T.-Y. A Diamond Bomb for Obtaining Powder Pictures at High Pressures. *Rev. Sci. Instrum.* **1950**, *21*, 815–815. DOI: 10.1063/1.1745728.

- (47) Jamieson, J. C. Introductory Studies of High-Pressure Polymorphism to 24,000 Bars by X-Ray Diffraction with Some Comments on Calcite II. *J. Geol.* **1957**, *65*, 334–343. DOI: 10.1086/626433.
- (48) Jamieson, J. C.; Lawson, A. W.; Nachtrieb, N. D. New Device for Obtaining X-ray Diffraction Patterns from Substances Exposed to High Pressure. *Rev. Sci. Instrum.* **1959**, *30*, 1016–1019. DOI: 10.1063/1.1716408.
- (49) Weir, C. E.; Lippincott, E. R.; Van Valkenburg, A.; Bunting, E. N. Infrared Studies in the 1- to 15-Micron Region to 30,000 Atmospheres. *J. Res. Natl. Bur. Stand. A Phys. Chem.* **1959**, *63A*, 55–62. DOI: 10.6028/jres.063A.003.
- (50) Katrusiak, A. High-Pressure Crystallography. *Acta Cryst. A* **2008**, *64*, 135–148. DOI: 10.1107/S0108767307061181.
- (51) Merrill, L.; Bassett, W. A. Miniature Diamond Anvil Pressure Cell for Single Crystal X-ray Diffraction Studies. *Rev. Sci. Instrum* **1974**, *45*, 290–294. DOI: 10.1063/1.1686607.
- (52) Piermarini, G. J. High Pressure X-Ray Crystallography with the Diamond Cell at NIST/NBS. *J. Res. Natl. Inst. Stand. Technol.* **2001**, *106*, 889–920. DOI: 10.6028/jres.106.045.
- (53) Seal, M. Diamond Anvil Technology. In *High-Pressure Research in Mineral Physics: A Volume in Honor of Syun-iti Akimoto*. American Geophysical Union: Washington, D. C., 1987, 35–40. DOI: 10.1029/GM039p0035.
- (54) Boehler, R.; De Hantsetters, K. New Anvil Designs in Diamond-Cells. *High Press. Res.* **2004**, *24*, 391–396. DOI: 10.1080/08957950412331323924.
- (55) O'Bannon, E. F., III; Jenei, Z.; Cynn, H.; Lipp, M. J.; Jeffries, J. R. Contributed Review: Culet Diameter and the Achievable Pressure of a Diamond Anvil Cell: Implications for the Upper Pressure Limit of a Diamond Anvil Cell. *Rev. Sci. Instrum.* **2018**, *89*, 111501. DOI: 10.1063/1.5049720.
- (56) Bell, P. M.; Mao, H. K.; Goettel, K. Ultrahigh Pressure: Beyond 2 Megabars and the Ruby Fluorescence Scale. *Science* **1984**, *226*, 542–544. DOI: 10.1126/science.226.4674.542.
- (57) Anzellini, S.; Dewaele, A.; Occelli, F.; Loubeyre, P.; Mezouar, M. Equation of State of Rhenium and Application for Ultra High Pressure Calibration. *J. Appl. Phys.* **2014**, *115*, 043511–043524. DOI: 10.1063/1.4863300.
- (58) Schiferl, D.; Fritz, J. N.; Katz, A. I.; Schaefer, M.; Skelton, E. F.; Qadri, S. B.; Ming, L. C.; Manghnani, M. H. Very High Temperature Diamond-Anvil Cell for X-Ray Diffraction: Application to the Comparison of the Gold and Tungsten High-Temperature-High-Pressure Internal Standards. In *High-Pressure Research in Mineral Physics: A Volume in Honor of Syun-iti Akimoto*; American Geophysical Union: Washington, D. C., **1987**, 75–83.
- (59) Rosa, A. D.; Merkulova, M.; Garbarino, G.; Svitlyk, V.; Jacobs, J.; Sahle, C. J.; Mathon, O.; Munoz, M.; Merkel, S. Amorphous Boron Composite Gaskets for *in Situ* High-Pressure and High-Temperature Studies. *High Press. Res.* **2016**, *36*, 564–574. DOI: 10.1080/08957959.2016.1245297.
- (60) Tateiwa, N.; Haga, Y.; Matsuda, T. D.; Fisk, Z. Magnetic Measurements at Pressures above 10 GPa in a Miniature Ceramic Anvil Cell for a Superconducting Quantum Interference Device Magnetometer. *Rev. Sci. Instrum.* **2012**, *83*, 053906–053912. DOI: 10.1063/1.4722945.
- (61) Manaa, M. R. Molecules to Microbes: In Situ Studies of Organic Systems Under Hydrothermal Conditions. In *Chemistry at Extreme Conditions*; Manaa, M. R., Ed.; Elsevier Science: London, England, **2005**, 83–86. DOI: 10.1016/B978-0-444-51766-1.X5000-8.

- (62) Weir, S.T. *Electrical Transport Experiments at High Pressure*; No. LLNL-PROC-410546. Lawrence Livermore National Lab. (LLNL), Livermore, CA (United States), **2009**.
- (63) Klotz, S.; Chervin, J. C.; Munsch, P.; Le Marchand, G. Hydrostatic Limits of 11 Pressure Transmitting Media. *J. Phys. D. Appl. Phys* **2009**, *42*, 075413–075426. DOI: 10.1088/0022-3727/42/7/075413.
- (64) Angel, R. J.; Bujak, M.; Zhao, J.; Gatta, G. D.; Jacobsen, S. D. Effective Hydrostatic Limits of Pressure Media for High-Pressure Crystallographic Studies. *J. Appl. Cryst.* **2007**, *40*, 26–32. DOI: 10.1107/s0021889806045523.
- (65) Piermarini, G. J.; Block, S.; Barnett, J.D. Hydrostatic Limits in Liquids and Solids to 100 Kbar. *J. Appl. Phys* **1973**, *44*, 5377–5382. DOI: 10.1063/1.1662159.
- (66) LeSar, R.; Ekberg, S. A.; Jones, L. H.; Mills, R. L.; Schwalbe, L. A.; Schiferl, D. Raman Spectroscopy of Solid Nitrogen up to 374 Kbar. **1979**, *32*, 131–134, DOI: 10.1016/0038-1098(79)91073-1.
- (67) Takemura, K. Evaluation of the Hydrostaticity of a Helium-Pressure Medium with Powder X-Ray Diffraction Techniques. *J. Appl. Phys.* **2001**, *89*, 662–668. DOI: 10.1063/1.1328410.
- (68) Varga, T.; Wilkinson, A. P.; Angel, R. J. Fluorinert as a Pressure-Transmitting Medium for High-Pressure Diffraction Studies. *Rev. Sci. Instrum.* **2003**, *74*, 4564–4566. DOI: 10.1063/1.1611993.
- (69) Sidorov, V. A.; Sadykov, R. A. Hydrostatic Limits of Fluorinert Liquids Used for Neutron and Transport Studies at High Pressure. *J. Phys. Condens. Matter* **2005**, *17*, S3005–S3008. DOI: 10.1088/0953-8984/17/40/002.
- (70) Yokogawa, K.; Murata, K.; Yoshino, H.; Aoyama, S. Solidification of High-Pressure Medium Daphne 7373. *Jpn. J. Appl. Phys.* **2007**, *46*, 3636–3639. DOI: 10.1143/jjap.46.3636.
- (71) Murata, K.; Yokogawa, K.; Yoshino, H.; Klotz, S.; Munsch, P.; Irizawa, A.; Nishiyama, M.; Iizuka, K.; Nanba, T.; Okada, T.; Shiraga, Y.; Aoyama, S. Pressure Transmitting Medium Daphne 7474 Solidifying at 3.7 GPa at Room Temperature. *Rev. Sci. Instrum.* **2008**, *79*, 085101 DOI: 10.1063/1.2964117.
- (72) Kunz, M. Mapping Completeness. *IUCrJ* **2021**, *8*, 855–856. DOI: 10.1107/S2052252521011106.
- (73) Tchoń, D.; Makal, A. Maximizing Completeness in Single-Crystal High-Pressure Diffraction Experiments: Phase Transitions in 2°AP. *IUCrJ* **2021**, *8*, 1006–1017. DOI: 10.1107/S2052252521009532.
- (74) Patyk, E.; Skumiel, J.; Podsiadło, M.; Katrusiak, A. High-Pressure (+)-Sucrose Polymorph. *Angew. Chem. Int. Ed* **2012**, *51*, 2146–2150. DOI: 10.1002/anie.201107283.
- (75) Hilfiker, R., von Raumer, M., *Polymorphism in the Pharmaceutical Industry: Solid Form and Drug Development*, 1st ed.; Eds.; Wiley-VCH Verlag: Weinheim, Germany, **2019**.
- (76) Datta, S.; Grant, D. J. W. Crystal Structures of Drugs: Advances in Determination, Prediction and Engineering. *Nat. Rev. Drug Discov.* **2004**, *3*, 42–57. DOI: 10.1038/nrd1280.
- (77) Bernstein, J. *Polymorphism in Molecular Crystals*, *IUCr, Monographs on Crystallography*. Clarendon Press, Oxford **2002**.
- (78) Censi, R.; Di Martino, P. Polymorph Impact on the Bioavailability and Stability of Poorly Soluble Drugs. *Molecules* **2015**, *20*, 18759–18776. DOI: 10.3390/molecules201018759.

- (79) Correa, C. Guidelines for the Examination of Pharmaceutical Patents: Developing a Public Health Perspective. *Work. Pap.* **2007**.
- (80) Boldyrev, V. V. Mechanochemical Modification and Synthesis of Drugs. *J. Mater. Sci.* **2004**, *39*, 5117–5120. DOI: 10.1023/b:jmsc.0000039193.69784.1d.
- (81) Kim, S.; Wei, C.; Kiang, S. Crystallization Process Development of an Active Pharmaceutical Ingredient and Particle Engineering via the Use of Ultrasonics and Temperature Cycling. *Org. Process Res. Dev.* **2003**, *7*, 997–1001. DOI: 10.1021/op034107t.
- (82) Loh, Z. H.; Samanta, A. K.; Sia Heng, P. W. Overview of Milling Techniques for Improving the Solubility of Poorly Water-Soluble Drugs. *Asian J. Pharm. Sci.* **2015**, *10*, 255–274. DOI: 10.1016/j.ajps.2014.12.006.
- (83) *Handbook of Stability Testing in Pharmaceutical Development: Regulations, Methodologies, and Best Practices*; Huynh-Ba, K., Ed.; Springer: New York, NY, **2010**.
- (84) Heinz, A.; Strachan, C. J.; Gordon, K. C.; Rades, T. Analysis of Solid-State Transformations of Pharmaceutical Compounds Using Vibrational Spectroscopy. *J. Pharm. Pharmacol.* **2010**, *61*, 971–988. DOI: 10.1211/jpp.61.08.0001.
- (85) Bauer, J.; Spanton, S.; Henry, R.; Quick, J.; Dziki, W.; Porter, W.; Morris, J. Ritonavir: An Extraordinary Example of Conformational Polymorphism. *Pharm. Res.* **2001**, *18*, 859–866. DOI: 10.1023/a:1011052932607.
- (86) Fabbiani, F. P. A.; Allan, D. R.; David, W. I. F.; Davidson, A. J.; Lennie, A. R.; Parsons, S.; Pulham, C. R.; Warren, J. E. High-Pressure Studies of Pharmaceuticals: An Exploration of the Behavior of Piracetam. *Cryst. Growth Des.* **2007**, *7*, 1115–1124. DOI: 10.1021/cg0607710.
- (87) Fabbiani, F. P. A.; Allan, D. R.; David, W. I. F.; Moggach, S. A.; Parsons, S.; Pulham, C. R. High-Pressure Recrystallisation—a Route to New Polymorphs and Solvates. *CrystEngComm* **2004**, *6*, 504–511. DOI: 10.1039/b406631f.
- (88) Fabbiani, F. P. A.; Allan, D. R.; Dawson, A.; David, W. I. F.; McGregor, P. A.; Oswald, I. D. H.; Parsons, S.; Pulham, C. R. Pressure-Induced Formation of a Solvate of Paracetamol. *Chem. Commun.* **2003**, No. 24, 3004–3005. DOI: 10.1039/b310394c.
- (89) Oswald, I. D. H.; Pulham, C. R. Co-Crystallisation at High Pressure—an Additional Tool for the Preparation and Study of Co-Crystals. *CrystEngComm* **2008**, *10*, 1114–1116. DOI: 10.1039/b805591b.
- (90) Patyk-Kaźmierczak, E.; Kaźmierczak, M. Hydrate vs Anhydrate under a Pressure-(De)Stabilizing Effect of the Presence of Water in Solid Forms of Sulfamethoxazole. *Cryst. Growth Des.* **2021**, *21*, 6879–6888. DOI: 10.1021/acs.cgd.1c00784.
- (91) Wu, C.-Y.; Ruddy, O. M.; Bentham, A. C.; Hancock, B. C.; Best, S. M.; Elliott, J. A. Modelling the Mechanical Behaviour of Pharmaceutical Powders during Compaction. *Powder Technol.* **2005**, *152*, 107–117. DOI: 10.1016/j.powtec.2005.01.010.
- (92) Seibert, K. D.; Collins, P. C.; Fisher, E. Milling Operations in the Pharmaceutical Industry. In *Chemical Engineering in the Pharmaceutical Industry*; John Wiley & Sons, Inc.: Hoboken, NJ, USA, **2010**, 365–378.
- (93) Luisi, B. S.; Medek, A.; Liu, Z.; Mudunuri, P.; Moulton, B. Milling-Induced Disorder of Pharmaceuticals: One-Phase or Two-Phase System? *J. Pharm. Sci.* **2012**, *101*, 1475–1485. DOI: 10.1002/jps.23035.

- (94) Matsumoto, T.; Ichikawa, J.-I.; Kaneniwa, N.; Otsuka, M. Effect of Environmental Temperature on the Polymorphic Transformation of Phenylbutazone during Grinding. *Chem. Pharm. Bull.* **1988**, *36*, 1074–1085. DOI: 10.1248/cpb.36.1074.
- (95) Brittain, H. G. Effects of Mechanical Processing on Phase Composition. *J. Pharm. Sci.* **2002**, *91*, 1573–1580. DOI: 10.1002/jps.10115.
- (96) Kaneniwa, N.; Otsuka, M. Effect of Grinding on the Transformations of Polymorphs of Chloramphenicol Palmitate. *Chem. Pharm. Bull.* **1985**, *33*, 1660–1668. DOI: 10.1248/cpb.33.1660.
- (97) Lin, S.-Y.; Cheng, W.-T.; Wang, S.-L. Thermodynamic and Kinetic Characterization of Polymorphic Transformation of Famotidine during Grinding. *Int. J. Pharm.* **2006**, *318*, 86–91. DOI: 10.1016/j.ijpharm.2006.03.021.
- (98) Adeleye, O. A. Relationship between Compression Pressure, Mechanical Strength and Release Properties of Tablets. *Polim. Med.* **2019**, *49*, 27–33. DOI: 10.17219/pim/111888.
- (99) Chan, H. K.; Doelker, E. Polymorphic Transformation of Some Drugs under Compression. *Drug Dev. Ind. Pharm.* **1985**, *11*, 315–332. DOI: 10.3109/03639048509056874.
- (100) Chawla, G.; Bansal, A. K. Effect of Processing on Celecoxib and Its Solvates. *Pharm. Dev. Technol.* **2004**, *9*, 419–433. DOI:10.1081/pdt-200035800.
- (101) Koradia, V.; Tenho, M.; Lopez de Diego, H.; Ringkjøbing-Elema, M.; Møller-Sonnergaard, J.; Salonen, J.; Lehto, V.-P.; Rantanen, J. Investigation of Solid Phase Composition on Tablet Surfaces by Grazing Incidence X-Ray Diffraction. *Pharm. Res.* **2012**, *29*, 134–144. DOI:10.1007/s11095-011-0520-8.
- (102) Guerain, M. A Review on High Pressure Experiments for Study of Crystallographic Behavior and Polymorphism of Pharmaceutical Materials. *J. Pharm. Sci.* **2020**, *109*, 2640–2653. DOI: 10.1016/j.xphs.2020.05.021.
- (103) Sharma, C. V.; Mehta, V. Paracetamol: Mechanisms and Updates. *Contin. Educ. Anaesth. Crit. Care Pain* **2014**, *14*, 153–158. DOI: 10.1093/bjaceaccp/mkt049.
- (104) Shakhtshneider, T. P.; Boldyreva, E. V.; Vasilchenko, M. A.; Ahsbahs, H.; Uchtmann, H. Anisotropy of Crystal Structure Distortion in Organic Molecular Crystals of Drugs Induced by Hydrostatic Compression. *J. Struct. Chem.* **1999**, *40*, 892–898. DOI: 10.1007/bf02700697.
- (105) Boldyreva, E. V. High-Pressure Studies of the Anisotropy of Structural Distortion of Molecular Crystals. *J. Mol. Struct.* **2003**, *647*, 159–179. DOI: 10.1016/s0022-2860(02)00520-3.
- (106) Dawson, A.; Allan, D. R.; Belmonte, S. A.; Clark, S. J.; David, W. I. F.; McGregor, P. A.; Parsons, S.; Pulham, C. R.; Sawyer, L. Effect of High Pressure on the Crystal Structures of Polymorphs of Glycine. *Cryst. Growth Des.* **2005**, *5*, 1415–1427. DOI: 10.1021/cg049716m.
- (107) Boldyreva, E. V.; Ivashevskaya, S. N.; Sowa, H.; Ahsbahs, H.; Weber, H.-P. Effect of Hydrostatic Pressure on the γ -Polymorph of Glycine. 1. A Polymorphic Transition into a New δ -Form. *Z. Kristallogr. Cryst. Mater.* **2005**, *220*, 50–57. DOI: 10.1524/zkri.220.1.50.58886.
- (108) Moggach, S. A.; Allan, D. R.; Clark, S. J.; Gutmann, M. J.; Parsons, S.; Pulham, C. R.; Sawyer, L. High-Pressure Polymorphism in L-Cysteine: The Crystal Structures of L-Cysteine-III and L-Cysteine-IV. *Acta Cryst. B* **2006**, *62*, 296–309. DOI: 10.1107/S0108768105038802.
- (109) Ostrowska, K.; Kropidłowska, M.; Katrusiak, A. High-Pressure Crystallization and Structural Transformations in Compressed R, S-Ibuprofen. *Cryst. Growth Des.* **2015**, *15*, 1512–1517. DOI: 10.1021/cg5018888.

- (110) Bridgman, P. W. Polymorphism at High Pressures. *Proc. Am. Acad. Arts Sci.* **1916**, 52 (3), 91–188. DOI: 10.2307/20025675.
- (111) Lamelas, F. J.; Dreger, Z. A.; Gupta, Y. M. Raman and X-Ray Scattering Studies of High-Pressure Phases of Urea. *J. Phys. Chem. B* **2005**, 109, 8206–8215. DOI: 10.1021/jp040760m.
- (112) Olejniczak, A.; Ostrowska, K.; Katrusiak, A. H-Bond Breaking in High-Pressure Urea. *J. Phys. Chem. C Nanomater. Interfaces* **2009**, 113, 15761–15767. DOI: 10.1021/jp904942c.
- (113) Patyk-Kaźmierczak, E.; Kaźmierczak, M. A New High-Pressure Benzocaine Polymorph - towards Understanding the Molecular Aggregation in Crystals of an Important Active Pharmaceutical Ingredient (API). *Acta Cryst. B* **2020**, 76, 56–64. DOI: 10.1107/S2052520619016548.
- (114) Katrusiak, A. Crystallographic Autostereograms. *J. Mol. Graph. Model.* **2001**, 19, 363–367. DOI: 10.1016/s1093-3263(00)00085-1.
- (115) Hirota, S.; Yamauchi, O. Weak Interactions and Molecular Recognition in Systems Involving Electron Transfer Proteins. *Chem. Rec.* **2001**, 1, 290–299. DOI: 10.1002/tcr.1014.
- (116) Sinha, N.; Smith-Gill, S. J. Electrostatics in Protein Binding and Function. *Curr. Protein Pept. Sci.* **2002**, 3, 601–614. DOI: 10.2174/1389203023380431.
- (117) Tanford, C. Contribution of Hydrophobic Interactions to the Stability of the Globular Conformation of Proteins. *J. Am. Chem. Soc.* **1962**, 84, 4240–4247. DOI: 10.1021/ja00881a009.
- (118) Paigen, K. On the Regulation of DNA Transcription. *J. Theor. Biol.* **1962**, 3, 268–282. DOI: 10.1016/s0022-5193(62)80017-4.
- (119) Ohmine, I.; Saito, S. Water Dynamics: Fluctuation, Relaxation, and Chemical Reactions in Hydrogen Bond Network Rearrangement. *Acc. Chem. Res.* **1999**, 32, 741–749. DOI: 10.1021/ar970161g.
- (120) Steiner, T. The Hydrogen Bond in the Solid State. *Angew. Chem. Int. Ed Engl.* **2002**, 41, 49–76. DOI: 10.1002/1521-3773(20020104)41:1<48::aid-anie48>3.0.co;2-u.
- (121) Sutton, C.; Risko, C.; Brédas, J.-L. Noncovalent Intermolecular Interactions in Organic Electronic Materials: Implications for the Molecular Packing vs Electronic Properties of Acenes. *Chem. Mater.* **2016**, 28, 3–16. DOI: 10.1021/acs.chemmater.5b03266.
- (122) McMullan, R. K.; Thomas, R.; Nagle, J. F. Structures of the Paraelectric and Ferroelectric Phases of $\text{NaD}_3(\text{SeO}_3)_2$ by Neutron Diffraction: A Vertex Model for the Ordered Ferroelectric State. *J. Chem. Phys.* **1982**, 77, 537–547. DOI: 10.1063/1.443635.
- (123) Jeffrey, G. A. *An Introduction to Hydrogen Bonding*; Oxford University Press: Oxford, **1997**.
- (124) Arunan, E.; Desiraju, G. R.; Klein, R. A.; Sadlej, J.; Scheiner, S.; Alkorta, I.; Clary, D. C.; Crabtree, R. H.; Dannenberg, J. J.; Hobza, P.; Kjaergaard, H. G.; Legon, A. C.; Mennucci, B.; Nesbitt, D. J. Definition of the Hydrogen Bond (IUPAC Recommendations 2011). *Pure Appl. Chem.* **2011**, 83, 1637–1641. DOI: 10.1351/pac-rec-10-01-02.
- (125) Mora, A. J.; Avila, E. E.; Delgado, G. E.; Fitch, A. N.; Brunelli, M. Temperature Effects on the Hydrogen-Bond Patterns in 4-Piperidinecarboxylic Acid. *Acta Cryst. B* **2005**, 61, 96–102. DOI: 10.1107/S0108768104031738.

- (126) Wang, Q.; Yan, T.; Wang, K.; Zhu, H.; Cui, Q.; Zou, B. Pressure-Induced Reversible Phase Transition in Thiourea Dioxide Crystal. *J. Chem. Phys.* **2015**, *142*, 244701–244709. DOI: 10.1063/1.4922842.
- (127) Katrusiak, A.; Szafranski, M.; Podsiadlo, M. Pressure-Induced Collapse of Guanidinium Nitrate N-H···O Bonded Honeycomb Layers into a 3-D Pattern with Varied H-Acceptor Capacity. *Chem. Commun.* **2011**, *47*, 2107–2109. DOI: 10.1039/c0cc02630a.
- (128) Hofmeister, A. M.; Cynn, H.; Burnley, P. C.; Meade, C. Vibrational Spectra of Dense, Hydrous Magnesium Silicates at High Pressure; Importance of the Hydrogen Bond Angle. *Am. Mineral.* **1999**, *84*, 454–464. DOI: 10.2138/am-1999-0330.
- (129) Williams, Q.; Guenther, L. Pressure-Induced Changes in the Bonding and Orientation of Hydrogen in FeOOH-Goethite. *Solid State Commun.* **1996**, *100*, 105–109. DOI: 10.1016/0038-1098(96)00374-2.
- (130) Gorbaty, Y. U. E.; Bondarenko, G. V.; Kalinichev, A. G.; Okhulkov, A. V. The Effect of Pressure on Hydrogen Bonding in Water: IR Study of ν_{OD} HDO at Pressures of up to 1500 Bar. *Mol. Phys.* **1999**, *96*, 1659–1665. DOI: 10.1080/00268979909483109.
- (131) Moggach, S. A.; Marshall, W. G.; Parsons, S. High-Pressure Neutron Diffraction Study of L-Serine-I and L-Serine-II, and the Structure of L-Serine-III at 8.1 GPa. *Acta Cryst. B* **2006**, *62*, 815–825. DOI: 10.1107/S010876810601799X.
- (132) Sikora, M.; Katrusiak, A. Pressure-Controlled Neutral–Ionic Transition and Disorder of NH···N Hydrogen Bonds in Pyrazole. *J. Phys. Chem. C* **2013**, *117*, 10661–10668. DOI: 10.1021/jp401389v.
- (133) Sikka, S. K.; Sharma, S. M. The Hydrogen Bond under Pressure. *Phase Transit.* **2008**, *81*, 907–934. DOI: 10.1080/01411590802098864.
- (134) Patyk, E.; Katrusiak, A. Transformable H-Bonds and Conformation in Compressed Glucose. *Chem. Sci.* **2015**, *6*, 1991–1995. DOI: 10.1039/c4sc03588g.
- (135) Patyk, E.; Jenczak, A.; Katrusiak, A. Giant Strain Geared to Transformable H-Bonded Network in Compressed β -D-Mannose. *Phys. Chem. Chem. Phys.* **2016**, *18*, 11474–11479. DOI: 10.1039/c6cp01286h.
- (136) Forman, R. A.; Piermarini, G. J.; Barnett, J. D.; Block, S. Pressure Measurement Made by the Utilization of Ruby Sharp-Line Luminescence. *Science* **1972**, *176*, 284–285. DOI: 10.1126/science.176.4032.284.
- (137) Mao, H. K.; Xu, J.; Bell, P. M. Calibration of the Ruby Pressure Gauge to 800 Kbar under Quasi-Hydrostatic Conditions. *J. Geophys. Res.* **1986**, *91*, 4673–4676. DOI: 10.1029/jb091ib05p04673.
- (138) Innokenty Kantor, Fluorescence pressure calculation and thermocouple tools. Online, <http://kantor.50webs.com/ruby.htm>.
- (139) Dewaele, A.; Torrent, M.; Loubeyre, P.; Mezouar, M. Compression Curves of Transition Metals in the Mbar Range: Experiments and Projector Augmented-Wave Calculations. *Phys. Rev. B* **2008**, *78*, 104102–104115. DOI: 10.1103/physrevb.78.104102.
- (140) Budzianowski, A.; Katrusiak, A. High-Pressure Crystallographic Experiments with a CCD-Detector. In *High-Pressure Crystallography. NATO Science Series (Series II: Mathematics, Physics and Chemistry)*; Katrusiak, A., Mcmillan, P., Eds.; Springer: Dordrecht, **2004**; Vol. 140.
- (141) Rigaku Oxford Diffraction Ltd, Yarnton, Oxfordshire, CrysAlis PRO, **2017–2021**.

- (142) Sheldrick, G. M. A Short History of SHELX. *Acta Cryst. A* **2008**, *64*, 112–122. DOI: 10.1107/S0108767307043930.
- (143) Sheldrick, G. M. Crystal Structure Refinement with SHELXL. *Acta Cryst. C* **2015**, *71*, 3–8. DOI: 10.1107/S2053229614024218.
- (144) Dolomanov, O. V.; Bourhis, L. J.; Gildea, R. J.; Howard, J. A. K.; Puschmann, H. OLEX2: A Complete Structure Solution, Refinement and Analysis Program. *J. Appl. Cryst.* **2009**, *42*, 339–341. DOI: 10.1107/s0021889808042726.
- (145) Wöhler, F.; Liebig, J. Untersuchungen über das Radikal der Benzoesäure. *Ann. Pharm.* **1832**, *3*, 249–282. DOI: 10.1002/jlac.18320030302.
- (146) Bernstein, J.; Hagler, A. T. Conformational Polymorphism. The Influence of Crystal Structure on Molecular Conformation. *J. Am. Chem. Soc.* **1978**, *100*, 673–681. DOI: 10.1021/ja00471a001.
- (147) Katrusiak, A. Rigid H₂O Molecule Model of Anomalous Thermal Expansion of Ices. *Phys. Rev. Lett.* **1996**, *77*, 4366–4369. DOI: 10.1103/PhysRevLett.77.4366.
- (148) Katrusiak, A. Modelling Hydrogen-bonded Crystal Structures beyond Resolution of Diffraction Methods. *Pol. J. Chem.* **1998**, *72*, 449–459.
- (149) Katrusiak, A. Geometric Effects of H-Atom Disordering in Hydrogen-Bonded Ferroelectrics. *Phys. Rev. B Condens. Matter* **1993**, *48*, 2992–3002. DOI: 10.1103/physrevb.48.2992.
- (150) Tomkowiak, H.; Olejniczak, A.; Katrusiak, A. Pressure-Dependent Formation and Decomposition of Thiourea Hydrates. *Cryst. Growth Des.* **2013**, *13*, 121–125. DOI: 10.1021/cg301254a.
- (151) Roszak, K.; Katrusiak, A. High-Pressure and Environment Effects in Selenourea and Its Labile Crystal Field around Molecules. *Acta Crystallogr. B Struct. Sci. Cryst. Eng. Mater.* **2021**, *77*, 449–455. DOI: 10.1107/S205252062100398X.
- (152) Ng, S. W.; Naumov, P.; Ibrahim, A. R.; Fun, H.-K.; Chantrapromma, S.; Wojciechowski, G.; Brzezinski, B.; Hanna, J. V. X-Ray and Spectroscopic Re-Investigation of the 1:1 Complex Formed between Urotropine and Resorcinol. *J. Mol. Struct.* **2002**, *609*, 89–95. DOI: 10.1016/s0022-2860(01)00945-0.
- (153) Horikoshi, R.; Nambua, C.; Mochida, M. Supramolecular Assembly of Ferrocenes via Hydrogen Bonds: Dimensional Variation in Ferrocenylpyrimidine Complexes with Carboxylic Acids and Aromatic Alcohols. *New J. Chem.* **2004**, *28*, 26–33. DOI: 10.1039/b306699a
- (154) Barooah, N.; Sarmaa, R. J.; Batsanov, A. S.; Baruah, J. B. Structural Aspects of Adducts of N-Phthaloylglycine and Its Derivatives. *J. Mol. Struct.* **2006**, *791*, 122–130. DOI: 10.1016/j.molstruc.2006.01.025
- (155) Bridgman, P. W. Thermodynamic Properties of Twelve Liquids Between 20° and 80° and up to 12000 kgm. per sq. cm. *Proc. Am. Acad. Arts Sci.* **1913**, *49*, 3–113. DOI: 10.2307/20025445
- (156) Zieliński, W.; Katrusiak, A. Hydrogen Bonds NH···N in Compressed Benzimidazole Polymorphs. *Cryst. Growth Des.* **2013**, *13*, 696–700. DOI: 10.1021/cg301374z
- (157) Zieliński, W.; Katrusiak, A. Colossal Monotonic Response to Hydrostatic Pressure in Molecular Crystal Induced by a Chemical Modification. *Cryst. Growth Des.* **2014**, *14*, 4247–4253. DOI: 10.1021/cg5008457

(158) Paliwoda, D.; Dziubek, K. F.; Katrusiak, A. Imidazole Hidden Polar Phase. *Cryst. Growth Des.* **2012**, *12*, 4302–4305. DOI: 10.1021/cg300852t

(159) McCrone, W. C. *Polymorphism. In Physics and Chemistry of the Organic Solid State*. Vol. 2; Fox, D., Labes, M. M., Weissberger, M., Eds.; Wiley Interscience: New York, **1965**.

Appendix A: Summary

My thesis tells *The story of resorcinol crystals and a new perspective for stabilizing high-pressure polymorphs at ambient conditions*. Resorcinol is an important natural product and chemical compound of many applications, including technological ones. Resorcinol is also important from the point of view of the history of science, as it was the first organic compound for which the structures of two polymorphs were determined by X-ray diffraction in the 1930s. Actually, those historic determinations were puzzling, and they continued to be puzzling in the most recent times, because both polymorphs have the same space-group symmetry type and the high-temperature polymorph β is denser than the low-temperature one (α); in 2016 a still denser polymorph ε was discovered, which was even more puzzling. I have shown that polymorph β is not stable under pressure, as it was suggested, and that polymorph ε is the high-pressure form of resorcinol between 0.2 and 0.7 GPa, above which still another new polymorph ζ is stable. This was a surprising outcome because polymorph ε was discovered under ambient pressure (0.1 MPa), but only in the mixture with tartaric acid and with polymorph β . I have obtained polymorph ε in its pure form (without additions), as a single crystal, and I have shown that it is unstable below 0.2 GPa. I have also shown that resorcinol is prone to form solvates under pressure: I have obtained two new hydrates (mono- and duotritohydrate) and the methanol solvate. These solvates are quite intriguing by themselves, as the monohydrate and mono-methanol solvates are isostructural, but the monohydrate is metastable with respect to duotritohydrate, while the duotritomethanol solvate was not found. Also, the duotritohydrate forms a passivation layer on the surface of monohydrate crystals, protecting the metastable phase from dissolution. I established that it is characteristic to all resorcinol phases that they transform between phases with a wide hysteresis, which hampers the investigations of resorcinol forms. Therefore, I had to use the methods of high-pressure in situ isothermal and isochoric recrystallizations in the diamond anvil cell for outlining the pressure/temperature phase diagram and also the preference diagram for the solvates. I consider the discovery of the new polymorph ζ of resorcinol and of the solvates and their stability relations to be a significant achievement. Particularly, polymorph ζ is the first layered structure of pure resorcinol and the first centrosymmetric structure. As for the general achievements, the phase diagram of pure resorcinol indicated that polymorph ε cannot exist under ambient pressure and therefore it was somehow stabilized – I found the method of stabilizing high-pressure phases and tested it not only for resorcinol, but also for other compounds. Thus, this new method to recover and

stabilize high-pressure polymorphs is quite general method for other organic compounds. In fact, my research shows that high-pressure polymorphs can be used for practical applications, which can solve one of the big challenges of high-pressure research, *i.e.* overcoming the instability of the obtained high-pressure polymorphs at ambient conditions. Some of the puzzles connected to the polymorphism of resorcinol still remain unsolved, but certainly many new information about the polymorphs and crystalline forms of resorcinol have been provided in my thesis. Besides the thesis, these results have been summarized in three articles on resorcinol published in *Crystal Growth & Design* and in *Journal of Physical Chemistry C*.

In the first article (R1), I show that the polymorphs α and β can be compressed up to 5.6 GPa and that their α -to- β phase transition does not occur at 0.5 GPa. However, the hydrogen bonds network in polymorphs α show some destabilizing effects close to 0.5 GPa, which is due to the molecular reorientations in the compressed crystal environment. This structural feature of hydrogen bonds OH \cdots O can be the reason for observations by the NMR and IR techniques of the α -to- β phase transition reported in the literature.

Solvates of resorcinol with water and methanol have been discussed in article R2. The monohydrate and duotritohydrate revealed a formation of the passivation layer protecting the metastable form from dissolution. Surprisingly, the duotritohydrate, the more stable and higher-pressure form is disordered, while the monohydrate contains geometrically unfavourable hydrogen bond (by over 0.3 Å longer than expected for OH \cdots O bonds) in its structure.

In article R3, two new high-pressure polymorphs ε and ζ of resorcinol have been revealed. Moreover, in this paper, we stabilized the high-pressure polymorph ε at ambient conditions by doping the resorcinol sample with tartaric acid. We have explained the mechanism leading to this stabilization by the effect of internal pressure. The range of this internal pressure induced by doping can be calculated according to the formula based on our model. These results of high-pressure polymorph stabilization for resorcinol have been consistent also for other well-known compounds (imidazole and benzimidazole derivatives), for which high-pressure polymorphs were obtained previously.

Appendix B: Summary in Polish (Streszczenie w języku polskim)

Moja praca dyplomowa opowiada **Historię kryształów rezorcynolu i nowych sposobów stabilizowania wysokociśnieniowych polimorfów w warunkach normalnych**. Rezorcynol jest ważnym produktem naturalnym i związkem chemicznym o wielu zastosowaniach, w tym technologicznych. Rezorcynol jest również ważny z punktu widzenia historii nauki, ponieważ był pierwszym związkiem organicznym dla którego w latach 30-tych XX wieku określono struktury dwóch odmian polimorficznych metodą dyfrakcji rentgenowskiej. Jednakże, uzyskane wtedy wyniki nawet do niedawna stanowiły zagadkę, ponieważ obie formy mają symetrię tej samej grupy przestrzennej, a wysokotemperaturowa odmiana β ma wyższą gęstość niż niskotemperaturowa odmiana polimorficzna (α); w 2016 roku odkryto formę ϵ o jeszcze wyższej gęstości, co było jeszcze bardziej zagadkowe. Wykazałam, że wbrew wcześniejszym przypuszczeniom to nie odmiana polimorficzna β jest stabilna pod ciśnieniem, lecz faza ϵ jest wysokociśnieniową formą rezorcynolu w ciśnieniu w zakresie między 0.2 a 0.7 GPa, a powyżej tego ciśnienia stabilna jest jeszcze inna forma rezorcynolu, nowy polimorf ζ . Był to zaskakujący wynik, ponieważ odmiana polimorficzna ϵ odkryta została pod ciśnieniem atmosferycznym (0.1 MPa), jednak otrzymana została jedynie, gdy w próbce znajdowała się domieszka kwasu winowego i polimorfu β . W wyniku moich badań uzyskałam formę ϵ w czystej postaci (bez dodatków) jako monokryształ i wykazałam, że jest ona niestabilna poniżej 0.2 GPa. Wykazałam również, że rezorcynol ma skłonność do tworzenia solwatów pod ciśnieniem: uzyskałam dwa nowe hydraty (mono- i duotritohydrat) oraz solwat z metanolem. Odkryte solwaty są same w sobie dość intrygujące, ponieważ monohydrat i solwat z metanolem (w stosunku 1:1) są izostrukuralne, ale monohydrat jest metastabilny w stosunku do duotritohydratu, podczas gdy solwat duotritometanolu nie został znaleziony. Ponadto, duotritohydrat tworzy warstwę pasywacyjną na powierzchni kryształów monohydratu, dzięki czemu są one chronione przed rozpuszczeniem pomimo ich metastabilności. Stwierdziłam, że dla wszystkich faz rezorcynolu charakterystyczne jest występowanie dużej histerezy dla przejść między fazami, co utrudnia ich badania. Dlatego w celu określenia ciśnieniowo-temperaturowego wykresu fazowego oraz wykresu warunków tworzenia solwatów, konieczne było zastosowanie metod izotermicznej i izochorycznej rekrytalizacji wysokociśnieniowej z zastosowaniem komory z kowadełkami diamentowymi. Uważam, że odkrycie nowej odmiany

polimorficznej ζ i solwatów rezorcynolu, oraz wyznaczenie zakresów ich stabilności są znaczącym osiągnięciem. W szczególności odkrycie formy ζ , która jest pierwszą warstwową strukturą czystego rezorcynolu i pierwszą strukturą centrosymetryczną. W kontekście ogólnych osiągnięć, wykazałam na podstawie diagramu fazowego czystego rezorcynolu, że odmiana ε nie może istnieć pod ciśnieniem atmosferycznym w związku z czym musi ona być w jakiś sposób ustabilizowana. Doprowadziło mnie to do znalezienia metody stabilizacji faz wysokociśnieniowych, która przetestowana została nie tylko dla rezorcynolu, ale także dla innych związków. Zatem, ta nowa metoda uzyskiwania i stabilizacji wysokociśnieniowych odmian polimorficznych stosowana być może dla innych związków organicznych. Moje badania pokazują więc, że wysokociśnieniowe odmiany polimorficzne mogą być wykorzystane w praktyce, dzięki rozwiązaniu jednego z wielkich wyzwań badań wysokociśnieniowych, tj. przewyciężenia niestabilności otrzymanych wysokociśnieniowych odmian polimorficznych w warunkach atmosferycznych. Niektóre zagadki związane z polimorfizmem rezorcynolu wciąż pozostają nierozwiązane, niemniej moja praca z pewnością dostarcza wiele nowych informacji na temat odmian polimorficznych i form krystalicznych tego związku. Wyniki stanowiące podstawę tej dysertacji, zostały podsumowane w trzech artykułach naukowych na temat rezorcynolu opublikowanych w czasopismach *Crystal Growth & Design* oraz w *Journal of Physical Chemistry C*.

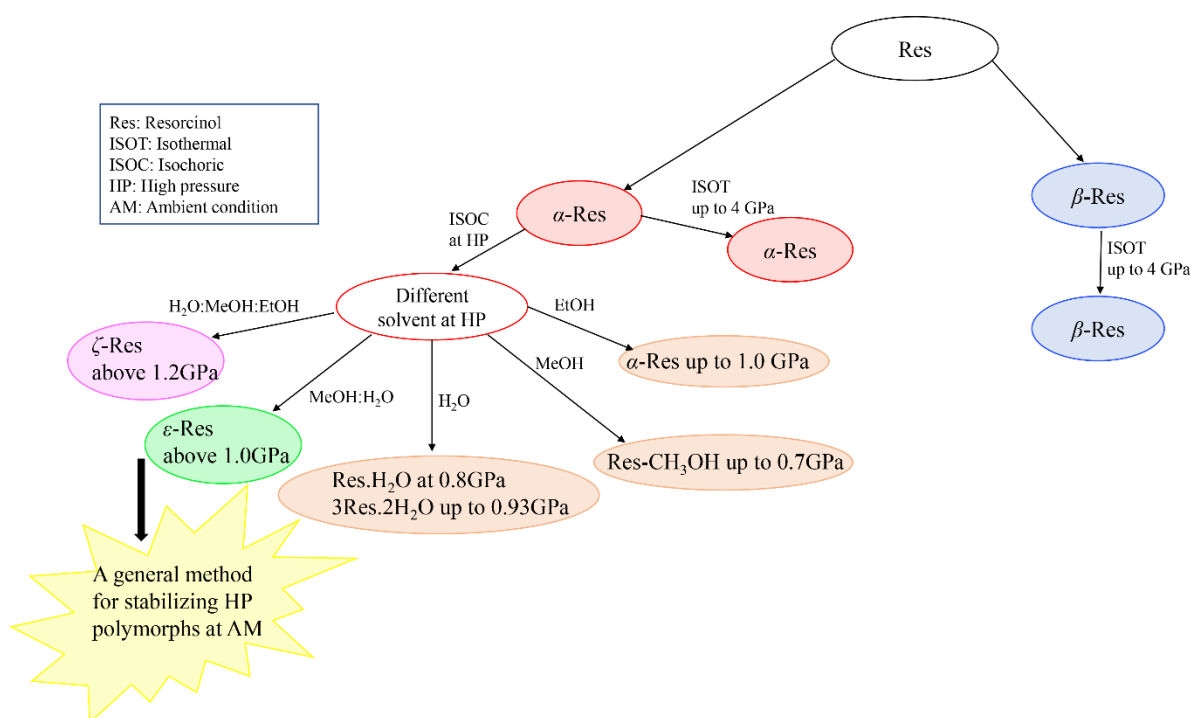
W pierwszym artykule (R1) pokazuję, że odmiany polimorficzne α i β mogą zostać ściśnięte do ciśnienia równego 4.0 GPa bez zajścia przejścia fazowego z formy α do β w ciśnieniu 0.5 GPa. Niemniej sieć wiązań wodorowych w odmianie polimorficznej α wykazuje pewne efekty destabilizujące w ciśnieniu bliskim 0.5 GPa, co spowodowane jest zmianą położenia cząsteczek w ściśniętym kryształ. To z kolei może być powodem zaobserwowania przejścia fazowego z formy α do β , opisanego w literaturze na podstawie wyników badań NMR i IR.

Solwaty rezorcynolu z wodą i metanolem zostały omówione w artykule R2. Monohydrat i duotritohydrat ujawniły tworzenie się warstwy pasywacyjnej chroniącej formę metastabilną przed rozpuszczeniem. Co zaskakujące, duotritohydrat, bardziej stabilna forma powstająca w wyższym ciśnieniu jest nieuporządkowana, a w strukturze monohydratu występuje geometrycznie niekorzystne wiązanie wodorowe (o ponad 0.3 Å dłuższe niż by oczekiwano dla wiązań OH \cdots O).

W artykule R3 przedstawiłam dwie nowe wysokociśnieniowe odmiany polimorficzne ε i ζ rezorcynolu. Ponadto w tej publikacji pokazałam, że wysokociśnieniową odmianę

polimorficzną ϵ można ustabilizować w warunkach atmosferycznych poprzez domieszkowanie próbki rezorcynolu kwasem winowym. Mechanizm prowadzący do tej stabilizacji wyjaśniliśmy efektem ciśnienia wewnętrznego. Zakres tego wewnętrznego ciśnienia wywołanego domieszkowaniem można obliczyć według wzoru opartego na naszym modelu. Wyniki stabilizacji wysokociśnieniowej odmiany polimorficznej rezorcynolu są zgodne z wynikami uzyskanymi dla innych dobrze znanych związków (pochodnych imidazolu i benzimidazolu), których wysokociśnieniowe odmiany polimorficzne zostały otrzymane w przeszłości.

Achievement infographic:



Appendix C: Crystallographic data

Selected crystallographic data of resorcinol polymorphs α , β , ε , γ and ζ and the molecular conformation. This table concerns only the polymorphs, for which the crystals were obtained and the crystallographic data was determined experimentally by X-ray diffraction; for polymorph γ only the unit-cell dimensions and the space-group symmetry were proposed basing on a powder X-ray diffraction measurement, while the full structural information was obtained for other polymorphs α , β , ε and ζ .

Polymorph	α	β	γ	ε	ζ
Pressure (GPa)	0.80(2)	0.91(2)	5.60	0.25(2)	0.70(2)
Space group	$Pna2_1$	$Pna2_1$	$Pnna$	$P2_12_12_1$	$P2_1/c$
Unit cell a (Å)	10.2830(19)	7.5918(6)	7.3346	17.876(5)	10.6348(8)
b	9.1431(7)	12.629(15)	11.486(7)	10.464(6)	9.5004(16)
c	5.5953(3)	5.3029(14)	9.246(5)	5.7045(16)	10.873(2)
β (°)	90	90	90	90	114.713(15)
Volume (Å ³)	526.06(11)	508.4(6)	778.938	1067.0(8)	997.9 (3)
Z/Z'	4/1	4/1	8/1	8/2	8/2
D_x (g/cm ³)	1.390	1.439	-	1.371	1.446
Conformer*	<i>anti-anti</i>	<i>anti-syn</i>	-	<i>anti-syn</i>	<i>anti-syn</i>
Reference	R1	R1	19	R3	R3

*The hydroxyl-group conformation is associated with torsion angles C2-C1-O1-H and C2-C3-O3-H3.

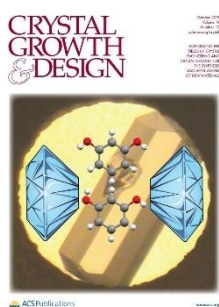
Appendix D: Scientific articles

(R1) Pressure-Dependent Crystallization Preference of Resorcinol Polymorphs

F. Safari, A. Olejniczak, A. Katrusiak,

Cryst. Growth Des. **2019**, *19*, 5629–5635.

DOI: 10.1021/acs.cgd.9b00610



Declarations of co-authors contribution to this article, included in this thesis:

In paper “Pressure-Dependent Crystallization Preference of Resorcinol Polymorphs” published in *Cryst. Growth Des.* **2019**, *19*, 5629–5635, I have done the experimental part of this research and prepared manuscript and all plots and tables. I assess my contribution as 80%.


In paper “Pressure-Dependent Crystallization Preference of Resorcinol Polymorphs” published in *Cryst. Growth Des.* **2019**, *19*, 5629–5635, I have checked the result of experiments especially such as Cifs files and tables and also, I have supported F. Safari if she had some problems with the experiments. I assess my contribution as 10%.

In paper “Pressure-Dependent Crystallization Preference of Resorcinol Polymorphs” published in *Cryst. Growth Des.* **2019**, *19*, 5629–5635, I have suggested the subject, discussed the research and results and participated in writing this publication. I assess my contribution as 10%.

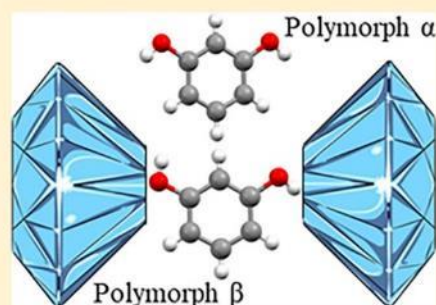
Pressure-Dependent Crystallization Preference of Resorcinol Polymorphs

Fatemeh Safari, Anna Olejniczak,[✉] and Andrzej Katrusiak*[✉]

Faculty of Chemistry, Adam Mickiewicz University, Uniwersytetu Poznańskiego 8, 61-614 Poznań, Poland

 Supporting Information

ABSTRACT: Polymorph α of resorcinol, at ambient pressure stable to 365 K when it transforms to polymorph β , is exceptionally resistant to high pressure. The crystals of polymorph α can be compressed to over 4 GPa without transforming to the β phase. We have performed high-pressure recrystallization of resorcinol aqueous and methanol solutions, and they yielded polymorph α below 0.5 GPa and polymorph β above this pressure. Our single-crystal X-ray diffraction studies on resorcinol polymorphs in a diamond-anvil cell reveal the structural origins of the phase transition. The high pressure changes the angular dimensions of bistable hydrogen bonds OH \cdots O, which destabilizes the H-atoms and the structure of polymorph α above 0.5 GPa, consistent with the calorimetric and NMR results. The high-temperature, high-pressure polymorph β achieves the more dense packing through the changed conformation of one of the hydroxyl groups and the considerable twisting of the hydrogen bonds necessary for the formation of additional C–H \cdots π bonds. The large temperature and pressure hysteresis of the polymorphs α and β are connected with the different topologies of their O–H \cdots O networks.



INTRODUCTION

Resorcinol, an intermediate often used in chemical practice and a pharmaceutical agent, was one of the first organic compounds for which the phenomenon of polymorphism was described and the first organic compound for which the structures of both polymorphs were determined in 1938 by Robertson and Ubbelohde.^{1,2} Until today, the resorcinol crystals belong to the best known examples of polymorphs.³ However, despite numerous studies of resorcinol by X-ray diffraction,⁴ NMR,⁵ Raman and IR spectroscopy,⁶ and by other methods, there are still unresolved issues regarding the low-temperature phase α , stable below 365 K, and high-temperature polymorph β , stable from 365 K to the melting point at 383 K.⁴ For example, it is intriguing that these two significantly different polymorphs α and β crystallize in the same orthorhombic space group $Pna2_1$. Moreover, it is counterintuitive that the lower-temperature polymorph α is less dense than the high-temperature β phase.⁶ These and other aspects of the resorcinol properties have prompted renewed interest and frequent studies on this generally applied chemical agent.⁷ Besides, resorcinol can be considered a model structure representing a large group of similar natural and synthetic compounds often applied in laboratory practice and chemical technologies. For example, the crystals of natural product orcinol (3,5-dihydroxytoluene) is known in two polymorphic forms, too, and like resorcinol it is prone to form various cocrystalline compounds.⁸

Despite the simple molecular structure, resorcinol can exist in several conformations, described as *anti-anti*, *anti-syn*, and *syn-syn* depending on the hydroxyl proton position with

respect to atom C2 in molecular fragment HO–C–C–OH (Figure 1). Phases α and β differ in the conformation and

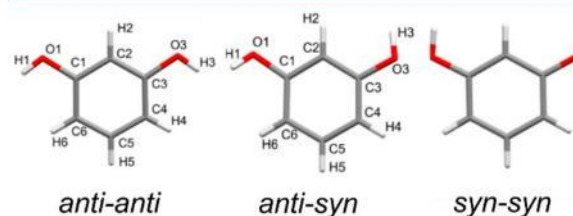


Figure 1. Resorcinol molecules in conformations *anti-anti* and *anti-syn* as present in polymorphs α and β (this study) and conformation *syn-syn* (as present in the cocrystal of resorcinol with 1,2-bis(4-pyridyl)ethane(4,4'-bipyeth)).¹¹

hence can be described as conformational polymorphs.³ The conformational transformations of resorcinol and its analogues are considered the key molecular property responsible for the polymorphism and extensive cocrystallization of these compounds.⁸ Presently there are 77 resorcinol single- and multicomponent crystals deposited in the Cambridge Structural Database (CSD), of which in 25 compounds the molecule assumes conformation *anti-anti* and in 22 compounds conformation *anti-syn*; all 30 resorcinol molecules present in conformation *syn-syn* have been found exclusively

Received: May 8, 2019

Revised: July 26, 2019

Published: August 14, 2019

in cocrystals. Most importantly, in the crystals of resorcinol, its cocrystals, and analogues, the molecular conformation (of hydroxyl groups) is coupled to the directions of intermolecular H-bonds. Consequently, the molecular conformation and the framework of H-bonded molecules are coupled. It was shown for the groups of 1,3-cyclohexane derivatives as well as for the OH...O bonded ferroelectrics, so-called KH_2PO_4 (often abbreviated KDP) type ferroelectrics,^{9,10} that the molecular conformation and the configuration of H-bonds in aggregates affect the proton dynamics and phase transitions.

The large density difference between resorcinol polymorphs α and β prompted the assumption that high pressure would compress the low-density α phase into the β phase, despite enormous structural differences between their structures.^{6,12} Raman studies revealed that at room temperature the α -to- β phase transition occurs at 0.50 GPa,¹³ but when the pressure was increased in large steps, phase α persisted until 1.0 GPa, and then the mixture of coexisting phases α and β was observed until 2.5 GPa.¹² This result is consistent with the NMR measurements of spin-lattice relaxation times in the temperature range 280–380 K and pressure up to 800 MPa, revealing the α -to- β phase transition at 0.4 GPa.⁵ However, the compression of the powdered samples of resorcinol in polymorphs α and β did not cause their transition up to 4.0 and 5.0 GPa, respectively.¹⁴ Besides, new high-pressure phases of resorcinol were reported: phase γ was observed by X-ray powder diffraction above 5.0 GPa;⁵ phase δ was detected by Raman spectroscopy above 2.5 GPa;¹³ and also the orthorhombic ϵ polymorph of space group $P2_12_12_1$ was found.¹⁵ The P - T phase diagram of resorcinol is outlined in Figure 2 (Table S1). However, to our knowledge, no direct evidence of the α -to- β phase transformation at 0.50 GPa was ever observed for single crystals. Also no reverse β -to- α phase transition has been observed neither by us nor reported in the literature.

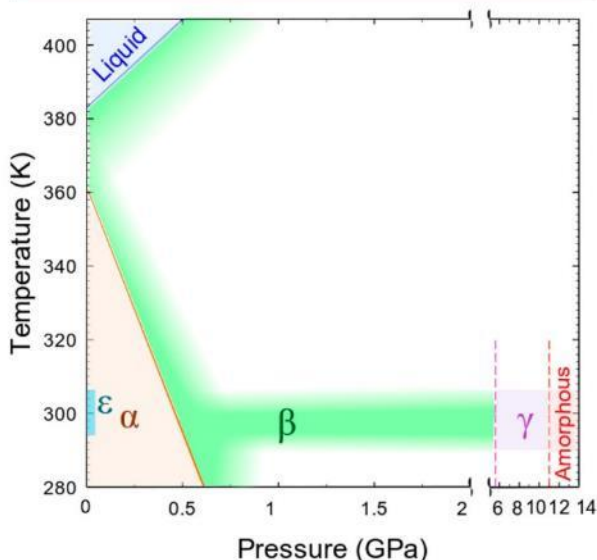


Figure 2. P - T diagram of resorcinol phases (labeled by Greek letters) according to this study and references.^{6,13} Note the changed abscissa-axis scale behind the break. The unexplored territories are left white.

EXPERIMENTAL SECTION

Single crystals of α -resorcinol were prepared by slowly evaporating the methanol and toluene solutions at ambient pressure and room temperature. The β polymorph was obtained by performing the crystallization above 365 K, both at ambient and elevated pressure. Single crystals of polymorph β were stored for weeks at normal conditions with no signs of their transformation.

The ambient and high-pressure single-crystal X-ray diffraction data were measured with a four-circle KUMA X-ray diffractometer with graphite monochromated Mo $K\alpha$ radiation. Previously described procedures were applied for the crystal centering and data collection;¹⁶ the UB-matrix determination and data reduction were performed with program CrysAlisPro15.¹⁷ The structures were refined by full-matrix least-squares on F^2 using the program Shelx-T incorporated in Olex2.^{18,19}

The structures of polymorphs α and β were determined at ambient conditions (296 K/0.1 MPa), and then they were applied as the starting models for the refinements of the high-pressure structures. The ambient-pressure structures determined by us were the references for the analysis of changes induced by pressure in polymorphs α and β . The high-pressure experiments were performed in a Merrill-Bassett diamond anvil cell (DAC), modified by mounting the diamond anvils directly on the steel backing plates. Pressure was calibrated with a Photon Control spectrometer by the ruby-fluorescence method with a precision of 0.03 GPa, and the calibration was performed before and after the diffraction measurement.²⁰

Two types of high-pressure experiments were performed. In one series, the sample crystal was mounted inside the DAC chamber, and Daphne oil 74.74²¹ was used as a pressure-transmitting medium; a cotton fiber fixed the sample position in order to eliminate any strains while increasing pressure. We also applied the EtOH solution of resorcinol, saturated in order to prevent the dissolution of the α -resorcinol sample, as the hydrostatic fluid. In another series, aimed at investigating the stability of the α and β phases as a function of pressure, we grew single crystals in situ in the DAC chamber of resorcinol of methanol/water solutions. This method of crystallization, by increasing pressure in isothermal conditions close to the room temperature, was aimed at observing the preference for the formation of polymorphs α and β as a function of pressure. The isothermal compression usually led to the nucleation of several grains, after which by oscillating pressure we could select one of them for growing the single-crystal sample (Figure 3). Then its polymorphic form was verified by X-ray diffraction. The concentration of the starting

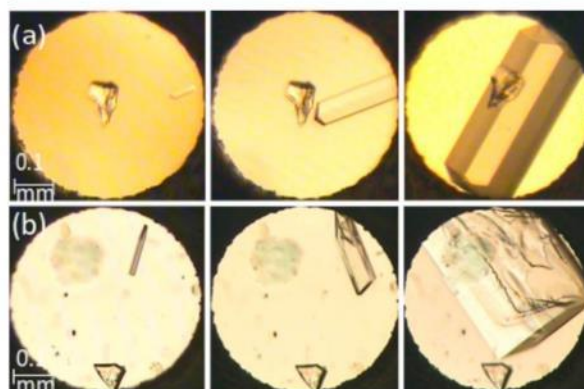


Figure 3. Single crystals of resorcinol grown of ethanol solution in the DAC chamber: (a) polymorph α isothermally (at 296 K) nucleated at 0.25 GPa (left), then isothermally compressed to 0.40 GPa (middle) and 0.50 GPa (right); as well as (b) polymorph β nucleated at isochoric conditions at 396 K after which temperature and pressure stabilized at 296 K/0.91 GPa (right). Small ruby chips for pressure calibration lie at the center (a) and bottom (b) of the DAC chambers.

Table 1. Selected Crystal Data of Resorcinol α and β at 296 K^a

polymorph	α	α	β	β
pressure (GPa)	0.0001	0.52	0.0001	0.50
space group	<i>Pna2</i> ₁	<i>Pna2</i> ₁	<i>Pna2</i> ₁	<i>Pna2</i> ₁
unit cell: <i>a</i> (Å)	10.5496(7)	10.345(4)	7.9269(3)	7.7108(15)
<i>b</i>	9.5704(7)	9.271(3)	12.6126(5)	12.611(5)
<i>c</i>	5.6693(5)	5.6111(10)	5.5206(2)	5.379(5)
volume (Å ³)	572.39(8)	538.1(3)	551.94(4)	523.1(7)
<i>Z</i> / <i>Z'</i>	4/1	4/1	4/1	4/1
<i>D</i> _x (g/cm ³)	1.278	1.359	1.325	1.398
$\Delta\eta_1 = \eta_s - \eta_d$ (°)	17.12	13.4	5.89	7.4
$\Delta\eta_3 = \eta_a - \eta_d$ (°)	2.26	-1.8	1.99	1.02

^aThe $\Delta\eta_1$ is the difference between angles O1...O3ⁱ-C3ⁱ (η_a) and C1-O1...O3ⁱ (η_d) in H-bond O1-H1...O3ⁱ; and $\Delta\eta_3$ is the analogous difference $\eta_a - \eta_d$ for O3-H3...O1ⁱⁱ (subscripts a and d denote the H-acceptor and H-donor sites).

solution was adjusted in a way that the nucleation occurred at various points of the pressure range 0.2–1.0 GPa (the lower the concentration, the higher the pressure was required for the nucleation to occur). Alternatively, when we aimed at the β phase, the recrystallization was performed in isochoric conditions; the sample could be heated above the phase transition temperature at 360 K, and then the temperature was gradually cooled down to room temperature.

The crystal data were determined at 0.12, 0.40, 0.52, 0.80, 1.04, 2.0, and 2.5 GPa (in Daphne oil as the hydrostatic medium) for polymorph α and at 0.50 and 0.91 GPa for polymorph β . Our diffraction data showed that the α -phase is monotonically compressed up to 2.5 GPa (Figures 3 and S1), and no phase transitions were detected. The crystal data of resorcinol polymorphs in high pressure are listed in Tables S2 and S3 in Supporting Information.

DISCUSSION

The crystallographic data of resorcinol polymorphs α and β at the normal conditions and high-pressure are summarized in Table 1 (cf. Tables S1–S3 in the Supporting Information). The isothermal recrystallizations of resorcinol polymorph α of the methanol/water solutions below 0.5 GPa confirm that it is stable in this pressure range (Figure S2). However, above 0.5 GPa both polymorphs α and β were obtained. These results of isothermal crystallizations suggest that polymorph β becomes favored above 0.5 GPa. The formation of polymorph β is consistent with the reports on the α -to- β transformation on increasing pressure above 0.5 GPa.^{5,6,13} The nucleation of polymorph α along with β above 0.5 GPa is in accordance with the Ostwald rule, which allows the formation of the metastable polymorphs when the substance is crystallized from the melt or solution.

The nucleation of both polymorphs above 0.5 GPa, in the stability region of polymorph β , is also an indication that their structures are significantly different and cannot easily transform between themselves. Owing to the significantly different molecular conformation (Figure 1), different crystal packing, molecular orientation (Figure 4), and H-bonding networks (Figure 5), polymorph β can be cooled down to room temperature, nearly 100 K below the temperature of the α -to- β transformation. Likewise, polymorph α can persist to about 4.0 GPa, about 3.5 GPa over the pressure-induced α -to- β transformation.

The three-dimensional H-bonding network in polymorph α (Figure 5) incorporates two types of polar helices running along the crystal [*z*] direction: C₄⁴ (8) between hydroxyl groups, where all O–H projections on the [*z*] axis are directed downward, and C₄⁴ (24) involving the molecular ring atoms,

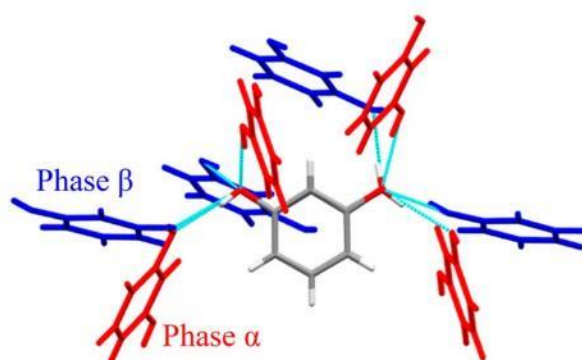


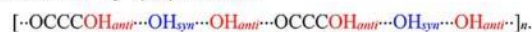
Figure 4. Resorcinol molecules with their rings exactly overlaid (gray) and their H-bonded neighbors in polymorphs α (red) and β (blue).²¹ The H-bonds are indicated in cyan.

where all O–H projections on the [*z*] axis are directed downward, too. The C₄⁴ (8) helix is smaller, and its one full turn consists of eight atoms, so its thread can be encoded as [\cdots HO \cdots HO \cdots HO \cdots HO \cdots]_n while the C₄⁴ (24) helix is larger in diameter and can be encoded as [\cdots OCCCCO \cdots HOCCCCO \cdots OCCCCO \cdots HOCCCCO \cdots]_n. The pitch of both the helices is exactly the same and equal to the unit-cell parameter *c*. It is also characteristic that each full turn of both helices involves four resorcinol molecules.

The H-bonding network in polymorph β incorporates two types of helices, too (Figure 5b): helix C₂² (12) involves two molecules per one full turn, and each of the molecules acts as the H-acceptor and H-donor (the hydroxyl group in the *syn* conformation), and helix C₆⁶ (20) involves two molecules and four hydroxyl groups from four neighboring molecules. The C₂² (12) helix can be encoded as



while the C₆⁶ (20) helix as



Apart from this topological difference between the H-bonded networks, there is a considerable difference in the crystals polarity because in polymorph α all projections of hydroxyl groups OH on the [*z*] axis are directed downward, whereas in polymorph β the projections on the [*z*] axis of groups OH_{syn} are directed upward and of groups OH_{anti} downward. The polarity of polymorphs α and β can be also considered in terms of the polarization of the conformers. The dipole moment (μ) of conformer *anti*–*anti* in polymorph α is

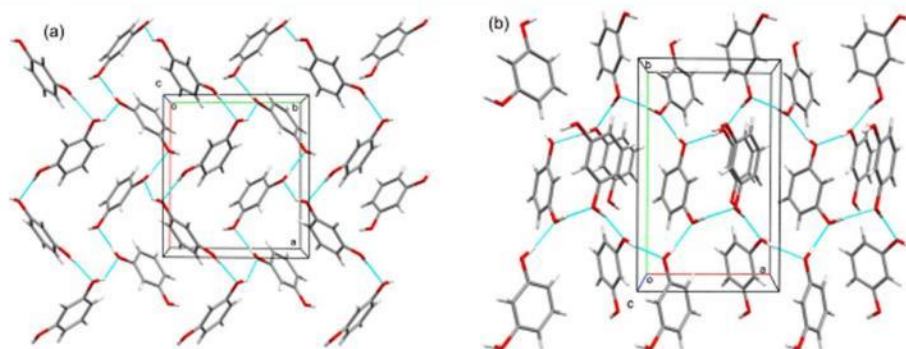


Figure 5. Auto-stereographic projections of (a) polymorph α at 0.52(2) GPa; and (b) polymorph β at 0.50(2) GPa. The H-bonds are indicated by the cyan lines.

3.08 D (debye = 3.336×10^{-30} C·m), compared to 1.57 D of molecule *anti-syn* in polymorph β ; the dipole moment of the *syn-syn* conformer is 2.07 D.^{22–24} More recent calculations give the μ projections (on the molecular axis passing through atoms C2 and C5) equal to -2.27 , 0.06 , and 2.37 D, respectively. According to these data, polymorph α is much more polar than polymorph β . The arrangement of polar molecules and groups has its consequences for the intermolecular interactions: the energy of electrostatic interactions for the parallel arrangement of dipoles is less favored than the antiparallel arrangement. The increased pressure reduces the intermolecular distance, and the interactions between parallel repelling dipoles can favor their conversion to the antiparallel attracting arrangement. These electrostatic interactions can contribute to the larger molecular volume of polymorph α compared to polymorph β .

It is also exceptional that in the low-temperature/low-pressure polymorph α the molecules assume the *anti-anti* conformation, by about 0.83 kJ mol $^{-1}$ less favored than the lowest-energy conformation *anti-syn*, present in polymorph β .²⁵ In most compounds, the less favored conformation is “forced” in the high-pressure phases, although the exceptions similar to that of resorcinol are known, too.²⁶ Thus there are two structural features of polymorph α that are energetically unfavorable compared to polymorph β : electrostatic interactions between dipoles close to parallel and the *anti-anti* conformation. In the compressed crystal, the dipoles are moved closer and their repelling increases, which can be considered as one of destabilizing factors contributing to the α -to- β transformation.

Polymorph α is clearly more strongly compressible than polymorph β in the initial range of pressure between 0.1 MPa and 2.0 GPa, but then their compression becomes approximately equal, and the V_m difference of about $\Delta V_m = 1$ Å 3 persists in the higher pressure range (Figure 6). It shows that the less efficient crystal packing of molecules in polymorph α (at 0.1 MPa 22.1% of void space accessible by spheres 0.5 Å in radius, compared to 15.2% in polymorph β) is a destabilizing factor of polymorph α , associated with the work energy difference $p\Delta V_m$ of about 1.2 kJ·mol $^{-1}$ at 0.5 GPa; 2.0 kJ·mol $^{-1}$ at 1.0 GPa, and 4.0 kJ·mol $^{-1}$ at 4.0 GPa.

It can be noted that the linear compression of polymorphs α and β is significantly different in all pressure range and that there is no indication that the compression becomes more similar in the region of 0.5 GPa or at still higher pressure (see Figures S2 and S4). Direction [y], most compressed in

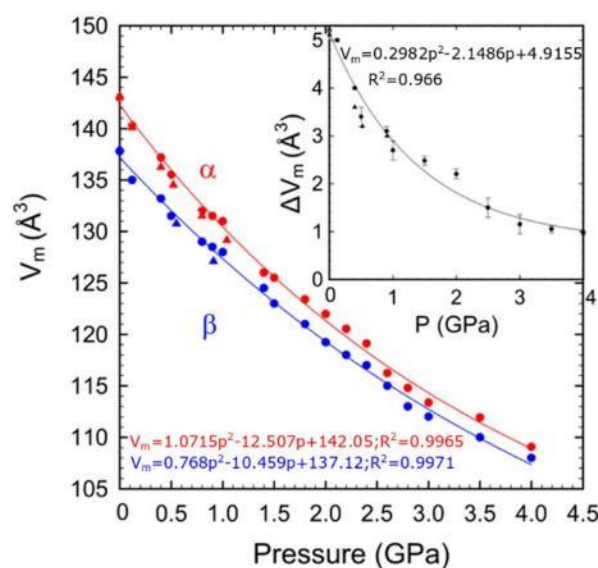


Figure 6. Molecular volume ($V_m = V/Z$) of resorcinol polymorphs α and β , plotted as a function of pressure up to 4 GPa. Triangles and circles represent our and Kichanov's et al.⁵ results. The inset shows the molecular volume difference ΔV_m between the polymorphs (see Figure S5).

polymorph α , is the least compressed direction of polymorph β ; and the polar direction [z] is the hardest direction of polymorph α , and it is the softest direction of polymorph β . The linear compression of the polymorphs further illustrates their significant differences, which are not reduced with pressure. This type of lattice strain rules out the isostructural relations between these polymorphs, despite the same space group symbol (Figure 6).

The pressure dependence of the lattice parameters demonstrates that the compression mechanism in both polymorphs relies on distortion of the H-bonded networks due to the shortening of H \cdots O distances and bending of the OH \cdots O angles of the H-bonds. In polymorph α , the distances in independent hydrogen bonds O1–H1 $_{anti}$ \cdots O3 $^i_{syn}$ (symmetry code: $x - 0.5, 1.5 - y, z$) and O3–H3 $_{anti}$ \cdots O1 $^i_{syn}$ (symmetry code: $1.5 - x, y - 0.5, z - 0.5$) are nearly identical, and they are compressed at very similar rates (Figure 7, Tables S5 and S8). The H-bond C–O \cdots O i angles on the H-donor site (in polymorph α associated with the *anti* direction: C1–O1 $_{anti}$ \cdots

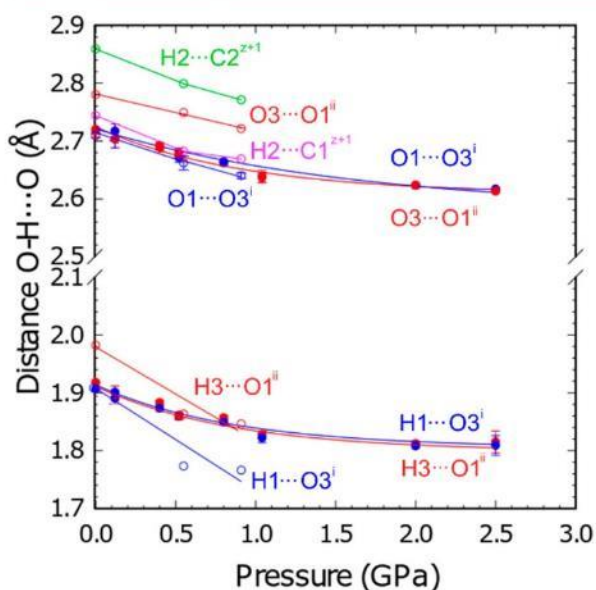


Figure 7. Pressure dependence of hydrogen-bond distances OH...O and O...O and in resorcinol polymorphs α (full circles) and β (empty circles); also the short distances H2...C2 (green) and H2...C1 (pink) in β -resorcinol have been indicated. Dimensions of hydrogen bonds O1H1...O3 are marked in blue, and those of O3H3...O1 are marked in red; the symmetry codes are in the text.

O3ⁱ_{syn} and C3–O3ⁱⁱ_{anti}...O1ⁱⁱ_{syn}) are very consistent (both of about 115.5°), and they are hardly pressure-dependent (Figure 8). The O...Oⁱ–Cⁱ angles on the H-acceptor site (in polymorph α they are associated with the *syn* direction: O1^{anti}...O3ⁱ_{syn}–C3ⁱ and O3^{anti}...O1ⁱⁱ_{syn}–C1ⁱⁱ), as expected, are larger than the H-donor C–O...Oⁱ angles;^{27,28} however, their

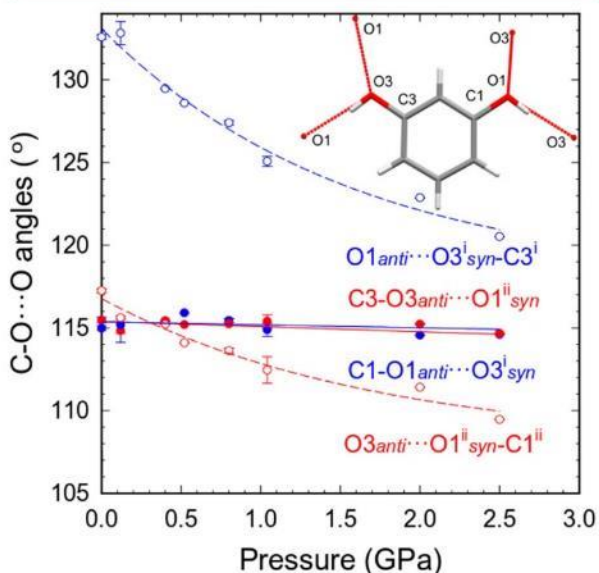


Figure 8. Pressure dependence of hydrogen-bond angles C–O...O on the H-donor side (full symbols and full lines) and on the H-acceptor side (open symbols and dashed lines) in polymorph α . The dimensions for hydrogen bond O1H1...O3ⁱ are marked in blue, and those for O3H3...O1ⁱⁱ are in red (cf. Table S6).

values are significantly different (Figure 8). Most importantly, H-acceptor angle O1^{anti}...O3ⁱ_{syn}–C3ⁱ, of 132.75(14)° at 0.1 GPa, is much larger than H-donor angles C1–O1^{anti}...O3ⁱ_{syn} and C3–O3^{anti}...O1ⁱⁱ_{syn}, both around 115°, which is strongly preferential for the hydroxyl H-atoms location in the *anti* sites. At 0.1 MPa, the other H-acceptor angle O3^{anti}...O1ⁱⁱ_{syn}–C1ⁱⁱ is 117.24(12), and therefore it favors the *anti* H-site, too. However, both the H-acceptor angles are reduced by the increasing pressure, and at about 0.4 GPa the H-acceptor angle O3^{anti}...O1ⁱⁱ_{syn}–C1ⁱⁱ becomes smaller than its H-donor counterpart C3–O3^{anti}...O1ⁱⁱ_{syn} (Figure 8). This interconversion locally destabilizes the H-site, although the H-bonding network of polymorph α is strongly stabilized by the substantial difference between H-donor and H-acceptor sides in bond C1–O1–H1^{anti}...O3ⁱ_{syn}–C3ⁱ. Pressure strongly reduces this difference, from 17.12° at 0.1 MPa to 5.91° at 2.50 GPa, and it can be extrapolated that at about 2.5 GPa this difference will become smaller than that of the H-destabilizing effect of bond C3–O3–H3^{anti}...O1ⁱⁱ_{syn}–C1ⁱⁱ (Figure 8). Thus, in that pressure range both the *anti* H-sites are destabilized, and the *syn* sites are favored for the geometrical reasons (Figure S6, Table S10). Theoretically, the relocation of H-atoms (either through the OH rotations or H-transfers) is possible; however, it would drastically change the electrostatic interactions in the crystal.

It is plausible that O3–H3 rotates first, and then the avalanche of the structural reconstructions follows, involving the H-bonds breaking, molecular shifts, and reorientations as well as the formation of the new H-bonding network of the β phase.

It can be noted that in polymorph β the distortions of the H-bonds from directions *syn* and *anti* on their H-acceptor side are very strong. In phase α , in both H-bonds the torsion angles C2–C–O...Oⁱ (where unprimed atoms are on the H-donor side and the primed one on the H-acceptor side) are close to 180° corresponding to the *anti* configuration and torsion angles O...Oⁱ–Cⁱ–C2ⁱ are close to 20° and 50°, which can be still classified as the *syn* configuration. In phase β , in hydrogen bond C1–O1–H1^{anti}...O3ⁱ_{syn}–C3ⁱ (symmetry code: 1.5 – x, y + 0.5, z + 0.5) the torsion angles C2–C–O...Oⁱ and O...Oⁱ–Cⁱ–C2ⁱ correspond to the *anti* and *syn* configurations (Figure S6), but in bond C3–O3–H3^{anti}...O1ⁱⁱ_{syn}–C1ⁱⁱ (symmetry code: 1–x, 1–y, z–0.5) the torsion angle O...Oⁱⁱ–Cⁱⁱ–C2ⁱⁱ on the acceptor side is close to 90° and cannot be classified as *syn* or *anti*. Thus, these configuration descriptors cannot be applied for the H-acceptor side in bond C3–O3–H3^{anti}...O1ⁱⁱ_{syn}–C1ⁱⁱ in phase β , and the actual value of the torsion angle O3...O1ⁱⁱ–C1ⁱⁱ–C2ⁱⁱ has been specified in their stead (Figure S6, Table S10). This is an important structural feature of phase β because these torsion angles of H-bonds O–H...O (Figure S7) allow that new hydrogen bonds C–H... π are formed, as indicated by short intermolecular contacts C2–H2...C6ⁱⁱ of 2.58 Å and C2–H2...C5ⁱⁱ of 2.63 Å. In phase β , the H-donor C–O...O angles are smaller than H-acceptor angles O...O1–C, at 0.1 MPa 117.79(12)° versus 119.78(2)° for H-bond O1–H1^{anti}...O3ⁱ–C3ⁱ and 113.69(4)° versus 119.58(5)° in H-bond O3–H3^{anti}...O1ⁱⁱ–C1ⁱⁱ, respectively. These angles are hardly pressure dependent in the investigated pressure range, as illustrated in Figure 8 (cf. Figure S8), so these magnitudes of pressure do not destabilize the β phase. It can be also noted that in both polymorphs the pressure reduces the inclination of molecules to the polar axis [z]. This reduced inclination is consistent with the increased polarity of crystals, which corresponds to the increased intermolecular electrostatic interactions of molecules

in the crystal structures. It is characteristic that the transformation from polymorph α to polymorph β considerably increases the inclination angle (Figure 9), and simultaneously

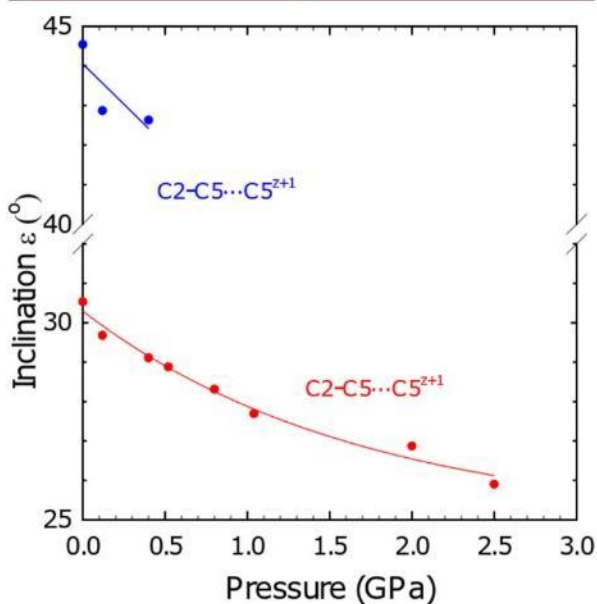


Figure 9. Inclination of the molecular axis $C5\cdots C2$ to the crystal axis $[z]$, plotted as a function of pressure for resorcinol polymorphs α (red) and β (blue).

the dipole moments of the anti–anti molecule (2.67 D) are reduced in the anti–syn molecule (1.42 D). Consequently, the polarity of the crystal is reduced and so are the electrostatic interactions in the structure of polymorph β .

CONCLUSIONS

Our study on resorcinol identified several pressure-induced structural features destabilizing polymorph α . The volume difference favoring the α -to- β transformation at high pressure has been confirmed. This more compact molecular packing in polymorph β leads to the formation of hydrogen bonds $C-H\cdots\pi$, absent in polymorph α . However, the formation of bonds $C-H\cdots\pi$ requires that the H-bonds are twisted off the planes of favored planar configurations *anti* and *syn*. It is apparent that the hydrogen-bonds network in polymorph α is destabilized by the reversal of $C-O\cdots O$ angles for bonds $O3_{anti}H\cdots O1_{syn}^{ii}$ and a gradual reduction of the difference in $C-O\cdots O$ angles on the H-donor and acceptor sides for bond $O1_{anti}H\cdots O3_{syn}^i$. Thus, it is plausible that high pressure destabilizes the positions of the hydroxyl H-atoms and that a similar effect can be the reason for the temperature-induced transformations.

The lack of correlations in the lattice dimensions between polymorphs α and β rules out their isostructural relation. The symmetry elements of space groups involve the unit translations, and these are considerably different for these polymorphs. Besides, these two structures are distinguishable by the different H-bonding networks and conformations of the hydroxyl hydrogen atoms.

ASSOCIATED CONTENT

Supporting Information

The Supporting Information is available free of charge on the ACS Publications website at DOI: 10.1021/acs.cgd.9b00610.

Tables with crystal data and structure refinements details, the short contacts $C-O\cdots O$ in high-pressure structures, plots of unit-cell parameters a , b , and c and unit-cell volume V , compression of unit-cell dimensions, relative volume changes as a function of pressure, geometric dimensions of hydrogen bonds $C-OH\cdots O$ as a function of pressure (PDF)

Accession Codes

CCDC 1913232–1913242 contain the supplementary crystallographic data for this paper. These data can be obtained free of charge via www.ccdc.cam.ac.uk/data_request/cif, or by emailing data_request@ccdc.cam.ac.uk, or by contacting The Cambridge Crystallographic Data Centre, 12 Union Road, Cambridge CB2 1EZ, UK; fax: +44 1223 336033.

AUTHOR INFORMATION

Corresponding Author

*E-mail: katran@amu.edu.pl. Phone: +48 61 829 1590.

ORCID

Anna Olejniczak: 0000-0002-4460-4362

Andrzej Katrusiak: 0000-0002-1439-7278

Funding

The authors are grateful to the Center of Advanced Technology for granting the access to X-ray diffractometers. This study was supported by the Polish Ministry of Higher Education; F.S. is grateful to the EU European Social Fund, Operational Program Knowledge Education Development, Grant POWR.03.02.00–00-I026/16.

Notes

The authors declare no competing financial interest.

REFERENCES

- Robertson, J. M. The Structure of Resorcinol a quantitative X-ray investigation. *Proc. R. Soc. London A* **1936**, *157*, 79–99.
- Robertson, J. M.; Ubbelohde, A. R. A New Form of Resorcinol. *Proc. R. Soc. London A* **1938**, *167*, 122–135.
- Bernstein, J. Polymorphism – A Perspective. *Cryst. Growth Des.* **2011**, *11*, 632–650.
- Bacon, G. E.; Curry, N. A. A Study of α -Resorcinol by Neutron Diffraction. *Proc. R. Soc. London A* **1956**, *235*, 552–559.
- Kichanov, S. E.; Kozlenko, D. P.; Bilski, P.; Wasicki, J.; Nawrocik, W.; Medek, A.; Hancock, B. C.; Lukin, E. V.; Lathe, C.; Dubrovinsky, L. S.; Savenko, B. N. The Polymorphic Phase Transformations in Resorcinol at High Pressure. *J. Mol. Struct.* **2011**, *1006*, 337–343.
- Deb, S. K.; Rekha, M. A.; Roy, A. P.; Vijayakumar, V.; Meenakshi, S.; Godwal, B. K. Raman-Scattering Study of High-Pressure Phase Transition and Amorphization of Resorcinol. *Phys. Rev. B: Condens. Matter Mater. Phys.* **1993**, *47*, 11491–11494.
- Dressler, H. *Resorcinol, Its Uses and Derivatives*; Springer Science +Business Media: New York, 1994; DOI: 10.1007/978-1-4899-0999-2
- Mukherjee, A.; Grobelny, P.; Thakur, T. S.; Desiraju, G. R. Polymorphs, Pseudopolymorphs, and Co-Crystals of Orcinol: Exploring the Structural Landscape with High Throughput Crystallography. *Cryst. Growth Des.* **2011**, *11*, 2637–2653.
- Zhang, Q.; Chen, F.; Kioussis, N.; Demos, S. G.; Radousky, H. B. Ab Initio Study of the Electronic and Structural Properties of the

Ferroelectric Transition in KH_2PO_4 . *Phys. Rev. B: Condens. Matter Mater. Phys.* **2001**, *65*, 024108–024110.

(10) Katrusiak, A. Geometric Effects of H-atom Disordering in Hydrogen-Bonded Ferroelectrics. *Phys. Rev. B: Condens. Matter Mater. Phys.* **1993**, *48*, 2992–3002.

(11) Papaefstathiou, G. S.; MacGillivray, L. R. Discrete versus Infinite Molecular Self-Assembly: Control in Crystalline Hydrogen-Bonded Assemblies Based on Resorcinol. *Org. Lett.* **2001**, *3*, 3835–8.

(12) Ebisuzaki, Y.; Askari, L. H.; Bryan, A. M.; Nicol, M. F. Phase Transition in Resorcinol. *J. Chem. Phys.* **1987**, *87*, 6659–6664.

(13) Druźbicki, K.; Mikuli, E.; Palka, N.; Zalewski, S.; Ossowska-Chruściel, M. D. Polymorphism of Resorcinol Explored by Complementary Vibrational Spectroscopy (FT-RS, THz-TDS, INS) and First-Principles Solid-State Computations (Plane-Wave DFT). *J. Phys. Chem. B* **2015**, *119*, 1681–1695.

(14) Rao, R.; Sakuntala, T.; Godwal, B. K. Evidence for High-Pressure Polymorphism in Resorcinol. *Phys. Rev. B: Condens. Matter Mater. Phys.* **2002**, *65*, No. 054108.

(15) Zhu, Q.; Shtukenberg, A. G.; Carter, D. J.; Yang, T.; Yu, J.; Chen, M.; Raiteri, P.; Oganov, A. R.; Pokroy, B.; Polishchuk, I.; Bygrave, P. J.; Day, G. M.; Rohl, A. L.; Tuckerman, M. E.; Kahr, B. Resorcinol Crystallization from the Melt: A New Ambient Phase and New “Riddles”. *J. Am. Chem. Soc.* **2016**, *138*, 4881–4889.

(16) Budzianowski, A.; Katrusiak, A. High-Pressure Crystallographic Experiments with a CCD Detector. In *High Pressure Crystallography*; Katrusiak, A.; McMillan, P. J., Eds.; NATO Science Series; Kluwer: Dordrecht, The Netherlands 2004; pp 101–112, DOI: 10.1007/978-1-4020-2102-2.

(17) *Xcalibur CCD System, Crys Alis Pro Software System*, version 1.171.33; Oxford Diffraction Ltd.: Wrocław, Poland. 2009

(18) Dolomanov, O. V.; Bourhis, L. J.; Gildea, R. J.; Howard, J. A. K.; Puschmann, H. OLEX2: a Complete Structure Solution, Refinement and Analysis Program. *J. Appl. Crystallogr.* **2009**, *42*, 339–341.

(19) Sheldrick, G. M. A Short History of SHELX. *Acta Crystallogr., Sect. A: Found. Crystallogr.* **2008**, *64*, 112–122.

(20) Piermarini, G. J.; Block, S.; Barnett, J. D.; Forman, R. A. Calibration of the Pressure Dependence of the R1 Ruby Fluorescence Line to 195 Kbar. *J. Appl. Phys.* **1975**, *46*, 2774–2780.

(21) Merrill, L.; Bassett, W. A. Miniature Diamond Anvil Pressure Cell for Single Crystal X-ray Diffraction Studies. *Rev. Sci. Instrum.* **1974**, *45*, 290–294.

(22) Bombicz, P. The Way from Isostructurality to Polymorphism. Where are the borders? The Role of Supramolecular Interactions and Crystal Symmetries. *Crystallogr. Rev.* **2017**, *23*, 118–151.

(23) Lander, J. J.; Svirbely, W. J. The Dipole Moments of Catechol, Resorcinol and Hydroquinone. *J. Am. Chem. Soc.* **1945**, *67*, 322–324.

(24) Rudyk, R.; Molina, M. A. A.; Gómez, M. I.; Blanco, S. E.; Ferretti, F. H. Solvent Effects on the Structure and Dipole Moment of Resorcinol. *J. Mol. Struct.: THEOCHEM* **2004**, *674*, 7–14.

(25) Anwar, J.; Chatchawalsaisin, J.; Kendrick, J. Asymmetric Crystal Growth of α -Resorcinol from the Vapor Phase: Surface Reconstruction and Conformational Change Are the Culprits. *Angew. Chem., Int. Ed.* **2007**, *46*, 5537–5540.

(26) Cai, W.; Katrusiak, A. Conformationally Assisted Negative Area Compression in Methyl Benzoate. *J. Phys. Chem. C* **2013**, *117*, 21460–21465.

(27) Katrusiak, A. Modelling Hydrogen-bonded Crystal Structures beyond Resolution of Diffraction Methods. *Pol. J. Chem.* **1998**, *72*, 449–459.

(28) Katrusiak, A. Rigid H_2O Molecule Model of Anomalous Thermal Expansion of Ices. *Phys. Rev. Lett.* **1996**, *77*, 4366–4369.

(R2) Pressure-Promoted Solvation of Resorcinol

F. Safari, A. Olejniczak, A. Katrusiak,
Cryst. Growth Des. **2020**, *20*, 3112–3118.
DOI: 10.1021/acs.cgd.9b01732

Declarations of co-authors contribution to this article, included in this thesis:

In paper “Pressure-Promoted Solvation of Resorcinol” published in *Cryst. Growth Des.* **2020**, *20*, 3112–3118, I have done the experimental part of this research and prepared manuscript and all plots and tables. I assess my contribution as 80%.

In paper “Pressure-Promoted Solvation of Resorcinol” published in *Cryst. Growth Des.* **2020**, *20*, 3112–3118, I have helped in solving the crystal structures which was obtained by F. Safari, and I also checked and corrected the crystallographic data. I assess my contribution as 10%.

In paper “Pressure-Promoted Solvation of Resorcinol” published in *Cryst. Growth Des.* **2020**, *20*, 3112–3118, I have suggested the subject, discussed the research and results and participated in writing this publication. I assess my contribution as 10%.

Pressure-Promoted Solvation of Resorcinol

Fatemeh Safari, Anna Olejniczak, and Andrzej Katrusiak*

Cite This: *Cryst. Growth Des.* 2020, 20, 3112–3118

Read Online

ACCESS |

Metrics & More

Article Recommendations

Supporting Information

ABSTRACT: Under ambient conditions resorcinol (Res), $C_6H_4(OH)_2$, favorably crystallizes from methanol and aqueous solutions as the anhydrate, in the form of polymorph α at room temperature. Anhydrous polymorph β can be obtained above 360 K. However, above 0.80 GPa the monohydrate Res·H₂O is formed from the aqueous solution. The monohydrate is less stable than the duotrihydrate 3Res·2H₂O, which nucleates later. The latter forms a tight passivation layer on the surface of monohydrate crystals and protects them from dissolution. Between 0.20 and 1.0 GPa the duotrihydrate is more favored than the previously reported Res polymorphs α and β . From a methanol solution above 0.40 GPa the methanol monosolvate Res·CH₃OH precipitates. In Res·H₂O resorcinol molecules assume the *syn-syn* conformation, and in 3Res·2H₂O independent *syn-syn* and *anti-anti* conformers are present. The *anti-anti* molecule is orientationally disordered, despite the fact that usually the disorder requires extra space, while the high pressure suppresses the volume. In all three new solvates, the solvent molecules mediate the H bonding between the hydroxyl groups. The formation of solvates can be rationalized by the low potential energy of *syn-syn* conformers as well as the volume gain of the solvates in comparison to the summed volumes of the pure resorcinol crystal and stoichiometric amounts of the solvent. The strong preference of the analogous orcinol (5-methylresorcinol) for the monohydrate formation under normal conditions is unchanged under high pressure.



INTRODUCTION

Pure compounds and their solvates and cocrystals can significantly differ in their physical and chemical properties. Therefore, such different forms of chemical compounds are often investigated to improve the performance of products.^{1–3} The investigation of hydrates is of particular importance, because humid air and solvents are usually involved in the manufacturing and formulation processes of (drug) compounds. Hydrate formation concerns at least one-third of organic compounds.^{4,5} However, presently there are still no general methods of predicting the preference for the formation of the pure or solvated forms. It was shown that high pressure can promote the formation of solvates for compounds that crystallize exclusively in the pure form under ambient conditions: for example, thiourea, C(NH₂)₂S, at 0.5 GPa forms the monohydrate, C(NH₂)₂S·H₂O, and above 0.7 GPa the duotrihydrate, 3C(NH₂)₂S·2H₂O,⁶ and the monohydrate of 1,4-diazabicyclo[2.2.2]octane dihydrobromide (hereafter dabco2HBr; 1,4-diazabicyclo[2.2.2]octane = dabco) above 0.48 GPa forms monohydrate dabco2HBr·H₂O polymorphs.⁷ High-pressure crystallization proved to be an efficient method for obtaining hydrates and other solvates of organic compounds: for example, dabco salts,^{8–10} 4,4'-bipyridinium perchlorate,¹¹ 5,6-dimethylbenzimidazole,¹² xylazine hydrochloride,¹³ and diphenylanthracene¹⁴ as well as pharmaceutical compounds of β -chlorpropamide¹⁵ and deoxycholic acid.¹⁶ It was shown that the preferred formation of these hydrates is connected with an

increase in their volume, in comparison to the volumes of the exact amount of the pure host compound crystallized separately and with the solvent present in the form of either a liquid or solid depending on the thermodynamic conditions;^{6–10} also the formation of new types of intermolecular bonds plays an important role.^{17,18}

The reverse effect of pressure favoring the crystallization of separate compounds has also been observed, but less frequently. For example, the isochoric crystallization of thiourea from an aqueous solution above 1.0 GPa yields the pure thiourea and ice VI, the methane hydrate, strongly preferred by pressure, decomposes above 8.0 GPa,¹⁹ and Y₂(C₂O₄)₃·10H₂O undergoes a partial dehydration at 1 GPa, forming monoclinic Y₂(C₂O₄)₃·6H₂O as single-crystalline inclusions in the original phase.²⁰

Presently, we have investigated the preferences of resorcinol and orcinol (Figure 1) for crystallization as either the pure or solvated compounds under high pressure. Resorcinol crystallizes exclusively as the anhydrate from aqueous solutions under the standard conditions, which contrasts with the analogous orcinol,

Received: December 30, 2019

Revised: February 14, 2020

Published: February 19, 2020



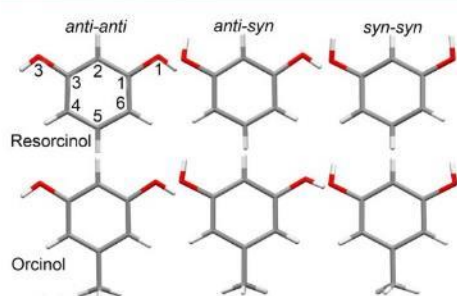


Figure 1. Resorcinol and orcinol conformers. Atomic labels usually applied in the literature and in this report are shown in the first drawing.

where hydrate formation is strongly favored. Resorcinol and its derivatives as well as isomeric quinol compounds²¹ are applied as medicines, and they can also be used as monomers (or as reactive additives) which increase the molecular weight of (pre)polymers. They can also be used in adhesives for wood.²² The active ingredients in the extracts of various plants contain resorcinol derivatives, which are primarily used in the treatment of cancer, osteoporosis, gastric ulcers, and other diseases.²³

Five polymorphs of pure resorcinol, labeled α and β (the same space group $Pna2_1$),^{24,25} γ ($Pnna$),^{26,27} δ (space group unknown),^{26,27} and ϵ (space group $P2_12_12_1$)²⁸ have been reported. The density of the α polymorph, which is stable under normal conditions, is lower than that of the high-temperature polymorph β .²⁹ Their structures were determined by X-ray diffraction in the 1930s,^{24,25} the structure of the α polymorph was one of the first for an organic compound to be determined by neutron diffraction in 1956,³⁰ and the ϵ polymorph was discovered in 2016. Despite such a long and varied record of experimental studies, no hydrates of resorcinol have been reported, which contrasts with a strong preference of orcinol (a close analogue of resorcinol) to form the hydrate. Our present study is aimed at determining the thermodynamic preferences of resorcinol solvates and to form an understanding of the mechanisms favoring the formation of solvates at high pressure. To study these preferences, we have performed high-pressure recrystallizations of resorcinol in aqueous, methanol, and ethanol solutions. We have also performed high-pressure crystallizations of orcinol, to allow a comparison of the results obtained from the study of these two similar compounds.

EXPERIMENTAL SECTION

The high-pressure crystallizations of the aqueous and methanol solutions were performed in a modified diamond anvil cell (DAC).³¹ Resorcinol solutions of various concentrations were used in order to start the nucleation at pressure under a range of isochoric and isothermal conditions.³² The in situ isothermal crystallization of the aqueous solutions, at 296 K, yielded the monohydrate $C_6H_4(OH)_2 \cdot H_2O$ at 0.8 GPa (Figure 2). The monohydrate precipitates as a powdered mass, and when the pressure was released to 0.35 GPa, all grains but one were dissolved and a bigger single crystal was grown by slowly increasing the pressure to 0.93 GPa (Figure 2). The crystallization process took about 2 h, and we noticed that after about 20 min at 0.93 GPa the crystal surface was covered by a layer of tightly packed tiny crystals of another new form (Figure 2). This monohydrate sample could be kept for days without visible changes. However, we have established that a release of pressure causes the passivation layer, most likely formed of hydrate $3Res \cdot 2H_2O$, to dissolve followed by the monohydrate dissolving gradually, while a single crystal of the duotritohydrate grew until the monohydrate disappeared (Figure 3). The conclusion that the passivation layer is formed of the

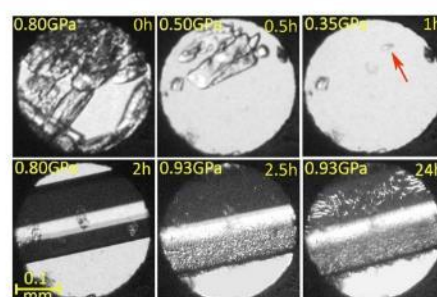


Figure 2. Isothermal crystallization of $Res \cdot H_2O$ at 296 K up to 0.93 GPa and of $3Res \cdot 2H_2O$ at 0.93 GPa. Two small ruby chips for the pressure calibration lie at the edge of the DAC chamber. The seed is indicated by the red arrow.

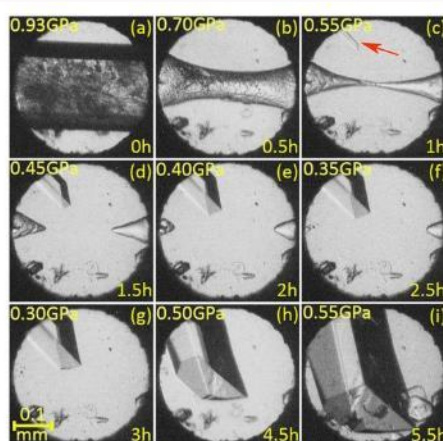


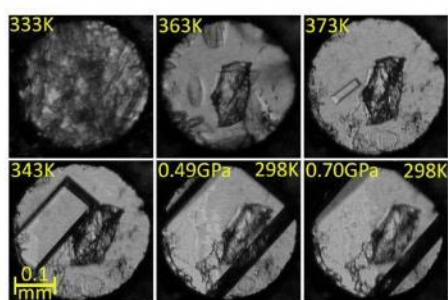
Figure 3. A $Res \cdot H_2O$ crystal (cf. Figure 2) covered by tiny $3Res \cdot 2H_2O$ crystals at 296 K/0.93 GPa (a). After the pressure is released (b–d), dissolution concomitant with the single-crystal nucleation of $3Res \cdot 2H_2O$ ((c), the seed indicated by the red arrow) and its further growth causes a further gradual reduction of pressure (e–g). Then (h, i), the pressure was increased to continue the growth. Several small ruby chips for the pressure calibration lie along the bottom edge of the DAC chamber.

duotritohydrate is based on the observation that this is the stable form of resorcinol in the aqueous solution between 0.2 and 1.0 GPa and that no other form of resorcinol could be obtained under these conditions. The $Res \cdot H_2O$ and $3Res \cdot 2H_2O$ crystals can be easily distinguished by their morphology, unit cell parameters, and symmetry (Figures 2 and 3 and Table 1); however, the crystal grains constituting the passivation layer are too small for such considerations. It can be noted that the 3:2 host molecules to crystallization water molecules ratio is relatively rare among hydrates. For this reason a common name for this hydrate stoichiometry is used, and in a few research papers^{33,34} a “2/3 hydrate” term was used. We have suggested the term “duotritohydrate”, used in the literature.^{35,36}

In the second series of experiments, resorcinol was crystallized in the DAC of the methanol solution. The new resorcinol monosolvate $C_6H_4(OH)_2 \cdot CH_3OH$ nucleated under isochoric conditions at 0.4 GPa, and then it was isothermally compressed up to 0.70 GPa (Figure 4 and Table 1). Finally, orcinol was recrystallized in order to also check its stability under the high-pressure conditions. The orcinol monohydrate $C_7H_6(OH)_2 \cdot H_2O$ was fully dissolved either in methanol or in water. The isochoric recrystallizations from the methanol solution yielded the monohydrate $C_7H_6(OH)_2 \cdot H_2O$ at 0.2 GPa; likewise, the recrystallizations of aqueous solution at 0.2 GPa also yielded the monohydrate (Figures S1 and S2).

Table 1. Selected Crystallographic Data of Resorcinol Solvates^a

	Res-CH ₃ OH			
	Res-H ₂ O	3Res-2H ₂ O	0.49 MPa	0.70 GPa
pressure	0.80 GPa	0.93 GPa	0.49 MPa	0.70 GPa
space group	<i>P</i> 2 ₁ 2 ₁ 2 ₁	<i>C</i> 2/ <i>c</i>	<i>P</i> 2 ₁ 2 ₁ 2 ₁	<i>P</i> 2 ₁ 2 ₁ 2 ₁
unit cell				
<i>a</i> (Å)	5.6567(18)	8.0312(8)	6.0242(12)	5.9240(3)
<i>b</i> (Å)	7.6544(5)	8.1080(6)	8.1523(12)	8.1201(3)
<i>c</i> (Å)	13.226(3)	26.01(4)	14.32(3)	14.087(9)
β (deg)	90	95.31	90	90
<i>V</i> (Å ³)	572.7(2)	1686(2)	703.4(14)	677.6(4)
<i>Z</i> / <i>Z'</i>	4/1	12/1.5	4/1	4/1
<i>D_x</i> (g/cm ³)	1.486	1.435	1.342	1.393
conformation	<i>syn-syn</i>	<i>syn-syn</i> and <i>anti-anti</i>	<i>syn-syn</i>	<i>syn-syn</i>

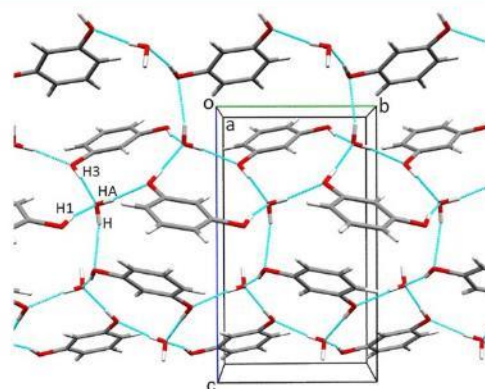
^aCf. Table S1 in the Supporting Information.**Figure 4.** Isochoric crystallization of Res-CH₃OH at 0.49 GPa and subsequent (the last panel) isothermal compression of the single crystal to 0.70 GPa. An irregular ruby chip for pressure calibration lies at the center of the chamber.

The pressure in the DAC chamber was calibrated by the ruby-fluorescence method with a Photon Control Inc. spectrometer, with an accuracy of 0.02 GPa.³⁷ The calibration was repeated before and after each diffraction measurement.³⁸ The single-crystal data have been measured with a KUMA KM4-CCD diffractometer. The CrysAlis software³⁹ was used for the data collections⁴⁰ and preliminary reduction of data after correcting the intensities for the effects of DAC absorption, sample shadowing by the gasket, and sample absorption.^{41,42} The reflections overlapping with diamond reflections were eliminated. The structures were refined with full-matrix least squares on *F*² using SHELX-L.^{43,44} Phenyl hydrogen atoms were ideally positioned according to the molecular geometry. The hydroxyl and water H atoms were located on the difference Fourier maps and then included in the refinements in the positions consistent with the molecular dimensions (O–H distance, 0.85 Å, C–O–H angle, 109.30°; H–O–H angle, 109.5°). The crystallographic and experimental details are given in Table S1 and deposited in the CIF format in the Cambridge Structure Database with CCDC numbers 1974181–1974186 and 1974294–1974295. The CIFs can be requested free of charge from <https://www.ccdc.cam.ac.uk>.

DISCUSSION

Chemical compounds often display a strong preference for crystallization in the form of either anhydrides or hydrates, when the crystallization is performed in the laboratory in open vials. In many cases, the presence of moisture in the atmospheric air suffices for the hydrate formation, even when the pure compound is dissolved in (initially) dry solvent but the solution is not then sealed from the atmosphere. There are also

compounds that form anhydrides or hydrates depending on the composition of the solution, air humidity, temperature, etc. Many compounds crystallize as anhydrides even from aqueous solutions. Resorcinol belongs to this latter group. Resorcinol has been thoroughly studied for decades, with five polymorphs (α , β , γ , δ , and ϵ) reported, but no hydrate of resorcinol was obtained. At the same time resorcinol favorably forms cocrystals with various compounds and presently there are 121 such multi-component deposits in the Cambridge Structure Database (version 1.23). Moreover, orcinol (5-methylresorcinol), despite being a close analogue of resorcinol, displays a strong preference for the formation of hydrates. Namely, under standard conditions orcinol favorably forms a monohydrate and dry solvents are required to obtain the anhydrate (two polymorphs of pure orcinol are known).⁴⁵ Hence, our present study is aimed at understanding the strong preference of resorcinol to form the anhydrate. We have applied high-pressure crystallization to establish whether this promotes hydrate formation by resorcinol. Recrystallizations from methanol and aqueous solutions in the DAC yielded new forms of resorcinol, as either polymorph α or β , up to 0.5 GPa. However, presently we have established that the pressure efficiently induces the formation of hydrates and a methanol solvate of resorcinol. The resorcinol monohydrate is formed in isothermal crystallization at 0.80 GPa. Then the surface of the monohydrate was tightly covered by many tiny crystals of duotrihydrate, 3C₆H₄(OH)₂·2H₂O (Figure 2). We have established that Res-H₂O is metastable, but it is protected from dissolution by the passivation layer of 3Res-2H₂O crystals. In the crystal structure of Res-H₂O, the water molecule mediates the hydrogen bonds between the hydroxyl groups (Figure 5). There are four symmetry-

**Figure 5.** Autostereogram⁵¹ of the molecular packing in Res-H₂O at 0.80 GPa/296 K. The OH...O hydrogen bonds are indicated as cyan lines, and the labels of H atoms participating in the H bonds are specified.

independent OH...O hydrogen bonds. Their dimensions are given in Table S3 and plotted in Figure S3. All of the OH...O bonds bind water and resorcinol molecules, while no water...water or resorcinol...resorcinol bonds are present (Figures 5 and 6).

In the structure of 3Res-2H₂O, there are two independent molecules of resorcinol; one of them (labeled A) is ordered in a general position, whereas the other (molecule B) is disordered and located on an inversion center (Figure 6). The water molecule lies in a general position. The water molecule forms three hydrogen bonds to resorcinol molecule A and one H₂O...

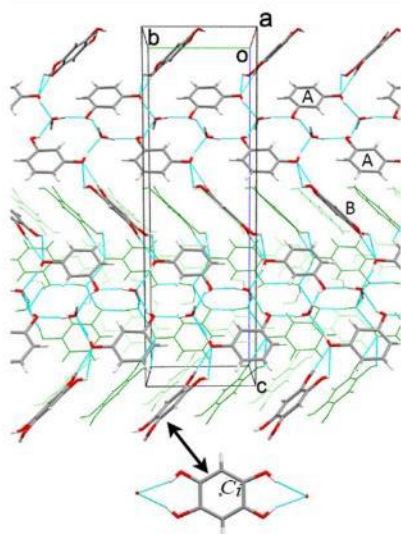


Figure 6. Molecular packing in 3Res·2H₂O at 0.93 GPa/296 K. H-B bonds are indicated by cyan lines. Capital letters A and B label the independent resorcinol molecules. Two overlapping positions of disordered half-occupied molecules B are shown, also viewed perpendicular to the ring at the bottom (indicated by the arrow).

H₂O hydrogen bond. Each resorcinol molecule A is OH...O bonded to three water molecules and to one molecule B. Each molecule B is OH...O bonded to two molecules A. The H-bonding pattern is shown in Figure 6 (cf. Table S3). The disorder of molecule B can be described as a nearly perfect superposition of the benzene ring with its half-occupied sites of hydroxyl group substituents at C1, C3, and their C_r-transformed sites C1' and C3'. The conformation of the hydroxyl groups is *syn-syn* in molecule A and *anti-anti* in molecule B. It is characteristic that a very similar type of disordered molecular orientation was reported for resorcinol cocrystals with hexamine⁴⁶ and bis(5-ferrocenylpyrimidine).⁴⁷ In these two cocrystals the disordered molecules are in an *anti-anti* configuration. In resorcinol cocrystallized with *N*-phthaloylglycine,⁴⁸ the *syn-syn* conformer of resorcinol is disordered. Other types of disorder of resorcinol molecules were observed in cocrystals with terpyridine⁴⁹ and several complexes of methylviologen.⁵⁰

The structure of Res·CH₃OH determined at 0.49 and 0.70 GPa, of orthorhombic space group *P2₁2₁2₁*, is isostructural with resorcinol monohydrate (cf. Table 1 and Figures 5 and 7). In the structure of Res·CH₃OH, the resorcinol and methanol molecules are H-bonded into ribbons along [010].

Resorcinol molecules in pure polymorphs, solvates, and cocrystals assume the *anti-anti*, *anti-syn*, and *syn-syn* configurations (Figure 1). The DFT calculations at the RB3LYP/6-31G level of theory of the potential energy for isolated molecules indicate that the *anti-syn* conformer is 0.94 kJ mol⁻¹ more stable than *anti-anti* conformer and 2.15 kJ mol⁻¹ more stable than the *syn-syn* conformer. These values are smaller than the energy of cohesion forces in H-bonded crystals, but they can be significant enough to help the stability of the observed resorcinol forms.

We established that one of the H bonds in the monohydrate, O—H...O²⁶⁶⁴, has a dimension of nearly 3 Å (Figure 8) and is much longer than the analogous H bonds in other solvates and in pure resorcinol. It is plausible that some steric hindrances in the structure of Res·H₂O prevent the formation of the H-

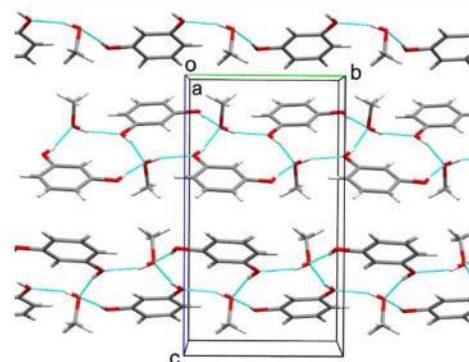


Figure 7. Autostereographic view of the structure of Res·CH₃OH at 0.49 GPa/296 K. The H bonds are indicated by cyan lines.

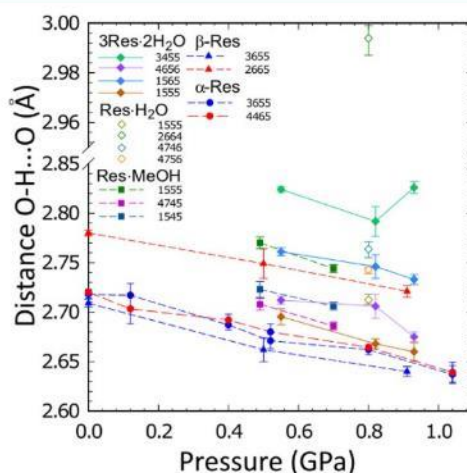


Figure 8. Pressure dependence of O...O H bond lengths in Res·H₂O, 3Res·2H₂O, and Res·CH₃OH, as well as in resorcinol polymorphs α and β . Symmetry operations indicated by ORTEP codes⁵³ are explicitly given in Table S9.

bonding network, efficiently using up all the available H donors and H acceptors. This could be the reason for the metastability of the Res·H₂O and its subsequent transformation to 3Res·2H₂O, where all hydroxyl groups and H₂O molecules can be linked by H bonds between 2.65 and 2.85 Å (Figure 8).

The molecular volumes of Res·H₂O, 3Res·2H₂O, and Res·CH₃OH are somewhat smaller than the sums of volumes of the stoichiometric amounts of pure resorcinol and solvent molecules

$$V_m(\text{Res}\cdot\text{H}_2\text{O}) < V_m(\text{Res}) + V_m(\text{H}_2\text{O})$$

$$V_m(3\text{Res}\cdot 2\text{H}_2\text{O}) < 3V_m(\text{Res}) + 2V_m(\text{H}_2\text{O})$$

$$V_m(\text{Res}\cdot\text{CH}_3\text{OH}) < V_m(\text{Res}) + V_m(\text{CH}_3\text{OH})$$

where V_m is the molecular volume of the solvates, the pure resorcinol polymorph β (stable in the considered range of pressure), and the solvents (Figure 9). In these comparisons we have applied volumes of the separate components (resorcinol polymorph β and liquid solvents) compressed to the appropriate pressure conditions (Figure 10).^{52,54}

This result indicates that the volume gain is a significant factor for the formation of these solvates. The energy associated with

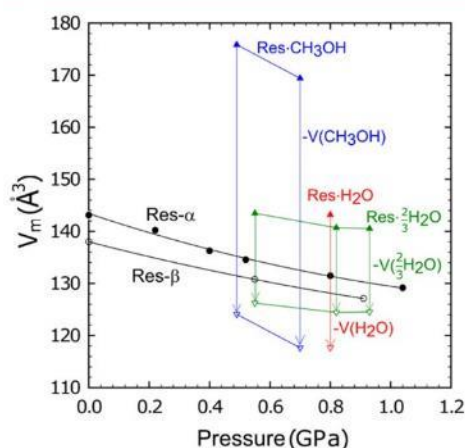


Figure 9. Pressure dependence of molecular volume referred to one resorcinol molecule in polymorphs α (black circles), β (empty black circles),⁵² Res- H_2O (red triangle), 3Res- $2\text{H}_2\text{O}$ (green triangles), and Res- CH_3OH (blue triangles). The vertical arrows indicate the difference in the solvate and appropriate amounts of the solvate volume (water or methanol).⁵⁴

this volume difference in comparison to β -resorcinol is 4.8 kJ mol^{-1} for Res- H_2O at 0.8 GPa, 1.2 kJ mol^{-1} for 3Res- $2\text{H}_2\text{O}$ at 0.45 GPa and 1.7 kJ mol^{-1} at 0.82 GPa, and 3.6 kJ mol^{-1} for Res- CH_3OH at 0.6 GPa. It appears that the effect of the largest work component gain for Res- H_2O is diminished by the inadequate H-bonding pattern in the structure (one of the possible H bonds cannot be formed)—hence the internal energy of the Res- H_2O structure increases and it is metastable in comparison to 3Res- $2\text{H}_2\text{O}$, as schematically illustrated in Figure 10. The energy of one hydrogen bond between two hydroxyl groups can be roughly estimated as several kJ mol^{-1} ; therefore, this value can be significant for changing the balance between the resorcinol solvates.

CONCLUSIONS

We have found that high pressure favors the formation of new solvates, which are unstable under ambient conditions. These new forms are resorcinol monohydrate, duotrihydrate, and monomethanol solvates. The stability of these new solvates at

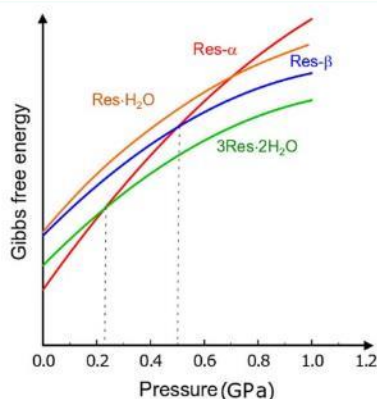


Figure 10. Schematic diagram of Gibbs free energy versus pressure at 296 K for resorcinol polymorphs α (red line),⁵² β (blue),⁵² Res- H_2O (orange), and 3Res- $2\text{H}_2\text{O}$ (green).

high pressure can be associated with the formation of new H bonds and with a volume gain of the solvates in comparison to the summed volume of their components. The H bonding plays a direct role in the molecular aggregation, as the solvent molecules mediate most of the H bonds between the resorcinol hydroxyl groups. The metastability of the monohydrate has been associated with a disadvantageous molecular arrangement hampering the formation of one of the possible $\text{OH}\cdots\text{O}$ bonds. Surprisingly, the more stable duotrihydrate is disordered, as one of its independent molecules assumes two orientations in the structure. This contrasts with the general assumption that high pressure eliminates orientational disorder. Although none of the new solvates could be recovered to ambient conditions, the revealed mechanisms of the pressure effects can prove useful for obtaining new stable solvates of this and other compounds. The comparison of resorcinol and orcinol illustrates that a relatively small structural difference (the methanol group at C5 in orcinol) can cause a drastic effect in the solvation of similar compounds. Such differences can be reduced, to some extent, by pressure, as has been presently observed for resorcinol hydrates promoted by high pressure. However, none of the resorcinol hydrates is isostructural with the orcinol monohydrate (similarly, as none of their anhydrate polymorphs are isostructural either).

ASSOCIATED CONTENT

Supporting Information

The Supporting Information is available free of charge at <https://pubs.acs.org/doi/10.1021/acs.cgd.9b01732>.

Additional photos of resorcinol crystals, crystal data and structure refinement details, and a plot showing the pressure dependence of geometric dimensions of hydrogen bonds $\text{OH}\cdots\text{O}$ as a function of pressure (PDF)

Accession Codes

CCDC 1974181–1974186 and 1974294–1974295 contain the supplementary crystallographic data for this paper. These data can be obtained free of charge via www.ccdc.cam.ac.uk/data_request/cif, or by emailing data_request@ccdc.cam.ac.uk, or by contacting The Cambridge Crystallographic Data Centre, 12 Union Road, Cambridge CB2 1EZ, UK; fax: +44 1223 336033.

AUTHOR INFORMATION

Corresponding Author

Andrzej Katrusiak – Faculty of Chemistry, Adam Mickiewicz University 61-614 Poznań, Poland; orcid.org/0000-0002-1439-7278; Phone: +48 61 829 1590; Email: katran@amu.edu.pl

Authors

Fatemeh Safari – Faculty of Chemistry, Adam Mickiewicz University 61-614 Poznań, Poland; orcid.org/0000-0002-4584-339X

Anna Olejniczak – Faculty of Chemistry, Adam Mickiewicz University 61-614 Poznań, Poland; orcid.org/0000-0002-4460-4362

Complete contact information is available at: <https://pubs.acs.org/doi/10.1021/acs.cgd.9b01732>

Author Contributions

The manuscript was written through contributions of all authors. All authors have given approval to the final version of the manuscript.

Funding

This study was supported by the Polish Ministry of Higher Education; F.S. is grateful to the EU European Social Fund, Operational Program Knowledge Education Development, grant POWR.03.02.00–00-1026/16 and project OPUS 10 UMO-2015/19/B/ST5/00262 from the Polish National Science Centre.

Notes

The authors declare no competing financial interest.

REFERENCES

- Bernstein, J. Polymorphism – A Perspective. *Cryst. Growth Des.* **2011**, *11*, 632–650.
- Singhal, D.; Curatolo, W. Drug Polymorphism and Dosage form Design: a Practical Perspective. *Adv. Drug Delivery Rev.* **2004**, *56*, 335–347.
- Blagden, N.; Matas, M.; Gavan, P. T.; York, P. Crystal Engineering of Active Pharmaceutical Ingredients to Improve Solubility and Dissolution rates. *Adv. Drug Delivery Rev.* **2007**, *59*, 617–630.
- Stahly, G. P. Diversity in Single- and Multiple-Component Crystals. The Search for and Prevalence of Polymorphs and Co-Crystals. *Cryst. Growth Des.* **2007**, *7*, 1007–1026.
- Cruz-Cabeza, A. J.; Reutzel-Edens, S. M.; Bernstein, J. Facts and Fictions about Polymorphism. *Chem. Soc. Rev.* **2015**, *44*, 8619–8635.
- Tomkowiak, H.; Olejniczak, A.; Katrusiak, A. Pressure-Dependent Formation and Decomposition of Thiourea Hydrates. *Cryst. Growth Des.* **2013**, *13* (1), 121–125.
- Andrzejewski, M.; Olejniczak, A.; Katrusiak, A. Humidity Control of Isostructural Dehydration and Pressure-induced Polymorphism in 1,4-Diazabicyclo [2.2.2] octane Dihydrobromide Monohydrate. *Cryst. Growth Des.* **2011**, *11*, 4892–4899.
- Olejniczak, A.; Podsiadlo, M.; Katrusiak, A. High Pressure Used for Producing a New Solvate of 1,4-Diazabicyclo [2.2.2] octane Hydroiodide. *New J. Chem.* **2016**, *40*, 2014–2020.
- Olejniczak, A.; Katrusiak, A. Pressure-Induced Hydration of 1,4-Diazabicyclo [2.2.2] octane Hydroiodide (dabcoHI). *Cryst. Growth Des.* **2011**, *11*, 2250–2256.
- Aniola, M.; Olejniczak, A.; Katrusiak, A. Pressure-Induced Solvate Crystallization of 1,4-Diazabicyclo [2.2.2] octane Perchlorate with Methanol. *Cryst. Growth Des.* **2014**, *14*, 2187–2191.
- Aniola, M.; Katrusiak, A. Pressure Effects on Crystallization, Polymorphism, and Solvation of 4,4'-Bipyridinium Perchlorate. *Cryst. Growth Des.* **2017**, *17*, 3134–3141.
- Zielinski, W.; Katrusiak, A. Pressure-Induced Preference for Solvation of 5,6-Dimethylbenzimidazole. *CrystEngComm* **2016**, *18*, 3211–3215.
- Olejniczak, A.; Krükle-Berziga, K.; Katrusiak, A. Pressure-Stabilized Solvates of Xylazine Hydrochloride. *Cryst. Growth Des.* **2016**, *16*, 3756–3762.
- Fabbiani, F. P. A.; Bergantini, S.; Gavezzotti, A.; Rizzato, S.; Moret, M. X-ray Diffraction and Computational Studies of the Pressure-Dependent Tetrachloroethane Solvation of Diphenylanthracene. *CrystEngComm* **2016**, *18*, 2173–2181.
- Zakharov, B. A.; Seryotkin, Y. V.; Tumanov, N. A.; Paliwoda, D.; Hanfland, M.; Kurmosov, A. V.; Boldyreva, E. V. The Role of Fluids in High-Pressure Polymorphism of Drugs: Different Behaviour of β -Chlorpropamide in Different Inert Gas and Liquid Media. *RSC Adv.* **2016**, *6*, 92629–92637.
- Tozuka, Y.; Kawada, D.; Oguchi, T.; Yamamoto, T. Supercritical Carbon Dioxide Treatment as a Method for Polymorph Preparation of Deoxycholic Acid. *Int. J. Pharm.* **2003**, *263*, 45–50.
- Drebushchak, V. A.; Ogienko, A. G.; Boldyreva, E. V. Polymorphic Effects at the Eutectic Melting in the H₂O–Glycine System. *J. Therm. Anal. Calorim.* **2013**, *111*, 2187–2191.
- Zieliński, W.; Katrusiak, A. Hydrate Smaller Than the Anhydrate. *CrystEngComm* **2015**, *17*, 5468–5473.
- Hirai, H.; Uchiyama, Y. High-Pressure Structures of Methane Hydrate Observed up to 8 GPa at Room Temperature. *J. Chem. Phys.* **2001**, *115*, 7066–7070.
- Zakharov, B.; Gribov, P.; Matvienko, A.; Boldyreva, E. Isostructural Crystal Hydrates of Rare-Earth Metal Oxalates at High Pressure: from Strain Anisotropy to Dehydration. *Z. Kristallogr. - Cryst. Mater.* **2017**, *232*, 751–757.
- Caspari, W. A. The Crystal Structure of Quinol. Part II. *J. Chem. Soc.* **1927**, *0*, 1093–1095.
- Alan, R.; Sabongi, J. *Resorcinol, Its Uses and Derivatives*; Springer: 1994; pp 5–86. DOI: 10.1007/978-1-4899-0999-2.
- Durairaj, R. B. *Resorcinol Chemistry, Technology and Applications*; Springer: 2005; pp 633–634. DOI: 10.1007/3-540-28090-1.
- Robertson, J. M. The Space Group of Resorcinol C₆H₆O₂. *Z. Kristallogr. - Cryst. Mater.* **1934**, *89*, 518–518.
- Ubbelohde, A. R.; Robertson, J. M. A New Form of Resorcinol. *Proc. R. Soc. A* **1937**, *140*, 239–239.
- Rao, R.; Sakuntala, T.; Godwal, B. K. Evidence for High-Pressure Polymorphism in Resorcinol. *Phys. Rev. B: Condens. Matter Mater. Phys.* **2002**, *65*, 054108.
- Kichanov, S. E.; Kozlenko, D. P.; Bilski, P.; Wąsicki, J.; Nawrocik, W.; Medek, A.; Hancock, B. C.; Lukin, E. V.; Lathe, C.; Dubrovinsky, L. S.; Savenko, B. N. The Polymorphic Phase Transformations in Resorcinol at High Pressure. *J. Mol. Struct.* **2011**, *1006*, 337–343.
- Zhu, Q.; Shtukenberg, A. G.; Carter, D. J.; Yang, T.; Yu, J.; Chen, M.; Raiteri, P.; Oganov, A. R.; Pokroy, B.; Polishchuk, I.; Bygrave, P. J.; Day, G. M.; Rohl, A. L.; Tuckerman, M. E.; Kahr, B. Resorcinol Crystallization From the Melt: a New Ambient Phase and New “Riddles”. *J. Am. Chem. Soc.* **2016**, *138*, 4881–4889.
- Lautz, H. Über die Beziehungen Instabiler Formen zu Stabilen. *Z. Phys. Chem.* **1913**, *84U*, 611–641.
- Bacon, G. E.; Curry, N. A. A Study of α -Resorcinol by Neutron Diffraction. *Proc. R. Soc. Lon. A* **1956**, *235*, 552–559.
- Merrill, L.; Bassett, W. A. Miniature Diamond Anvil Pressure Cell for Single Crystal X-ray Diffraction Studies. *Rev. Sci. Instrum.* **1974**, *45*, 290–294.
- Katrusiak, A. High-pressure crystallography. *Acta Crystallogr., Sect. A: Found. Crystallogr.* **2008**, *64*, 135–148.
- Jovanovski, G.; Kamenar, B. Two Ionic Saccharinates: (1a) Sodium Saccharinate 2/3 Hydrate, C₇H₄NO₃SNa₂·3H₂O (1b) Magnesium Disaccharinate Heptahydrate, (C₇H₄NO₃)₂Mg·7H₂O. *Cryst. Struct. Comm.* **1982**, *11*, 247–255.
- Bishop, R. Aspects of Crystallization and Chirality. In *Chirality in Supramolecular Assemblies: Causes and Consequences*; Keene, F. R., Ed.; Wiley: London, UK, 2016; p 81. DOI: 10.1002/9781118867334.ch3.
- Watts, N. *The Oxford New Greek Dictionary*; Berkley Books: 2008; pp 201, 445.
- <https://www.foundalis.com/lan/grknum.htm>.
- Piermarini, G. J.; Block, S.; Barnett, J. D.; Forman, R. A. Calibration of the Pressure Dependence of the R1 Ruby Fluorescence Line to 195 kbar. *J. Appl. Phys.* **1975**, *46*, 2774–2780.
- Mao, H. K.; Xu, J.; Bell, P. M. Calibration of the Ruby Pressure Gauge to 800 kbar Under Quasi-Hydrostatic Conditions. *J. Geophys. Res.* **1986**, *91*, 4673–4676.
- Budzianowski, A.; Katrusiak, A. High-Pressure Crystallographic Experiments with a CCD Detector. In *High-Pressure Crystallography*; Katrusiak, A., McMillan, P. F., Eds.; Kluwer: Dordrecht, The Netherlands, 2004; pp 101–112. DOI: 10.1007/978-1-4020-2102-2_7.
- Xcalibur CCD system, *CrysAlisPro Software System, Ver. 1.171.33*; Oxford Diffraction Ltd.: Wrocław, Poland, 2009.
- Katrusiak, A. REDSHABS, Program for the correcting reflections intensities for DAC absorption, gasket shadowing and sample crystal absorption; Adam Mickiewicz University: Poznań, Poland, 2003.

(42) Katrusiak, A. Shadowing and Absorption Corrections of Single-Crystal High-Pressure Data. *Z. Kristallogr. - Cryst. Mater.* **2004**, *219*, 461–467.

(43) Dolomanov, O. V.; Bourhis, L. J.; Gildea, R. J.; Howard, J. A. K.; Puschmann, H. OLEX2: a Complete Structure Solution, Refinement and Analysis Program. *J. Appl. Crystallogr.* **2009**, *42*, 339–341.

(44) Sheldrick, G. M. A Short History of SHELX. *Acta Crystallogr., Sect. A: Found. Crystallogr.* **2008**, *64*, 112–122.

(45) Mukherjee, A.; Grobelny, P.; ThakurGautam, S. T.; Desiraju, R. Polymorphs, Pseudopolymorphs and Co-Crystals of Orcinol: Exploring the Structural Landscape with High Throughput Crystallography. *Cryst. Growth Des.* **2011**, *11*, 2637–2653.

(46) Ng, S. W.; Naumov, P.; Ibrahim, A. R.; Fun, H. K.; Chantrapomma, S.; Wojciechowski, G.; Brzezinski, B. X-Ray and Spectroscopic Re-investigation of the 1:1 Complex Formed Between Urotropine and Resorcinol. *J. Mol. Struct.* **2002**, *609*, 89–95.

(47) Horikoshi, R.; Nambua, C.; Mochida, M. Supramolecular Assembly of Ferrocenes via Hydrogen Bonds: Dimensional Variation in Ferrocenylpyrimidine Complexes with Carboxylic Acids and Aromatic Alcohols. *New J. Chem.* **2004**, *28*, 26–33.

(48) Barooah, N.; Sarmaa, R. J.; Batsanov, A. S.; Baruah, J. B. Structural Aspects of Adducts of N-Phthaloylglycine and Its Derivatives. *J. Mol. Struct.* **2006**, *791*, 122–130.

(49) Trokowski, R.; Akinea, S.; Nabeshima, T. Selective Binding of Benzenediol Derivatives by Simultaneous Non-Covalent Interactions in Bis-Pt (II) Aza-Aromatic Host–Guest System. *Dalton Trans.* **2009**, *46*, 10359–10366.

(50) Imai, Y.; Kamona, K.; Kinuta, K.; Nobuob, T.; Sato, S.; Kuroda, R.; Matsubara, Y. An Iselective and Visual Inclusion Host System Using Charge-Transfer Complexes of 3,3'-Disubstituted-1,1'-bi-2-Naphthol and Methylviologen. *Tetrahedron Lett.* **2007**, *48*, 6321–6325.

(51) Katrusiak, A. Crystallographic Autostereograms. *J. Mol. Graphics Modell.* **2001**, *19*, 363–367.

(52) Safari, F.; Olejniczak, A.; Katrusiak, K. Pressure-Dependent Crystallization Preference of Resorcinol Polymorphs. *Cryst. Growth Des.* **2019**, *19*, 5629–5635.

(53) Johnson, C. K. ORTEP II; Oak Ridge National Laboratory: Oak Ridge, TN, 1976; Report ORNL-5138.

(54) Bridgman, P. W. Thermodynamic Properties of Twelve Liquids Between 20° and 80° and up to 12000 kgm. per sq. cm. *Proc. Am. Acad. Arts Sci.* **1913**, *49*, 3–113.

(R3) High-Pressure Polymorphs Nucleated and Stabilized by Rational Doping under Ambient Conditions

F. Safari, A. Katrusiak,

J. Phys. Chem. C **2021**, *42*, 23501–23509.

DOI: 10.1021/acs.jpcc.1c07297

Declarations of co-authors contribution to this article, included in this thesis:

In paper “High-Pressure Polymorphs Nucleated and Stabilized by Rational Doping under Ambient Conditions” published in *J. Phys. Chem. C* **2021**, *42*, 23501–23509, I have done the experimental part of this research and prepared manuscript and all plots and tables and I have solved all crystal structures. I assess my contribution as 80%.

In paper “High-Pressure Polymorphs Nucleated and Stabilized by Rational Doping under Ambient Conditions” published in *J. Phys. Chem. C* **2021**, *42*, 23501–23509, I have suggested the subject, discussed the research and general models and participated in writing this publication. I assess my contribution as 20%.

High-Pressure Polymorphs Nucleated and Stabilized by Rational Doping under Ambient Conditions

Fatemeh Safari and Andrzej Katrusiak*

Cite This: *J. Phys. Chem. C* 2021, 125, 23501–23509

Read Online

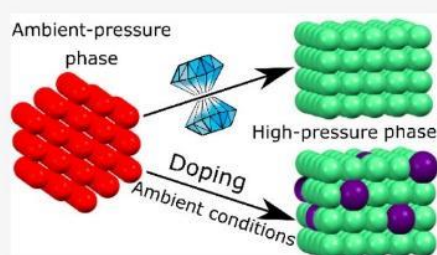
ACCESS |

Metrics & More

Article Recommendations

Supporting Information

ABSTRACT: High-pressure polymorphs can be obtained and stabilized at ambient pressure by utilizing dopants with more voluminous molecules, inducing internal strain in the structures. This effect has been confirmed for doped resorcinol and imidazole derivatives by nucleating and stabilizing their high-pressure phases under ambient conditions. The dopant molecular volume and concentration, as well as the bulk modulus of the polymorph in the binary system, are related to the stability region in the single-component phase diagram. High-pressure isothermal and isochoric recrystallizations yielded pure single crystals of resorcinol ϵ above 0.20 GPa and a new polymorph ζ above 0.70 GPa. These recrystallizations of pure resorcinol revealed within 1 GPa of the p – T phase diagram the boundaries and the stability regions of four resorcinol polymorphs α , β , ϵ , and ζ , contrary to the compression experiments on ambient-pressure polymorphs α and β , when the high-pressure phases were hidden behind the wide hysteresis extending to nearly 5 GPa. The hysteresis, originating from the H-bonding networks, hinders the formation of polymorphs ϵ and ζ when polymorphs α and β are compressed without melting or dissolving the crystals. Polymorph ζ is the only known resorcinol structure built of hydrogen-bonded layers.



INTRODUCTION

The wide variety of properties displayed by the same chemical compound in its different forms, such as polymorphs, glasses, size-scaled (nano)particles, and epitaxial layers, has stimulated research aimed at obtaining new materials desired for innovative and challenging applications. For example, studies on polymorphs of organic compounds have improved the performance of active pharmaceutical ingredients (APIs),^{1–5} polymorphs of photovoltaic materials, such as hybrid and purely inorganic perovskites, can cause undesired effects but also improve the performance of solar cells.⁶ Many methods for obtaining new polymorphs^{7,8} and for their theoretical prediction^{9,10} have been described. Among others, high pressure has been recognized as a very efficient tool for obtaining novel polymorphs and solvates of various compounds,^{11–13} such as paracetamol,¹⁴ urea,^{15,16} sucrose,¹⁷ benzimidazole,¹⁸ and others.^{19,20} However, most of the new forms obtained under high pressure and high/low temperature are unstable under normal conditions, which limits their practical applications. Here, we describe a simple method for obtaining and stabilizing high-pressure polymorphs under ambient conditions. These effects can be achieved by rationally doping a compound. In fact, the method of doping for obtaining new polymorphs is well-known;^{21,22} however, it was not connected to and optimized for specific regions of phase diagrams. The mechanism behind this phenomenon has been explained and verified for several compounds, but this study was inspired by intriguing inconsistencies in the phase diagram

of resorcinol²³ and by the recent discovery of polymorph ϵ obtained by mixing resorcinol with tartaric acid.²⁴

Resorcinol is an important chemical agent^{25,26} and the first organic compound for which, in the 1930s, the structures of two polymorphs were determined.^{27–29} Back then, the density of low-temperature polymorph α being lower than that of high-temperature polymorph β and their space-group symmetry type $Pna2_1$ ($Z = 4$) being the same despite considerable structural differences were counterintuitive. Since then, high-pressure polymorphs γ (space group $Pnna$) and δ (space group unknown)^{30,31} have also been postulated, but their structures have not been reported. Most recently, polymorph ϵ (space group $P2_12_12_1$) was found in the mixture with polymorph β obtained by freezing the melt of resorcinol with the addition of tartaric acid in the form of a thin film.²⁴ The structure of polymorph ϵ was determined from multicomponent powder X-ray diffraction (PXRD) combined with density functional theory (DFT) and molecular dynamics (MD) calculations. This discovery, quite puzzling after over a century of studies on this textbook example of polymorphs,² raised a number of questions, such as the availability of pure resorcinol polymorph

Received: August 17, 2021

Revised: September 30, 2021

Published: October 19, 2021



Table 1. Selected Crystallographic Data of Resorcinol Polymorphs α , β , ϵ , and ζ (cf. Tables S1 and S2) as Well as the Torsion Angles Describing the Molecular Conformation and H-Bond Directions

polymorph	α	β	ϵ	ϵ	ζ	ζ
pressure (GPa)	0.80(2)	0.91(2)	0.25(2)	0.96(2)	0.70(2)	1.2(2)
space group	$Pna2_1$	$Pna2_1$	$P2_12_12_1$	$P2_12_12_1$	$P2_1/c$	$P2_1/c$
unit cell a (Å)	10.2830(19)	7.5918(6)	17.876(5)	17.700(6)	10.6348(8)	10.465(3)
b	9.1431(7)	12.629(15)	10.464(6)	10.094(3)	9.5004(16)	9.425(5)
c	5.5953(3)	5.3029(14)	5.7045(16)	5.6096(6)	10.873(2)	10.787(6)
β (deg)	90	90	90	90	114.713(15)	113.70(4)
vol (Å ³)	526.06(11)	508.4(6)	1067.0(8)	1002.2(5)	997.9(3)	974.1(9)
Z/Z'	4/1	4/1	8/2	8/2	8/2	8/2
D_x (g/cm ³)	1.390	1.439	1.371	1.459	1.446	1.502
conformer ^a	anti-anti	anti-syn	anti-syn	anti-syn	anti-syn	anti-syn
C2–C1–O1–H (deg) ^b	173	–164	–151/–127	–152/–128	–163/156	–163/155
C2–C3–O3–H (deg)	–170	–17	–3/45	10/48	–1.6/19	5/17
C2–C1–O1...O3 (deg)	170.3	–161.5	–148/–128	–136/–128.5	–149.5/146	–150/145.35
C2–C3–O3...O1 (deg)	–163.3	–25.4	6/58	0.8/62.23	6.8/29.8	7.17/31.03

^aThe hydroxyl group conformation is associated with torsion angles C2–C1–O1–H and C2–C3–O3–H3. ^bThe values for symmetry-independent molecules A and B, in polymorphs ϵ and ζ , are separated with the slash.

ϵ , its stability region in the p – T phase diagram, the role of the dopant, and more general questions about metastability, detection of the total energy-minimum forms, and the roles of symmetry-independent units (Z') and molecular conformation. Undoubtedly, McCrone's famous statement "... that every compound has different polymorphic forms, and that, in general, the number of forms known for that compound is proportional to the time and money spent in research on that compound"³² has also been validated for resorcinol. Recent extensive studies on resorcinol as a function of temperature and pressure by X-ray and neutron diffraction, solid-state NMR, free-induction decay (FID) analysis, Raman spectroscopy, and other methods identified polymorph β as the high-pressure form of resorcinol up to 5 GPa, where it transforms to phase γ .^{30,31} Polymorph α could be isothermally compressed to 4 GPa; however, in other experiments, it transformed to polymorph β at 0.5 GPa.³¹ Recently, we investigated the structural origin of the pressure- and temperature-induced transformation between resorcinol phases α and β ;²³ two pressure ranges favoring the formation of resorcinol hydrates were also identified.³³

Presently, we have established that polymorph ϵ is the stable form of pure resorcinol from 0.20 to 0.70 GPa, at which point another polymorph ζ becomes stable. Single crystals of polymorphs ϵ and ζ were grown, and their structures were determined. The limiting pressure of 0.20 GPa, where single crystals of polymorph ϵ obtained from pure resorcinol immediately transformed to polymorph α , was most surprising in the context of the prolonged handling of polymorph ϵ obtained from the mixture with tartaric acid.²⁴ We have proposed a microstructural mechanism of doping stabilization of polymorph ϵ , and we have shown that this simple method also stabilizes high-pressure polymorphs of other compounds.

EXPERIMENTAL SECTION

High-Pressure Crystallizations. High-pressure experiments were performed in a diamond anvil cell (DAC)³⁴ modified by mounting the anvils directly on the steel supports with conical windows. Gaskets were made of steel foil 0.2 mm thick with a spark-eroded hole 0.35 mm in diameter. Polymorph ϵ nucleated above 0.20 GPa from the solution of resorcinol in a methanol/water 1:1 (vol) mixture (Figure S1).

In another series of experiments, polymorph ϵ nucleated and grew in the form of a single crystal from the aqueous solution in the presence of resorcinol monohydrate (Figure S2): first, the monohydrate crystal was grown in the DAC at 0.80 GPa, and after releasing the pressure to 0.35 GPa, it started to dissolve while another crystal nucleated. After further reduction of the pressure to 0.20 GPa, the monohydrate dissolved completely, and a crystal of ϵ -resorcinol was isothermally grown when the pressure was slowly increased up to 0.25 GPa (Figure S2); the crystal grew when the pressure was increased to 0.50 GPa, and then no change in the size or shape was noticed. On average, the crystallization of one single-crystal sample from its nucleation to the final equilibration of growth at room temperature required about 1–3 h of the controlled microscopic experiment. The crystals were studied in situ by single-crystal X-ray diffraction (SCXRD).

Characteristically, polymorphs α , β , and ϵ could be isothermally compressed to over 1 GPa, while high-pressure recrystallization between 0.20 and 0.70 GPa resulted in polymorph ϵ only. Above 0.70 GPa, a new polymorph ζ of pure resorcinol was crystallized from the saturated solution in MeOH/EtOH/H₂O (16:3:1) by the isochoric method (Figure S3). The SCXRD data were measured for this sample, and then again for the crystal isothermally compressed to 0.83, 1.00, and 1.20 GPa.

The pressure in the DAC chamber was calibrated by the ruby-fluorescence method before and after each diffraction measurement by using a Photon Control Inc. spectrometer of increased resolution, affording an accuracy of 0.02 GPa.^{35,36} A KUMA KM4-CCD diffractometer was used for SCXRD measurements. Data collection³⁷ and preliminary reduction of data after correcting the intensities for the effects of DAC absorption, sample shadowing by the gasket, and sample absorption were performed.^{38,39} The structures were refined with full-matrix least-squares on F^2 using SHELX-L.^{40,41} The crystallographic and experimental details are given in Table S1 and are deposited in CIF format in the Cambridge Structural Database with CCDC numbers 2084039–2084046.

Sample Doping by Melting. Samples of 4.1 mg of ambient-pressure polymorphs (α -phase) of selected compounds listed in Table 2 were mixed by grinding with a

Table 2. List of Selected Host Samples and Compounds Used as Dopants

host compound	dopant
resorcinol	L-tartaric acid (L-Ta)
resorcinol	D,L-tartaric acid (DL-Ta)
resorcinol	D-tartaric acid (D-Ta)
resorcinol	2-methyl benzimidazole (M-BzIm)
resorcinol	5,6-dimethylbenzimidazole (dM-BzIm).
imidazole (Im)	2-methyl benzimidazole (M-BzIm)
benzimidazole (BzIm)	2-methyl benzimidazole (M-BzIm)
benzimidazole (BzIm)	5,6-dimethylbenzimidazole (dM-BzIm)
2-methyl benzimidazole (M-BzIm)	5,6-dimethylbenzimidazole (dM-BzIm)

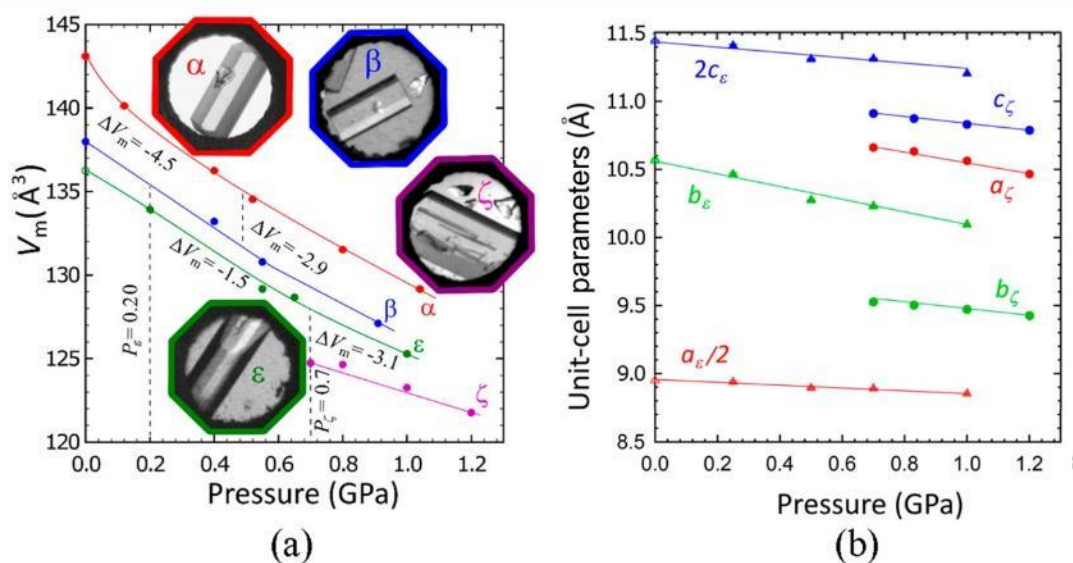


Figure 1. (a) Molecular volume ($V_m = V/Z$) of resorcinol polymorphs α , β , ϵ , and ζ plotted as a function of pressure. All ESDs are smaller than the plotted symbols. The empty symbol represents the ϵ phase obtained from a mixture of resorcinol with tartaric acid at 0.1 MPa (this data point was determined in ref 24). The insets show single crystals of polymorphs grown in situ in the DAC (cf. Figures S1–S3). (b) Unit-cell parameter as a function of pressure for polymorph ϵ (triangles) and polymorph ζ (circles); parameters a_ϵ and c_ζ have been divided and multiplied by 2, in order to accommodate all plots in one drawing.

dopant at 5, 15, and 25 wt % ratios and recrystallized by freezing the melt, following the procedure reported for α -resorcinol mixed with D-tartaric acid (D-Ta) by Zhu et al.²⁴ Each of these mixtures, as well as the reference sample of the pure compound, was heated on the thermal stage of a microscope until all crystal grains were molten, after which the samples were left to cool down to room temperature and recrystallize (Figure S9). The cooling of the molten mixture from ca. 370–300 K took about 10 min, but the molten sample froze in few seconds. Subsequently, the samples were characterized by PXRD using a Bruker D8 diffractometer operating in the θ - 2θ geometry with a Johansson monochromator, $\lambda(\text{Cu K}\alpha_1) = 1.54060$ \AA , and a LynxEye silicon-strip detector. The PXRD patterns were compared with the reference patterns calculated for the pure-compound phases as well as the applied dopant.^{42,43} In this way, the polymorphs constituting the samples were identified, and their ratio was established by comparing the intensities of reflections.

Milling Mixed Samples. Preparation of doped samples, analogous to those obtained in the melting and freezing process, by milling mixtures of 4.1 mg of the ambient-pressure polymorph with the dopants listed in Table 2 at 5, 10, 15, 20, and 25 wt % was attempted. The samples were milled in

hardened steel containers with several steel balls at a frequency of 30 Hz for 4 h. An MM 400 mill was used for all the powder samples. The subsequent PXRD patterns showed no changes in the ambient-pressure components in the mixtures, and no high-pressure polymorphs were detected.

RESULTS AND DISCUSSION

High-Pressure Crystallization. We used the methods of in situ isothermal recrystallization and isochoric recrystallization to explore the stability regions of resorcinol polymorphs under pressure. The crystallization conditions were additionally varied by changing the solvent (methanol, ethanol, water, and their various mixtures), concentration of resorcinol, and temperature and pressure region chosen for nucleating and growing crystals. The crystallization was performed slowly to prevent kinetic nucleation and to obtain high-quality single crystals; their morphology and high-accuracy XRD data were used for identifying the polymorphs. The crystallization process and transformations of the sample crystals and their compression and decompression were observed through a microscope. In this way, we could repetitively obtain and identify any of the four polymorphs α , β , ϵ , and ζ of pure resorcinol in the pressure region up to 1.20 GPa (Table 1).

High-quality single crystals of polymorph ϵ were grown in isochoric and isothermal conditions between 0.20 and 0.70 GPa (Figures S1 and S2). Upon releasing the pressure, the ϵ crystals were crushed into small pieces below 0.20 GPa due to the strain induced by the first-order phase transition to polymorph α , identified by PXRD both for the sample kept below 0.20 GPa in the DAC and for the powder recovered to ambient conditions. The single crystals of polymorph ϵ could be compressed to 1 GPa, at which they were crushed. By performing in situ PXRD measurements, we confirmed that the tiny fragments are still in the ϵ phase. The damage was due to mechanical reasons caused by anisotropic strain in the elongated crystal samples bridging the opposite edges of the steel gaskets (Figures S1 and S2), which plastically deformed when the pressure in the DAC was increased. All recrystallization procedures above 0.70 GPa resulted in crystals of a new polymorph ζ (Figure S3). All these observations show that polymorph ϵ of resorcinol is stable between 0.20 and 0.70 GPa and that polymorph ζ is stable at still higher pressure.

High-pressure SCXRD structural studies on polymorph ϵ showed that its molecular volume is smaller than those of polymorphs α and β in the all pressure ranges from 0.1 MPa to 1 GPa (Table 1, Figure 1a), but above 0.70 GPa, polymorph ζ is significantly denser than polymorph ϵ . This information corroborates the conclusions on the stability regions of polymorphs ϵ and ζ drawn from the high-pressure recrystallization, microscopic observations, and SCXRD/PXRD studies (Figure 1 and Figure S4). The p - T phase diagram outlined by us (Figure 3b) is consistent with the previous observations reported in the literature, with the reservation that, previously, the solid polymorphs α and β were only compressed and not dissolved. In those experiments, polymorphs α and β persisted to 5 GPa^{23,30,31} owing to the molecular conformations (Figure 2, Table 1) coupled to H-bonding networks (Table 1, Figure

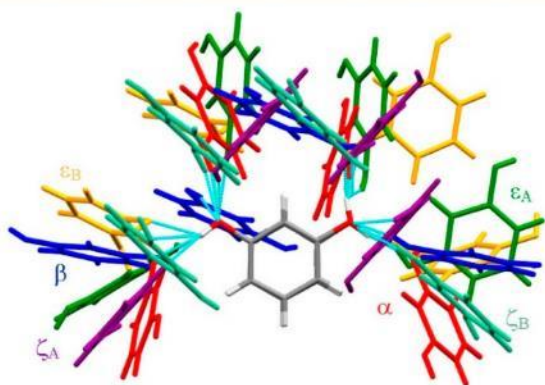


Figure 2. H-Bonded neighbors around the exactly superimposed central molecule (gray) in resorcinol polymorphs: α (red), β (navy blue), ϵ (green around molecule A and yellow around molecule B), and ζ (purple around molecule A and fern around molecule B). H-Bonds are indicated in cyan.

S6), preserving the present forms, although alternative structures could acquire a lower Gibbs free energy. This behavior, responsible for the extensive hysteresis,⁴⁴ clearly corresponds to different Gibbs functions associated with the polymorphs, as illustrated in Figure 3a. These results compared to those obtained in Kahr's group²⁴ led us to the conclusion that high hydrostatic pressure causes some effects similar to

those of doping resorcinol with tartaric acid, which results in the crystallization of polymorph ϵ at 0.1 MPa. Because of the instability of resorcinol ϵ at ambient pressure, we could not determine its unit-cell dimensions at 0.1 MPa, and in Figure 3, the dimensions previously determined by Kahr's group²⁴ for resorcinol doped with tartaric acid are plotted.

Apart from the lowest molecular volume (the highest density), the unique features of polymorph ζ —among the group of structurally determined resorcinol polymorphs α , β , ϵ , and ζ —are the centrosymmetric space group (Table 1) and that, in the crystal structure of ζ -resorcinol, the molecules are H-bonded into layers, which contrasts with the three-dimensional H-bonded networks in the other polymorphs (Figures S6–S8). It is remarkable that the compression of the layered structure of polymorph ζ is hardly anisotropic, as illustrated by the compression of the unit-cell parameters in Figure 1b. The polymorphs also differ in the conformations of hydroxyl groups, approximately described as either anti–anti (polymorph α) or anti–syn (polymorphs β , ϵ , and ζ). The descriptors “anti” and “syn” refer to the positions of ideally located hydroxyl hydrogen atoms with torsion angles C2–C1–O1–H and C2–C3–O3–H equal to 180° or 0°, respectively. The largest distortions from these ideal values are present in polymorph ϵ (Table 1). The hydroxyl group conformation indicates the direction of the H-bonds to the neighboring molecules (Figures S6–S8). The orientation of these close neighbors is further varied by torsion angles C–O...O–C (Figure 2). Undoubtedly, there are no easy paths for the molecules to change their arrangements and aggregation topologies by way of solid-to-solid phase transitions.

The polymorphic landscape of resorcinol as a function of pressure and temperature can be described by four Gibbs free energy functions shown in Figure 3a, and the p - T diagram in Figure 3b contains four polymorphs of resorcinol within the pressure range of 0–1 GPa. These results show that, at 300 K, polymorph β is metastable in all ranges of investigated pressure. Consequently, the recrystallization experiments yield the sequence of polymorphs α , ϵ , and ζ .

Owing to the wide hysteresis of resorcinol polymorphs, their volume compressibility $\beta_v = -(1/V) dV/dp|_{T=296\text{ K}}$ could be independently determined at 0.1 MPa at 296 K (Figure 1a): for polymorph α the compressibility, β_v is 0.140 GPa⁻¹; for polymorph β it is 0.091 GPa⁻¹; for polymorph ϵ it is 0.081 GPa⁻¹; for polymorph ζ the compressibility could be measured only above 0.7 GPa where it is equal to 0.048 GPa⁻¹. This significantly smaller β_v for polymorph ζ results from (i) the clearly nonlinear compressibility decreasing with increasing pressure for molecular crystals, as well as (ii) the reverse dependence of the compressibility on the density, clearly observed for polymorphs α , β , and ϵ (Figure 1a). These effects and the magnitudes of compressibility measured for resorcinol are typical of molecular crystals with hydrogen bonds. For example, in imidazole, at 0.1 MPa/296 K, β_v is 0.15 GPa⁻¹, but it decreases to 0.07 GPa⁻¹ at 0.7 GPa.⁴⁵ In benzimidazole at 0.1 MPa the compressibility is similar, about 0.13 GPa⁻¹, for polymorphs α and β , but the magnitude of β_v at 0.7 GPa in polymorph β decreases to 0.07 GPa⁻¹.¹⁸

Structural Model of Internal Pressure. The formation of polymorph ϵ in the frozen melt of resorcinol mixed with D-Ta suggested that mixing produces a similar effect as compression. Below, dopant molecules are indeed shown to be able to induce internal strain mimicking external compression. The generation of the internal doping pressure (p_d) requires that

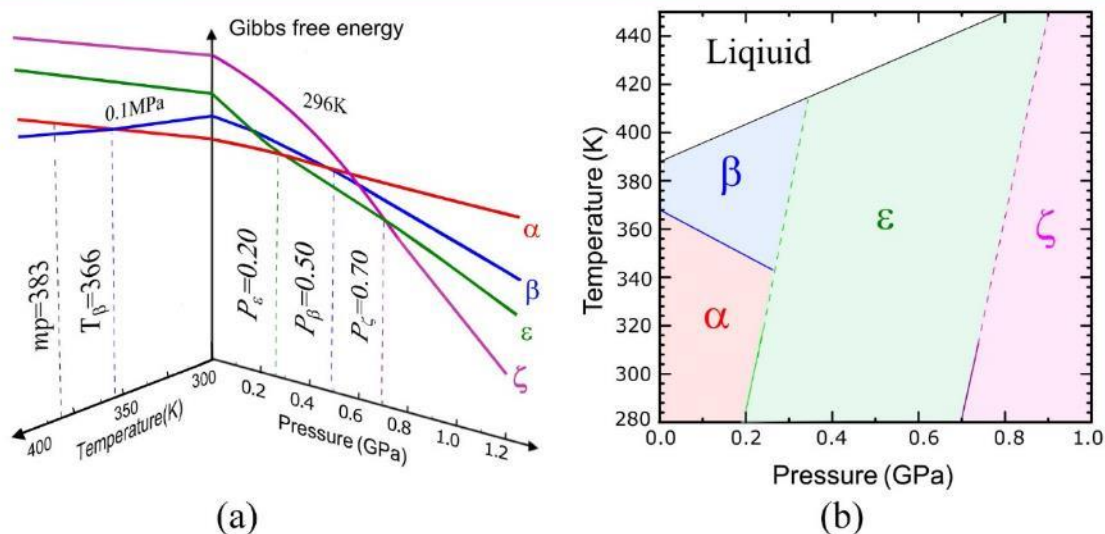


Figure 3. (a) Schematic diagram of the Gibbs free energy function vs pressure at 296 K and vs temperature at 0.1 MPa for resorcinol polymorphs α , β , ϵ , and ζ . Minimum pressure values for crystallizing polymorphs ϵ (P_ϵ) and ζ (P_ζ) are indicated; P_β marks the postulated equilibrium boundary pressure between polymorphs α and β in their metastable region. (b) p - T phase diagram of resorcinol; the dashed lines indicate phase boundaries extrapolated beyond those determined at 296 K in this study.

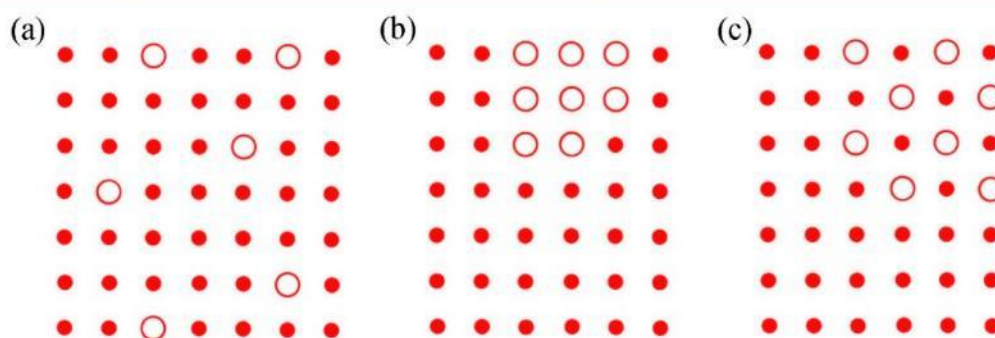


Figure 4. Schematic illustration of (a) a random distribution of single dopant molecules (large open circles), (b) dopant inclusion, and (c) dopant–host cocrystal inclusion in the host lattice (small dots).

the dopant molecule be embedded in the host structure, in which the host lattice is preserved (Figure 4a), and that no inclusions of dopant aggregates are formed (Figure 4, parts b and c). In the structure where the isolated dopant molecules are on average separated by n host molecules, the dopant-to-host molar ratio (c_d) is

$$c_d = [(n + 1)^3 - 1]^{-1} \quad (1)$$

According to this formula, the average separation $n = 1$ implies a molar ratio equal to 1:7 (14.3% dopant), $n = 2$ gives a ratio of 1:26 (3.8%), $n = 3$ gives a ratio of 1:80 (1.25%), etc. For large n values, c_d can be approximated by the molar concentration of the dopant in the mixture, equal to $(n + 1)^{-3}$. Assuming that the isotropic host and dopant molecules have a regular structure, the internal doping pressure can be assessed by the following formula:

$$p_d = K_o \cdot c_d \cdot \delta V / V_o \quad (2)$$

where K_o is the bulk modulus of the pure host compound, δV is the difference between the molecular volumes of the dopant and host, $\delta V = (V_d - V_o)$, and V_o is the molecular volume of

the pure host compound. Bulk modulus K_o can be substituted with volume compressibility ($K_o = 1/\beta_v$), and eq 2 can be rewritten in the form $p_d = (1/\beta_v)c_d\delta V/V_o$.

Equation 2 has been derived with the assumptions of isolated dopant molecules embedded in the host lattice, the same bulk modulus (K_o) describing the compression of the pure host and the doped crystal, and a spherical shape and isotropic interactions of all molecules. Thus, the effects of mismatched directional interactions, conformational flexibility, etc. are neglected. The obtained type of solid mixture (Figure 4) strongly depends on the method of crystallization and on the specific properties of the two compounds. For most compounds, the aggregation or cocrystallization of the dopant (Figure 4, parts b and c) can be expected to be favored by dynamic (slow) crystallization, while a random distribution of isolated dopant molecules in the host lattice (Figure 4a) is more likely to occur for kinetic processes, such as quick quenching of molten mixtures. Several different types of aggregation appear to be able to proceed simultaneously, but they can be dominated by the nucleation process. In quick and kinetic quenching of the melt, some parts of the components

can also form films or amorphize, which is difficult to detect by PXRD. When several types of solidification occur in the frozen melt, the actual concentration of isolated dopant molecules in the obtained solid solution is smaller than the ratio of mixed components. In fact, this effect is the main principle behind the zone-melting method. These considerations alone show that milling is very unlikely to result in a uniform distribution of single dopant molecules in the single-crystal grain (Figure S10). In practice, the dopant compound must be torn into single molecules and the host crystals cleaved along every second or third layer. Melting is much more suitable for this purpose, which has been fully confirmed by the positive results of our melting-and-freezing experiments and negative results of our milling experiments on mixing the various dopant and host compounds presented below.

In the real liquid solution of the dopant and host molten mixture, the larger dopant molecules exert some pressure. Likewise, in the crystal, the structure around larger dopant molecules is squeezed (Figure 5). This internal pressure

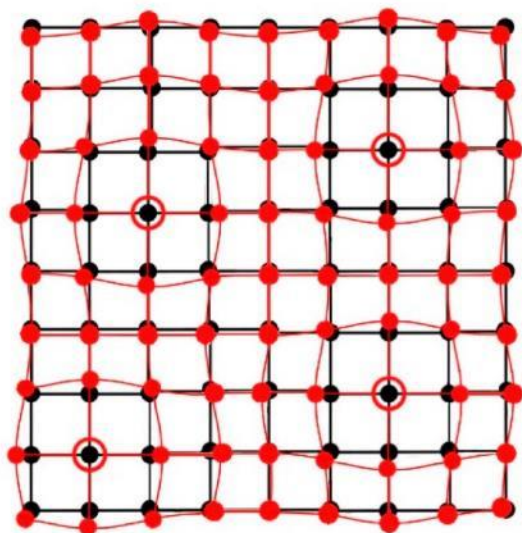


Figure 5. Schematic illustration of the effect of crystal doping (large open circles represent dopant molecules) on the crystal lattice: the lattice of a pure compound is represented by black lines, whereas red dots and lines represent the lattice strained under the internal pressure generated by large dopant molecules.

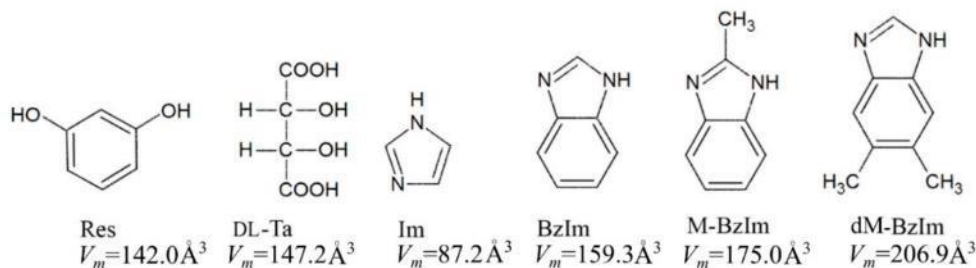
mimics the effect of external compression. Consequently, such doping of a compound can favor nucleation of high-pressure phases and their stabilization under ambient conditions. Figure 5 schematically illustrates that the microscopic strain induced by doping can be quite inhomogeneous, which can lead to a variety of nuclei and mixed phases in the kinetically frozen mixture. The double role of doping, i.e., the favored nucleation of the high-pressure polymorph and the stabilization of this polymorph by the dopant centers, can be explained by the internal pressure around the dopant molecules.

As explained above, the most efficient generation of strain is achieved when the dopant molecules do not form clusters in the structure of host compound. It is apparent that the equilibria between the intermolecular interactions of host–host, host–dopant, and dopant–dopant are essential for the homogeneous distribution of the dopant molecules in the host structure. Thus, apart from the molecular volume, also the compatibility of intermolecular forces types in the interactions, such as hydrogen bonds, van der Waals interactions, or halogen bonds, should be considered as the microscopic properties of the host and dopant compounds, or their hydrophilicity, lipophilicity, and miscibility as the macroscopic properties. Besides, the method of mixing the compounds may be crucial for obtaining the high dispersion of dopant molecules in the host structure, e.g., quick freezing from the melt, milling types, etc.

High-Pressure Polymorphs under Ambient Conditions. We tested the concept of doping pressure for crystallization of resorcinol and several imidazole derivatives, for which high-pressure phases were previously reported.^{18,20,45} The formulas of these compounds and their molecular volumes are shown in Scheme 1.

The dopant compounds were chosen according to their molecular volume, larger than that of the host compound. The volume of Ta molecules is only approximately 5% larger than that of resorcinol; however, the mismatched interactions with the crystal environment can cause additional strain. The results of quantitative PXRD on the frozen resorcinol–dopant mixtures are summarized in Table 3 and Table S6. The polymorphs were identified by comparing the measured PXRD patterns with those generated for the crystal structures of the polymorphs, and the quantities of the components were calculated from the intensities of reflections (Figures S11–S26). The 15 wt % addition of DL-Ta to resorcinol yielded the largest amount of polymorph ϵ (Table 3) mixed with polymorph β . In accordance with Ostwald's rule of stages, the presence of polymorph β is expected due to its stability

Scheme 1. Molecular Formulas, Abbreviations, and Molecular Volumes, V_m , of Compounds Used for Our Doping Tests at Ambient Pressure^a



^aThe V_m values of these compounds have been calculated according to their crystal data (refs 27 and 45–50).

Table 3. Polymorphs of Resorcinol Obtained in Molten and Frozen Resorcinol/Dopant Mixtures

dopant (wt %)	c_d	dopant pressure p_d (GPa)	resorcinol polymorphs
L-Ta 15%	0.1295	0.52	15% β :85% ϵ
D-Ta 15%	0.1295	0.52	12% β :88% ϵ
DL-Ta 15%	0.1295	0.52	10% β :90% ϵ
M-BzIm 15%	0.1470	0.42	77% β :23% ϵ
M-BzIm 25%	0.2777	0.79	31% β :69% ϵ
dM-BzIm 25%	0.2509	1.26	31% β :69% ϵ

temperature being below the melting point at 0.1 MPa. The internal pressures calculated according to eq 2 are given in Table 3 (Tables S4–S6).

Analogous experiments were conducted for imidazole and its derivatives (Table 4 and Table S6), for which the ambient- and

Table 4. Polymorphs of Imidazole, Benzimidazole (BzIm), and 2-Methylbenzimidazole (M-BzIm) Doped with the Compounds Listed in Table 2 (cf. Scheme 1) at 5, 15, and 25 wt % Ratios

dopant (wt %)	c_d	dopant pressure p_d (GPa)	Im polymorphs
BzIm 5%	0.0303	0.17	100% α
BzIm 25%	0.1920	1.11	35% α :65% β
M-BzIm 25%	0.1716	1.34	64% α :36% β
dopant (wt %)	c_d	dopant pressure p_d (GPa)	BzIm polymorphs
M-BzIm 5%	0.0469	0.07	100% β
M-BzIm 15%	0.1588	0.22	5% α :95% β
dM-BzIm 15%	0.1436	0.44	13% α :87% β
dopant (wt %)	c_d	dopant pressure p_d (GPa)	M-BzIm polymorphs
dM-BzIm 5%	0.0475	0.10	100% α
dM-BzIm 15%	0.1606	0.36	23% α :77% β
dM-BzIm 25%	0.3012	0.67	18% α :82% β

high-pressure polymorphs were previously determined.^{18,20,45} They showed results similar to those obtained for the doping experiments with resorcinol in that, in most cases, the high-pressure phases prevailed for benzimidazole (BzIm): the space-group symmetry of ambient-pressure polymorph α is $Pna2_1$,⁴⁷ and that of polymorph β stable above 0.23 GPa is $Pccn$.¹⁸ In the experiment of mixing BzIm with 5% dM-BzIm, we obtained a 100% yield of doped BzIm polymorph β . This was the only case of full yield of the high-pressure polymorph in all our experiments. This doped β -BzIm sample was stable for at least several months. The series of experiments on doping 2-methylbenzimidazole (M-BzIm) with 5,6-dimethylbenzimidazole (dM-BzIm) gave in the case of M-BzIm mixed with 5% dM-BzIm only the ambient-pressure phase α -M-BzIm, which was consistent with the internal pressure p_d (cf. eq 2, Table 4) being lower than the pressure of 0.26 GPa²⁰ required for stabilizing pure polymorph β -M-BzIm. However, 15% and 25% doping caused the formation of the β -M-BzIm polymorph as the main component of the frozen mixture (Table 4).

The absence of the higher-pressure polymorph ζ in any of the doped samples shows that sufficiently high internal strain cannot be generated by increasing the dopant concentration alone. It appears that when the dopant concentration exceeds some value (which may be different for different host and dopant compounds) the pressure does not increase linearly as a function of c_d , as suggested by eq 2. This can be expected, because the regions of the host structure decrease when c_d

increases and there are fewer single-dopant centers, which are most efficient in exerting strain on the host structure environment, while there are more larger clusters of the dopant molecules, less efficient in generating strain. Second, the higher-pressure polymorph (ζ) may require a close crystal packing possible only for tightly fitting identical molecules. It is also possible that Ostwald's rule of stages remains valid for the nucleation of polymorphs in the doped-sample conditions, even when the internal strain exceeds that required for a new phase. At present, more experimental information is required to better understand the doping and high-pressure polymorphism.

CONCLUSIONS

Rational doping by molecules larger than the host compound molecules can generate an internal strain in the melt, which mimics external compression and leads to high-pressure polymorphs. The doping pressure concept requires that single dopant molecules larger than the host molecules be randomly distributed in the host melt and crystal structure. Then, the internal pressure can be assessed from the molecular volume difference, dopant concentration, and host bulk modulus. The doping pressure is strongly inhomogeneous, but it shifts the thermodynamic equilibrium for nucleation toward high-pressure polymorphs and stabilizes them under ambient conditions. The optimized doping agent, its concentration, and the conditions when freezing the molten mixture can lead to a high or even full yield of desired high-pressure polymorphs. Undoubtedly, rational doping provides access to high-pressure polymorphs under ambient conditions and to their practical applications, for example, as APIs. The dopant properties can be adjusted for the envisaged applications of the product; for example, they may be chosen to improve the taste or bioaccessibility of the API. The high-pressure polymorphs of resorcinol appear much less puzzling than the polymorphs in varied-temperature studies alone. In the sequence of high-pressure phases, their increased density is obligatory, while their symmetry changes (Table 1) are not generally required, although they occur in most of the first-order phase transitions. These relations between resorcinol polymorphs α and β as a function of temperature, the unexpected density change, and the same space-group symmetry type appeared particularly confusing in the 1930s, when resorcinol happened to be the first example of structurally characterized polymorphs of any organic compound.^{27,28} The extended hysteresis of the transition between phases α and β only complicated the description. For these reasons, resorcinol was excluded from some of the most prominent reviews and textbooks on polymorphism. Presently, the case of resorcinol can be regarded as a clear illustration of the necessary and sufficient conditions in thermodynamics.⁵¹

ASSOCIATED CONTENT

Supporting Information

The Supporting Information is available free of charge at <https://pubs.acs.org/doi/10.1021/acs.jpcc.1c07297>.

Crystallographic data, powder diffraction data, and the internal dopant pressure calculation (PDF)

AUTHOR INFORMATION

Corresponding Author

Andrzej Katrusiak – Faculty of Chemistry, Department of Materials Chemistry, Adam Mickiewicz University, 61-614 Poznań, Poland; orcid.org/0000-0002-1439-7278; Phone: +48 61 829 1590; Email: katran@amu.edu.pl

Author

Fatemeh Safari – Faculty of Chemistry, Department of Materials Chemistry, Adam Mickiewicz University, 61-614 Poznań, Poland; orcid.org/0000-0002-4584-339X

Complete contact information is available at: <https://pubs.acs.org/10.1021/acs.jpcc.1c07297>

Author Contributions

F.S. and A.K. designed the research, performed the experiments, and wrote the manuscript. Both authors have approved the final version of the manuscript.

Notes

The authors declare no competing financial interest. The X-ray crystallographic structures reported in this study have been deposited at the Cambridge Crystallographic Data Centre under deposition numbers CSD 2084039–2084046. These data can be obtained free of charge from <https://www.ccdc.cam.ac.uk/>.

ACKNOWLEDGMENTS

The authors are grateful to the Center of Advanced Technology for granting access to the X-ray diffractometers. This study was supported by the Polish Ministry of Higher Education. F.S. is grateful to the EU European Social Fund, Operational Program Knowledge Education Development, Grant POWR.03.02.00-00-1026/16.

REFERENCES

- (1) Bernstein, J. *Polymorphism in Molecular Crystals*; Clarendon Press: Oxford, U.K., 2002.
- (2) Brittain, H. G. *Polymorphism in Pharmaceutical Solids*; Marcel Dekker: New York, 1999.
- (3) Hilfiker, R.; Raumer, M. V. *Polymorphism in the Pharmaceutical Industry: Solid Form and Drug Development*; Wiley-VCH Verlag GmbH & Co. KGaA: Weinheim, Germany, 2019.
- (4) Guthrie, S. M.; Smilgies, D. M.; Giri, G. Controlling Polymorphism in Pharmaceutical Compounds Using Solution Shearing. *Cryst. Growth Des.* **2018**, *18*, 602–606.
- (5) Fabbiani, F. P. A.; Pulham, C. R. High-pressure Studies of Pharmaceutical Compounds and Energetic Materials. *Chem. Soc. Rev.* **2006**, *35*, 932–942.
- (6) Szafranski, M.; Katrusiak, A. Photovoltaic Hybrid Perovskites under Pressure. *J. Phys. Chem. Lett.* **2017**, *8*, 2496–2506.
- (7) Berkovitch-Yellin, Z.; Van Mil, J.; Addadi, L.; Idelson, M.; Lahav, M.; Leiserowitz, L. Crystal Morphology Engineering by “Tailor-Made” Inhibitors: A New Probe to Fine Intermolecular Interactions. *J. Am. Chem. Soc.* **1985**, *107*, 3111–3122.
- (8) Levesque, A.; Maris, T.; Wuest, J. D. ROY Reclaims Its Crown: New Ways to Increase Polymorphic Diversity. *J. Am. Chem. Soc.* **2020**, *142*, 11873–11883.
- (9) Srirambhatla, V. K.; Guo, R.; Price, S. L.; Florence, A. J. Isomorphous Template Induced Crystallisation: A robust method for the targeted crystallisation of Computationally Predicted Metastable Polymorphs. *Chem. Commun.* **2016**, *52*, 7384–7386.
- (10) Arlin, J. B.; Price, L. S.; Price, S. L.; Florence, A. J. A Strategy for Producing Predicted Polymorphs: Catemeric Carbamazepine Form V. *Chem. Commun.* **2011**, *47*, 7074–7076.

- (11) Fabbiani, F. P. A.; Buth, G.; Levendis, D. C.; Cruz-Cabeza, A. J. Pharmaceutical Hydrates under Ambient Conditions from High-pressure Seeds: A Case Study of GABA Monohydrate. *Chem. Commun.* **2014**, *50*, 1817–1819.
- (12) Zakharov, B.; Gribov, P.; Matvienko, A.; Boldyreva, E. Isostructural Crystal Hydrates of Rare-earth Metal Oxalates at High Pressure: From Strain Anisotropy to Dehydration. *Z. Kristallogr. - Cryst. Mater.* **2017**, *232*, 751–757.
- (13) Zakharov, B. A.; Seryotkin, Y. V.; Tumanov, N. A.; Paliwoda, D.; Hanfland, M.; Kurmosov, A. V.; Boldyreva, E. V. The role of fluids in high-pressure polymorphism of drugs: different behaviour of β -Chlorpropamide in different inert gas and liquid media. *RSC Adv.* **2016**, *6*, 92629–92637.
- (14) Boldyreva, E. V.; Shakhshneider, T. P.; Ahsbahs, H.; Sowa, H.; Uchtmann, H. Effect of high Pressure on the Polymorphs of Paracetamol. *J. Therm. Anal. Calorim.* **2002**, *68*, 437.
- (15) Olejniczak, A.; Ostrowska, K.; Katrusiak, A. H-bond Breaking in High-pressure Urea. *J. Phys. Chem. C* **2009**, *113*, 15761–15767.
- (16) Roszak, K.; Katrusiak, A. Giant anomalous strain between high-pressure phases and the mesomers of urea. *J. Phys. Chem. C* **2017**, *121*, 778–784.
- (17) Patyk, E.; Skumiel, J.; Podsiadlo, M.; Katrusiak, A. High-pressure (+)-Sucrose Polymorph. *Angew. Chem., Int. Ed.* **2012**, *51*, 2146–2150.
- (18) Zieliński, W.; Katrusiak, A. Hydrogen Bonds NH \cdots N in Compressed Benzimidazole Polymorphs. *Cryst. Growth Des.* **2013**, *13*, 696–700.
- (19) Zieliński, W.; Katrusiak, A. Pressure-induced Preference for Solvation of 5,6-Dimethylbenzimidazole. *CrystEngComm* **2016**, *18*, 3211–3215.
- (20) Zieliński, W.; Katrusiak, A. Colossal Monotonic Response to Hydrostatic Pressure in Molecular Crystal Induced by a Chemical Modification. *Cryst. Growth Des.* **2014**, *14*, 4247–4253.
- (21) Li, P.; Chen, I. W.; Penner-Hahn, J. X-Ray-absorption Studies of Zirconia Polymorphs. II. Effect of Y₂O₃ Dopant on ZrO₂ Structure. *Phys. Rev. B: Condens. Matter Mater. Phys.* **1993**, *48*, 10074–10081.
- (22) Machala, L.; Tucek, J.; Zboril, R. Polymorphous Transformations of Nanometric Iron (III) Oxide: A Review. *Chem. Mater.* **2011**, *23*, 3255–3272.
- (23) Safari, F.; Olejniczak, A.; Katrusiak, A. Pressure-dependent Crystallization Preference of Resorcinol Polymorphs. *Cryst. Growth Des.* **2019**, *19*, 5629–5635.
- (24) Zhu, Q.; Shtukenberg, A. G.; Carter, D. J.; Yang, T.; Yu, J.; Chen, M.; Raiteri, P.; Oganov, A. R.; Pokroy, B.; Polishchuk, I. B.; et al. Resorcinol Crystallization from the Melt: A New Ambient Phase and New “Riddles”. *J. Am. Chem. Soc.* **2016**, *138*, 4881–4889.
- (25) Durairaj, R. B. *Resorcinol: Chemistry, Technology, and Applications*; Springer: Berlin, Germany, 2005.
- (26) Dressler, H. *Resorcinol: Its Uses and Derivatives*; Plenum Press: New York, 1994.
- (27) Robertson, J. M. The Structure of Resorcinol a Quantitative X-ray Investigation. *Proc. R. Soc. London A* **1936**, *157*, 79–99.
- (28) Robertson, J. M.; Ubbelohde, A. R. A new form of resorcinol. II. Thermodynamic properties in relation to structure. *Proc. R. Soc. London A* **1938**, *167*, 136–147.
- (29) Robertson, J. M. *Organic Crystals and Molecules*; Cornell University Press: Ithaca, NY, 1953; p 224.
- (30) Rao, R.; Sakuntala, T.; Godwal, B. K. Evidence for High-pressure Polymorphism in Resorcinol. *Phys. Rev. B: Condens. Matter Mater. Phys.* **2002**, *65*, 054108–15.
- (31) Kichanov, S. E.; Kozlenko, D. P.; Bilski, P.; Wąsicki, J.; Nawrocik, W.; Medek, A.; Hancock, B. C.; Lukin, E. V.; Lathe, C.; Dubrovinsky, L. S. N.; et al. The polymorphic phase transformations in resorcinol at high pressure. *J. Mol. Struct.* **2011**, *1006*, 337–343.
- (32) McCrone, W. C. Polymorphism. In *Physics and Chemistry of the Organic Solid State*, Vol. 2; Fox, D., Labes, M. M., Weissberger, M., Eds.; Wiley Interscience: New York, 1965.

- (33) Safari, F.; Olejniczak, A.; Katrusiak, A. Pressure-promoted Solvation of Resorcinol. *Cryst. Growth Des.* **2020**, *20*, 3112–3118.
- (34) Merrill, L.; Bassett, W. A. Miniature Diamond Anvil Pressure Cell for Single Crystal X-ray Diffraction Studies. *Rev. Sci. Instrum.* **1974**, *45*, 290–294.
- (35) Piermarini, G. J.; Block, S.; Barnett, J. D.; Forman, R. A. Calibration of the Pressure Dependence of the R1 Ruby Fluorescence Line to 195 kbar. *J. Appl. Phys.* **1975**, *46*, 2774–2780.
- (36) Mao, H. K.; Xu, J.; Bell, P. M. Calibration of the Ruby Pressure Gauge to 800 kbar under Quasi-hydrostatic Conditions. *J. Geophys. Res.* **1986**, *91*, 4673–4676.
- (37) *Xcalibur CCD System, CrysAlisPro Software System*, ver. 1.171.33; Oxford Diffraction Ltd.: Wrocław, Poland, 2009.
- (38) Budzianowski, A.; Katrusiak, A. High-pressure crystallographic experiments with a CCD detector. In *High-Pressure Crystallography*; Katrusiak, A., McMillan, P. F., Eds.; Kluwer: Dordrecht, The Netherlands, 2004.
- (39) Katrusiak, A. REDSHABS, Program for the Correcting Reflections Intensities for DAC Absorption, Gasket Shadowing and Sample Crystal Absorption; Adam Mickiewicz University: Poznań, Poland, 2003.
- (40) Katrusiak, A. Shadowing and Absorption Corrections of Single-crystal High-pressure Data. *Z. Kristallogr. - Cryst. Mater.* **2004**, *219*, 461–467.
- (41) Dolomanov, O. V.; Bourhis, L. J.; Gildea, R. J.; Howard, J. A. K.; Puschmann, H. OLEX2: A Complete Structure Solution, Refinement and Analysis Program. *J. Appl. Crystallogr.* **2009**, *42*, 339–341.
- (42) Sheldrick, G. M. A Short History of SHELX. *Acta Crystallogr., Sect. A: Found. Crystallogr.* **2008**, *64*, 112–122.
- (43) Macrae, C. F.; Bruno, I. J.; Chisholm, J. A.; Edgington, P. R.; McCabe, P.; Pidcock, E.; Rodriguez-Monge, L.; Taylor, R.; Van De Streek, J.; Wood, P. A. Mercury CSD 2.0 - New Features for the Visualization and Investigation of Crystal Structures. *J. Appl. Crystallogr.* **2008**, *41*, 466–470.
- (44) Katrusiak, A.; Szafranski, M.; Podsiadlo, M. Pressure-induced Collapse of Guanidinium Nitrate N-H...O Bonded Honeycomb Layers into a 3-D Pattern with Varied H-Acceptor Capacity. *Chem. Commun.* **2011**, *47*, 2107–2109.
- (45) Paliwoda, D.; Dziubek, K. F.; Katrusiak, A. Imidazole Hidden Polar Phase. *Cryst. Growth Des.* **2012**, *12*, 4302–4305.
- (46) Martinez-Carrera, S. The Crystal Structure of Imidazole at -150° . *Acta Crystallogr.* **1966**, *20*, 783–798.
- (47) Escande, A.; Galigné, J. L. Structure Cristalline du Benzimidazole, $C_7N_2H_8$: Comparaison des Résultats de Deux études Indépendantes. *Acta Crystallogr., Sect. B: Struct. Crystallogr. Cryst. Chem.* **1974**, *B30*, 1647–1648.
- (48) Lee, Y.; Scheidt, W. R. Structure of 5,6-Dimethylbenzimidazole. *Acta Crystallogr., Sect. C: Cryst. Struct. Commun.* **1986**, *42*, 1652–1654.
- (49) Obodovskaya, A. E.; Starikova, Z. A.; Belous, S. N.; Pokrovskaya, I. E. Crystal and Molecular Structure of 2-Methylbenzimidazole. *J. Struct. Chem.* **1992**, *32*, 421–422.
- (50) Bootsma, G. A.; Schoone, J. C. Crystal Structures of Mesotartaric Acid. *Acta Crystallogr.* **1967**, *22*, 522–532.
- (51) Ge, Y.; Montgomery, S. L.; Borrello, G. L. Can C_p be Less Than C_v ? *ACS Omega* **2021**, *6*, 11083–11085.